Baryon Number Violation beyond the Standard Model

Thesis by

Bartosz Fornal

In Partial Fulfillment of the Requirements

for the Degree of

Doctor of Philosophy

California Institute of Technology

Pasadena, California

2014

(Defended April 2, 2014)

Acknowledgements

First and most of all, I would like to express my enormous gratitude to Mark Wise, my scientific father. I feel extremely honored and privileged to have had Mark as my doctoral advisor. He is an incredible physicist and a wonderful mentor. Doing research under his guidance was the best scientific experience I could ever have. His unparalleled passion towards physics is truly inspiring and exponentiated my love for theoretical elementary particle physics, with which I started my graduate school. Thanks to Mark I will remember my time at Caltech as the best years of my life.

I would like to further thank the other members of my defense committee: Sean Carroll, David Politzer, Frank Porter, and John Preskill, for their precious time and interest in my graduate work. I feel very lucky to have had a chance to interact with them.

Next, I would like to acknowledge all my other collaborators: Pavel Fileviez Pérez, Benjamín Grinstein, Janna Levin, and Tim Tait, as well as Jonathan Arnold, Koji Ishiwata, Sogee Spinner, and Michael Trott. I broadened my knowledge of physics significantly by working with all of them.

I benefitted considerably from the discussions with the members of the Caltech Particle Theory Group, especially Clifford Cheung, Steven Frautschi, Hirosi Ooguri, and John Schwarz, as well as visitors, in particular Harald Fritzsch and Peter Minkowski.

I would like to thank the exceptional administrative staff at Caltech, especially Carol Silberstein, who always had time for me and could make even the most difficult arrangements possible.

Finally, I would like to thank my wife, Maja, for her love and support, and my son, Marek, for his constant smile and happiness. I am very grateful for the support I received from my parents, Maria and Bogdan, as well as my grandparents, Maria and Tadeusz, Stanisława and Franciszek. You were always there when I needed you. I love you all very much!

My research was funded in part by the Henry and Grazyna A. Bauer Fellowship, the Gordon and Betty Moore Foundation through Grant #776 to the Caltech Moore Center for Theoretical Cosmology and Physics, and the U.S. Department of Energy under Contract No. DE-FG02-92ER40701. I am also very grateful to Caltech for supporting me as a teaching assistant, and to the UC Irvine Particle Theory Group for their hospitality.

Abstract

This thesis describes simple extensions of the standard model with new sources of baryon number violation but no proton decay. The motivation for constructing such theories comes from the shortcomings of the standard model to explain the generation of baryon asymmetry in the universe, and from the absence of experimental evidence for proton decay. However, lack of any direct evidence for baryon number violation in general puts strong bounds on the naturalness of some of those models and favors theories with suppressed baryon number violation below the TeV scale. The initial part of the thesis concentrates on investigating models containing new scalars responsible for baryon number breaking. A model with new color sextet scalars is analyzed in more detail. Apart from generating cosmological baryon number, it gives nontrivial predictions for the neutron-antineutron oscillations, the electric dipole moment of the neutron, and neutral meson mixing. The second model discussed in the thesis contains a new scalar leptoquark. Although this model predicts mainly lepton flavor violation and a nonzero electric dipole moment of the electron, it includes, in its original form, baryon number violating nonrenormalizable dimension-five operators triggering proton decay. Imposing an appropriate discrete symmetry forbids such operators. Finally, a supersymmetric model with gauged baryon and lepton numbers is proposed. It provides a natural explanation for proton stability and predicts lepton number violating processes below the supersymmetry breaking scale, which can be tested at the Large Hadron Collider. The dark matter candidate in this model carries baryon number and can be searched for in direct detection experiments as well. The thesis is completed by constructing and briefly discussing a minimal extension of the standard model with gauged baryon, lepton, and flavor symmetries.

Contents

Chapter 1

Introduction

1.1 Motivation

One of the most fundamental questions in elementary particle physics is whether baryon number is an exact or just an approximate global symmetry. This is a highly nontrivial problem, since the conservation of baryon number insures the stability of ordinary matter. On the other hand, baryon number violation is essential for producing a baryon asymmetry in the early universe, as required for a successful mechanism of baryogenesis. Proton decay is predicted by grand unified theories at a rate that could be detected by present day experiments. Also, the type I seesaw mechanism for neutrino masses requires Majorana mass terms which break lepton number by two units, and since the weak interactions preserve the difference between baryon and lepton number at the classical and quantum level, this suggests that baryon number should be broken by two units as well. However, despite all those hints, no baryon number violating processes have been observed experimentally.

The standard model contains the ingredients necessary to generate a cosmological baryon asymmetry. Nevertheless, the quantity in which they appear is insufficient to fully explain baryogenesis. It is therefore important to investigate extensions of the standard model which can account for a new structure generating baryon number violation. This is the main motivation behind this thesis: proposing and analyzing simple models preserving all the virtues of the standard model, but at the same time incorporating new baryon number violating processes, and reconciling those models with the current null experimental result in searches for baryon number nonconservation, especially the absence of proton decay.

This thesis incorporates three published papers: [1], [2], and [3], which constitute Chapters 2, 3, and 4, respectively. The first and the second papers were written in collaboration with Mark Wise and Jonathan Arnold, and the third one in collaboration with Pavel Fileviez Pérez, Sogee Spinner, and Jonathan Arnold. Chapter 5 describes the details of an unpublished project with specific directions for future work. In addition, the thesis is supplemented with appendices providing details of most of the calculations.

1.2 Baryon number in the standard model

1.2.1 Standard model review

The standard model of particle physics is a chiral gauge theory describing the electromagnetic, weak, and strong interactions [4, 5, 6, 7, 8, 9], based on the gauge group

$$SU(3)_c \times SU(2)_L \times U(1)_Y \ . \tag{1.1}$$

The matter fields of the standard model are three spin $1/2$ generations of quarks and leptons, and a spin zero Higgs boson. The only particles carrying baryon number are the quarks, and they are assigned baryon number $1/3$. The leptons have lepton number 1. The gauge fields associated with the gauge group of the standard model are: G^A_μ, W^a_μ, and B_μ, where $A = 1, ..., 8$ and $a = 1, 2, 3$. The particle content is summarized in Table 1.1.

As a relativistic quantum field theory, the standard model is described by a Lagrangian which can be schematically written as

$$\mathcal{L}_{\rm SM} = \mathcal{L}_{\rm gauge} + \mathcal{L}_{\rm kinetic} + \mathcal{L}_{\rm Higgs} + \mathcal{L}_{\rm Yukawa} \ . \tag{1.2}$$

The various terms are:

$$\mathcal{L}_{\rm gauge} = -\tfrac{1}{4} G^A_{\mu\nu} G^{A\,\mu\nu} - \tfrac{1}{4} W^a_{\mu\nu} W^{a\,\mu\nu} - \tfrac{1}{4} B_{\mu\nu} B^{\mu\nu} \ , \tag{1.3}$$

$$\mathcal{L}_{\rm kinetic} = \bar{Q}^i_L \, i\not{D} \, Q^i_L + \bar{u}^i_R \, i\not{D} \, u^i_R + \bar{d}^i_R \, i\not{D} \, d^i_R + \bar{l}^i_L \, i\not{D} \, l^i_L + \bar{e}^i_R \, i\not{D} \, e^i_R \ , \tag{1.4}$$

$$\mathcal{L}_{\rm Higgs} = (D_\mu H)^\dagger \, (D^\mu H) - \lambda \left(H^\dagger H - \tfrac{v^2}{2} \right)^2 \ , \tag{1.5}$$

$$\mathcal{L}_{\rm Yukawa} = -g^{ij}_u \, \bar{Q}^i_L \, \epsilon \, H^* \, u^j_R - g^{ij}_d \, \bar{Q}^i_L \, H d^j_R - g^{ij}_e \, \bar{L}^i_L \, H e^j_R + \text{h.c.} \ . \tag{1.6}$$

Field	Spin	$SU(3)_c$	$SU(2)_L$	$U(1)_Y$	B	L
$Q^i_{L\alpha} = \begin{pmatrix} u^i_{L\alpha} \\ d^i_{L\alpha} \end{pmatrix}$	$1/2$	3	2	$1/6$	$1/3$	0
$u^i_{R\alpha}$	$1/2$	3	1	$2/3$	$1/3$	0
$d^i_{R\alpha}$	$1/2$	3	1	$-1/3$	$1/3$	0
$l^i_{L\alpha} = \begin{pmatrix} \nu^i_{L\alpha} \\ e^i_{L\alpha} \end{pmatrix}$	$1/2$	1	2	$-1/2$	0	1
$e^i_{R\alpha}$	$1/2$	1	1	-1	0	1
H	0	1	2	$1/2$	0	0
G^A_μ	1	8	1	0	0	0
W^a_μ	1	1	3	0	0	0
B_μ	1	1	1	0	0	0

Table 1.1: Particle content of the standard model. The quantum numbers of the fields under the gauge groups are listed along with their baryon and lepton numbers. Quarks and leptons come in three generations, as denoted by the index i.

The Yang-Mills part of the Lagrangian (1.3) is built from the field strength tensors of the three gauge groups in a gauge invariant way. The kinetic part (1.4) describes the dynamics of quarks and leptons, with the gauge covariant derivative given by

$$D_\mu = \partial_\mu + ig G^A_\mu T^A + ig_2 W^a_\mu T^a + ig_1 B_\mu Y \ , \tag{1.7}$$

where T^A, T^a, and Y are the $SU(3)$, $SU(2)$, and $U(1)$ generators, respectively. The third part of the Lagrangian (1.5) involves only the Higgs doublet, both the kinetic and potential terms. Finally, the Yukawa part (1.6) describes how the quarks and leptons interact with the Higgs boson. The g^{ij}'s are the Yukawa couplings with $i, j = 1, 2, 3$ being generation indices. The color and spinor indices are not included in Eqs. (1.4) and (1.6).

The $SU(2)_L \times U(1)_Y$ part of the Lagrangian symmetry is spontaneously broken by the vacuum expectation value of the Higgs doublet [10, 11, 12],

$$H = \begin{pmatrix} H^+ \\ H^0 \end{pmatrix} \quad \rightarrow \quad \langle H \rangle = \frac{1}{\sqrt{2}} \begin{pmatrix} 0 \\ v \end{pmatrix}, \tag{1.8}$$

and reduces to the electromagnetic $U(1)_{\mathrm{EM}}$. After symmetry breaking, the spin one gauge fields carrying the interactions are the photon (electromagnetic), W and Z bosons (weak), and gluons (strong). The photon and weak Z boson fields are linear combinations of the gauge fields B_μ and W^3_μ. The Higgs mechanism is responsible for giving masses to the matter fields (Yukawa couplings produce quark and lepton mass matrices), as well as the W and Z bosons. For an excellent review of the standard model with a more detailed mathematical formulation, see Ref. [13].

The standard model provides an extremely successful description of our world. It explains the results of most of the particle physics experiments with stunning accuracy. However, despite its countless triumphs, it is incomplete by itself, even in the low energy regime. The standard model:

- $\rightarrow$ does not explain the existence of dark matter, confirmed by many astronomical and astrophysical observations;
- $\rightarrow$ predicts massless neutrinos, whereas neutrino oscillation experiments clearly indicate nonzero neutrino masses;
- $\rightarrow$ suffers from the hierarchy problem: the natural scale for the Higgs mass is the Planck mass, by far greater than the measured $125\ \mathrm{GeV}$;
- $\rightarrow$ has a strong CP problem, since the upper limit on the observed CP violation in strong interactions (coming from neutron electric dipole moment measurements) is smaller than 10^{-10} of its expected value;
- $\rightarrow$ gives no explanation for the hierarchical pattern of the Yukawa couplings;
- $\rightarrow$ does not include an efficient mechanism for cosmological baryon number generation.

In the following two subsections we concentrate on the last issue mentioned above. We discuss baryon number violation in the standard model and explain why there is a problem with accommodating baryogenesis. This will serve as a motivation for building models with new sources of baryon number violation.

1.2.2 Baryon number nonconservation

The Lagrangian of the standard model is invariant under an accidental global baryon number symmetry. It is impossible to violate baryon number at the classical level, as well as at any order in perturbation theory, since the baryon number current is conserved:

$$\partial_\mu j^\mu_B = \partial_\mu \left[\frac{1}{3} \sum_i \left(\bar{Q}^i_L \gamma^\mu Q^i_L + \bar{u}^i_R \gamma^\mu u^i_R + \bar{d}^i_R \gamma^\mu d^i_R \right) \right] = 0 \, . \tag{1.9}$$

The lowest dimensional nonrenormalizable baryon number violating operators allowed by the standard model gauge symmetries are dimension-six,

$$\mathcal{O}_{(6)} \sim \frac{q\,q\,q\,l}{\Lambda^2} \, , \tag{1.10}$$

and are very suppressed. However, within the standard model, baryon number can also be broken nonperturbatively through the electroweak chiral anomaly.

At the quantum level, the baryon number symmetry is anomalous and the baryon current is no longer conserved [14, 15],

$$\partial_\mu j^\mu_B = \frac{3}{64\pi^2} \, \epsilon^{\alpha\beta\gamma\delta} \left(g_2^2 \, W^a_{\alpha\beta} W^a_{\gamma\delta} + g_1^2 \, B_{\alpha\beta} B_{\gamma\delta} \right) \neq 0 \, , \tag{1.11}$$

where the factor of three corresponds to the number of generations. The electroweak chiral anomaly is closely related to the vacuum structure of the standard model. To understand this quantitatively, let us define the Chern-Simons number (in the gauge where $W_0 = 0$),

$$n_{\rm CS}(t) \equiv \frac{g_2^3}{96\pi^2} \, \epsilon^{ijk} \epsilon^{abc} \int d^3x \; W^a_i W^b_j W^c_k \; , \tag{1.12}$$

and consider static gauge field configurations corresponding to different values of $n_{\rm CS}$. Those configurations which have integer $n_{\rm CS}$ are pure gauge configurations of zero energy. Such minima correspond to topologically distinct vacuum states. The change in baryon number for a transition between those vacua starting at time t_i and ending at t_f is

$$\Delta B = \int_{t_i}^{t_f} dt \int d^3x \; \partial_\mu j^\mu_B = 3\left[n_{\rm CS}(t_f) - n_{\rm CS}(t_i)\right] \; . \tag{1.13}$$

Now, $n_{\rm CS}$ is a topological number and takes only integer values. Therefore, the change in baryon number can occur only in multiples of three units. Between the minima the energies of the configurations are positive and create an energy barrier. The energy of the saddle point configuration, being an extremum of the static energy, is simply the height of this barrier. Such a configuration is known as the sphaleron [16, 17].

At zero temperature, the rate for quantum tunnelling through the energy barrier is exponentially suppressed [18],

$$\Gamma(T=0) \sim \exp\left[-\frac{16\pi^2}{g_2^2}\right] \simeq 10^{-165} \; , \tag{1.14}$$

so there is essentially no baryon number violation in this case. On the other hand, at finite temperature the barrier can be overcome by a thermal excitation. In the broken phase ($T \lesssim m_h$) the rate of sphaleron events is [19]

$$\Gamma(T \lesssim m_h) \sim T^4 \exp\left[-\frac{8\pi\, m_W(T)}{g_2^2\, T}\, f\left(\frac{m_h}{m_W}\right)\right] \tag{1.15}$$

and is suppressed as well (the function f takes values of order one). However, at temperatures above the electroweak symmetry breaking scale there is no longer any exponential suppression and the rate takes the form

$$\Gamma(T \gtrsim m_h) \; \sim \; \left(\frac{g_2^2}{4\pi}\right)^5 T^4 \; . \tag{1.16}$$

Determining when the sphalerons were active in the early universe requires analyzing the condition for thermal equilibrium, i.e., comparing the sphaleron rate within the thermal

volume $1/T^3$ with the Hubble expansion rate,

$$\frac{\Gamma}{T^3} \gtrsim H \sim \frac{T^2}{M_P} \,. \tag{1.17}$$

Inserting numerical values into Eq. (1.17) yields an upper bound of 10^{12} GeV on the temperature at which the sphaleron processes remain efficient. We conclude that the baryon number violation mechanism in the standard model works only at temperatures

$$125 \text{ GeV} \lesssim T \lesssim 10^{12} \text{ GeV} \,. \tag{1.18}$$

1.2.3 Generation of baryon asymmetry

There are three ingredients every model is required to have in order to produce a baryon asymmetry. Those are described by the three Sakharov conditions [20]:

(1) baryon number violation,

(2) C and CP violation,

(3) departure from thermal equilibrium.

The standard model contains all of those elements so, *a priori*, it could incorporate baryogenesis. However, the amount of baryon asymmetry generated in the standard model is much smaller than current observations indicate. The first condition, baryon number non-conservation, is satisfied by sphaleron transitions. As for the second criterion, although the standard model does violate charge conjugation symmetry C maximally (since it is a chiral theory), the main contribution to the conjugation-parity symmetry CP comes only from the Cabibbo-Kobayashi-Maskawa matrix [21, 22] and it was proven to be insufficient for producing the present baryon asymmetry of the universe [23, 24]. On top of this, the standard model does not fulfill the third Sakharov requirement since it cannot accommodate a large enough departure from equilibrium: for a Higgs particle of mass 125 GeV there is no first-order electroweak phase transition crucial for having an inequilibrium state.

The lack of an efficient mechanism for baryogenesis within the standard model leads us (in Chapter 2) to include new scalar particles in the spectrum, providing additional sources

of CP violation. The models we discuss have the potential of explaining the observable baryon asymmetry of the universe and do not suffer from tree-level proton decay. Some of them predict also new phenomena such as neutron-antineutron oscillations.

1.2.4 Proton decay

Since baryon number is conserved in the standard model at the perturbative level and the nonperturbative effects of the sphalerons change baryon number by a multiple of three units, proton decay can occur only through nonrenormalizable operators. The least suppressed nonrenormalizable operators of this type are dimension-six:

$$\begin{aligned}
&\frac{1}{\Lambda^2}\epsilon^{\alpha\beta\gamma}\left[(d_{R\alpha})^T C u_{R\beta}\right]\left[(u_{R\gamma})^T C e_R\right], \qquad \frac{1}{\Lambda^2}\epsilon^{\alpha\beta\gamma}\epsilon_{ij}\epsilon_{km}\left[(Q^i_{L\alpha})^T C Q^j_{L\beta}\right]\left[(Q^k_{L\gamma})^T C l^m_L\right],\\
&\frac{1}{\Lambda^2}\epsilon^{\alpha\beta\gamma}\epsilon_{ij}\left[(Q^i_{L\alpha})^T C Q^j_{L\beta}\right]\left[(u_{R\gamma})^T C e_R\right], \quad \frac{1}{\Lambda^2}\epsilon^{\alpha\beta\gamma}\epsilon_{ij}\left[(d_{R\alpha})^T C u_{R\beta}\right]\left[(Q^i_{L\gamma})^T C l^j_L\right],\\
&\frac{1}{\Lambda^2}\epsilon^{\alpha\beta\gamma}(\tau^a\epsilon)_{ij}(\tau^a\epsilon)_{km}\left[(Q^i_{L\alpha})^T C Q^j_{L\beta}\right]\left[(Q^k_{L\gamma})^T C l^m_L\right],
\end{aligned} \tag{1.19}$$

where C is the charge conjugation matrix and the generation indices were suppressed for simplicity. Those operators mediate proton decay since they violate baryon and lepton number by one unit. In light of a null experimental observation of proton decay, the operators above can be used to derive lower limits on the proton mean lifetime, with the most stringent constraint coming from the decay mode $p \to e^+\pi^0$ [25],

$$\tau_p > 8.2 \times 10^{33} \text{ years} . \tag{1.20}$$

In order to satisfy this experimental bound, the scale Λ of new physics has to be very high, $\Lambda \gtrsim 10^{16}$ GeV. This implies a huge desert between the electroweak scale and the scale Λ, at which the origin of baryon number violating interactions can be understood.

The effective operators (1.19) have their origin in degrees of freedom at the high scale, where the physics is probably governed by a grand unified theory (GUT). Actually, grand unification is one of the most compelling arguments behind the experimental searches for proton decay, since it predicts a proton decay rate at a level not far from current experimental detection capabilities.

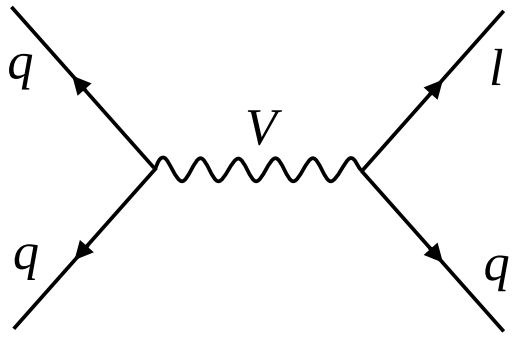

Figure 1.1: GUT vector boson exchange leading to proton decay.

Grand unified theories unify the three types of interactions in the standard model: strong, weak, and electromagnetic. They provide explanation to many puzzles of the standard model, like the quantization of electric charge, cancellation of chiral anomalies, and the origin of quantum numbers for quarks and leptons. The simplest and most studied grand unification theories are based on the gauge symmetry $SU(5)$ [26] and $SO(10)$ [27]. For a review of proton decay in grand unified theories, see Ref. [28].

Grand unification predicts new superheavy particles whose interactions with the standard model may violate baryon number at the perturbative level, causing proton decay. An example of a diagram involving a GUT vector boson leading to proton decay is shown in Fig. 1.1. This type of interaction is the origin of the nonrenormalizable dimension-six operators listed in (1.19). Denoting the mass of the new gauge boson by m_V, the proton decay rate can be estimated as

$$\Gamma_p = \frac{1}{\tau_p} \sim \frac{g_V^4}{16\pi^2}\frac{m_p^5}{m_V^4} \,, \tag{1.21}$$

where g_V is the coupling constant and m_p is the proton mass. Combining this estimate with the experimental bound (1.20) gives the lower limit on the mass of new vector bosons,

$$m_V \gtrsim 10^{16}\ \mathrm{GeV} \,, \tag{1.22}$$

which is in agreement with our previous bound on the scale Λ.

1.3 Neutron-antineutron oscillations

Apart from proton decay, which violates baryon number by one unit, an interesting and complimentary method of probing baryon number violation is to look for neutron-antineutron ($n\bar{n}$) oscillations, in which a neutron spontaneously changes into an antineutron. This process violates baryon number by two units (see Fig 1.2). There are various motivations for studying $n\bar{n}$ oscillations:

- $\rightarrow$ New physics behind $n\bar{n}$ oscillations may be responsible for creating a baryon asymmetry in the universe.

- $\rightarrow$ The process of $n\bar{n}$ oscillations is uniquely suited for studying the nature and scale of the seesaw mechanism. Since the neutrino Majorana mass term violates lepton number by two units, and the weak interactions conserve $B-L$ at the classical and quantum level, this suggests that $\Delta B = 2$ processes should exist as well.

- $\rightarrow$ Observation of $n\bar{n}$ oscillations would point to a relatively low scale of new physics, contradicting the picture of a desert between the electroweak scale and the grand unification scale. This is a consequence of the fact that $n\bar{n}$ oscillations are mediated by dimension-nine operators. In light of this fact, searches for $n\bar{n}$ oscillations can be viewed as complimentary to searches for proton decay: while proton decay experiments probe physics at the grand unification scale, the $n\bar{n}$ oscillation experiments are sensitive to physics at a scale as low as a TeV.

To better understand the phenomenon of $n\bar{n}$ oscillations, let us consider the dynamics of a two-level system consisting of a neutron and an antineutron described by an effective Hamiltonian. Its dynamics are governed by the following equation:

$$i\hbar \frac{\partial}{\partial t} \begin{pmatrix} n \\ \bar{n} \end{pmatrix} = \begin{pmatrix} E_n & \Delta m \\ \Delta m & E_{\bar{n}} \end{pmatrix} \begin{pmatrix} n \\ \bar{n} \end{pmatrix} \ . \tag{1.23}$$

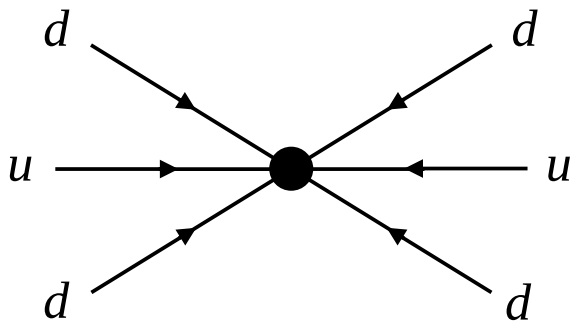

Figure 1.2: Diagram showing an interaction leading to neutron-antineutron oscillations.

The mixing parameter Δm contains information about the underlying theory which breaks baryon number by two units. The transition probability for a free neutron is given by

$$P_{n\to\bar{n}}(t) = \frac{(\Delta m)^2}{\frac{1}{4}(E_n - E_{\bar{n}})^2 + (\Delta m)^2} \sin^2\left(\sqrt{(E_n - E_{\bar{n}})^2 + (2\Delta m)^2}\, t\right) . \tag{1.24}$$

The oscillation time is defined as

$$\tau_{n\bar{n}} = \frac{\hbar}{|\Delta m|} . \tag{1.25}$$

For neutrons bound inside a nucleus, there is a relation between the measured nuclear instability lifetime and the corresponding $n\bar{n}$ oscillation time given by

$$\tau_{\rm bound} = T_R\, \tau_{n\bar{n}}^2 , \tag{1.26}$$

where T_R is obtained from nuclear structure calculations. A more thorough discussion of $n\bar{n}$ oscillations in various models is provided in Ref. [29].

Table 1.2 shows the experimental limit on the mixing parameter $|\Delta m|$. The strongest bound comes from the Super-Kamiokande nuclear decay experiment in Japan [30],

$$|\Delta m| < 2.7 \times 10^{-33}\ {\rm GeV} . \tag{1.27}$$

Experiment (year)	Type of search	Limit on $\lvert\Delta m\rvert$
Super-Kamiokande (2011)	nuclear decay in ^{16}O	$< 2.7 \times 10^{-33}$ GeV [30]
Soudan (2002)	nuclear decay in ^{56}Fe	$< 5.1 \times 10^{-33}$ GeV [31]
ILL (1994)	free neutrons	$< 7.7 \times 10^{-33}$ GeV [32]
NNbarX (prospective)	free neutrons	$\lesssim 7 \times 10^{-35}$ GeV [33]

Table 1.2: Best limits on the neutron-antineutron oscillation mixing parameter Δm from experiments of different type and the predicted sensitivity of the NNbarX experiment.

The search for $n\bar{n}$ oscillations in nuclear decay experiments becomes less efficient when we require higher sensitivity, which is the result of the atmospheric neutrino induced background. This is the reason why currently there is a focus on free neutron beam $n\bar{n}$ oscillation experiments. The prospective NNbarX experiment at Fermilab is exactly such an experiment. It should be able to probe $n\bar{n}$ oscillations in free neutron beams with a huge improvement in sensitivity by almost two orders of magnitude. In the case of no $n\bar{n}$ oscillation detection, the predicted upper limit for the mixing parameter will be

$$|\Delta m| \lesssim 7 \times 10^{-35} \text{ GeV} . \tag{1.28}$$

The limits (1.27) and (1.28) can be used to set current and future bounds on the couplings and masses of new particles, as will be shown in Chapter 2.

1.4 Lepton flavor violation

One of the most important open questions in flavor physics concerns the existence of processes violating flavor symmetry in the charged lepton sector. Some processes of this type would be:

$$\mu \to e\,\gamma , \quad \mu \to e \text{ conversion} , \quad \mu \to e\,e\,e . \tag{1.29}$$

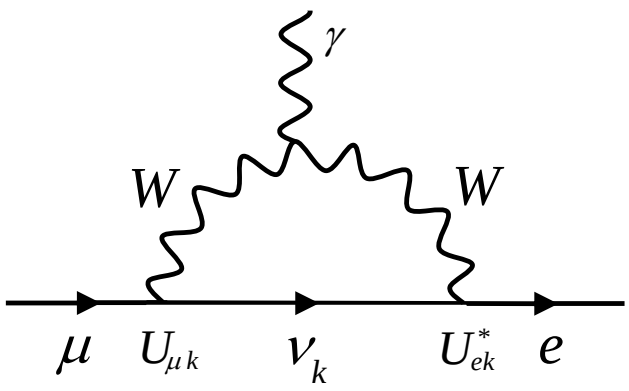

Figure 1.3: One of the diagrams contributing to the process $\mu \to e\,\gamma$ in the minimal extension of the standard model with massive neutrinos.

The standard model itself does not predict any charged lepton flavor violation, since it is invariant under the symmetry

$$U(1)_e \times U(1)_\mu \times U(1)_\tau \,. \tag{1.30}$$

Even in the minimal extension of the standard model with just the neutrino masses included, the predicted rates for charged lepton flavor violating processes are extremely suppressed.

To estimate the level of suppression, consider the process $\mu \to e\,\gamma$ in such a model. From Feynman diagrams like the one in Fig. 1.3, the branching ratio is given by [34]

$$B(\mu \to e\,\gamma) = \frac{\alpha}{2\pi}\left|\sum_i U_{ei}U^*_{\mu i}\frac{m^2_{\nu_i}}{m^2_W}\right|^2 \simeq \frac{\alpha}{2\pi}\left|U_{e3}U^*_{\mu 3}\frac{\Delta m^2_{\rm atm}}{m^2_W}\right|^2 \lesssim 10^{-54}\,, \tag{1.31}$$

where U is the Pontecorvo-Maki-Nakagawa-Sakata matrix [35, 36, 37]. Such a huge suppression highlights the importance of experimental searches for charged lepton flavor violation. With essentially no background, a positive signal would be a clear indication of physics beyond the standard model other than neutrino oscillations. Similar claims are not applicable in the quark sector. Quark flavor violation is well established within the standard model and described by the Cabibbo-Kobayashi-Maskawa matrix. It is not suppressed at all, making it incredibly hard to distinguish between small deviations from the standard model predictions and experimental uncertainties.

Experiment (year)	Process	Limit on branching ratio
MEG (2012)	$\mu \to e\,\gamma$	$< 5.7 \times 10^{-13}$ [38]
SINDRUM II (2006)	$\mu^- \mathrm{Au} \to e^- \mathrm{Au}$	$< 7.0 \times 10^{-13}$ [39]
SINDRUM (1988)	$\mu \to e\,e\,e$	$< 1.0 \times 10^{-12}$ [40]
COMET (prospective)	$\mu^- \mathrm{Al} \to e^- \mathrm{Al}$	$\lesssim 2.6 \times 10^{-17}$ [41]
Mu2e (prospective)	$\mu^- \mathrm{Al} \to e^- \mathrm{Al}$	$\lesssim 5.4 \times 10^{-17}$ [42]

Table 1.3: Best experimental limits on the branching ratios of various charged flavor violating processes and the predicted sensitivity of the COMET and the Mu2e experiments.

From an effective theory point of view, charged lepton flavor violation can be described by the nonrenormalizable dimension-five and dimension-six operators:

$$\frac{1}{\Lambda}\,\bar{l}_i \sigma_{\mu\nu} l_j F^{\mu\nu}\,, \quad \frac{1}{\Lambda^2}\,\bar{l}_i \gamma_\mu l_j \left(\bar{q}_k \gamma^\mu q_m + \bar{l}_k \gamma^\mu l_m\right), \tag{1.32}$$

where i, j, k and m are generation indices ($i \neq j$). The dimension-five operator encapsulates the lepton couplings to the electromagnetic field and describes the $\mu \to e\,\gamma$ effective vertex, as well as the tree-level part of the $\mu \to e$ conversion and the $\mu \to e\,e\,e$ process. The dimension-six operators are relevant for the four-fermion vertices responsible for the other contributions to $\mu \to e$ conversion and $\mu \to e\,e\,e$, but do not contribute to the $\mu \to e\,\gamma$ decay. The most stringent experimental limits on charged lepton flavor violation come from the $\mu \to e\,\gamma$ and $\mu \to e$ conversion experiments (see Table 1.3). Although the constraints are severe, the background is still suppressed by an additional forty orders of magnitude.

The state-of-the-art in measuring $\mu \to e\,\gamma$ is the MEG experiment in Switzerland, which provides the bound [38]

$$\mathrm{Br}(\mu \to e\,\gamma)_{\mathrm{MEG}} < 5.7 \times 10^{-13}\,. \tag{1.33}$$

The best limit on $\mu \to e$ conversion is set by SINDRUM II in Switzerland [39],

$$\mathrm{Br}(\mu \to e \ \text{conversion})_{\text{SINDRUM II}} < 7 \times 10^{-13} \,. \tag{1.34}$$

This result will be improved by four orders of magnitude by the Mu2e experiment at Fermilab, which by the year 2020 should reach the sensitivity [42]

$$\mathrm{Br}(\mu \to e \ \text{conversion})_{\text{Mu2e}} \lesssim 5 \times 10^{-17} \,. \tag{1.35}$$

Its future competitor, the COMET experiment in Japan, by 2020 should reach a similar sensitivity of [41]

$$\mathrm{Br}(\mu \to e \ \text{conversion})_{\text{COMET}} \lesssim 3 \times 10^{-17} \,. \tag{1.36}$$

Those high precision experiments are complimentary to the physics searches at the Large Hadron Collider (LHC). Although narrowed down to a single channel each, their signal would be very clean and provide evidence for new physics even before the LHC. Such a signal might be tied in some way to baryon number violation. In Chapter 3 we consider a model of this type, one that exhibits an enhancement of charged lepton flavor violation, but also contains dimension-five operators breaking baryon number. A discrete symmetry has to be imposed to forbid operators mediating proton decay in this model.

1.5 Baryon number in the minimal supersymmetric standard model

The minimal supersymmetric standard model (MSSM) [43] is viewed as one of the most promising candidates for physics beyond the standard model. It has a number of very attractive features, including that it:

- $\to$ does not suffer from the hierarchy problem;
- $\to$ contains a natural dark matter candidate;
- $\to$ explains gauge coupling unification;
- $\to$ is based on supersymmetry suggested by string theory.

Superfield	Particle content			$SU(3)_c$	$SU(2)_L$	$U(1)_Y$	B	L
	Spin 0	Spin $1/2$	Spin 1					
$\hat{Q}^i$	$\tilde{u}_L^i,\ \tilde{d}_L^i$	$u_L^i,\ d_L^i$	$-$	3	2	$1/6$	$1/3$	0
$(\hat{u}^c)^i$	$\tilde{u}_R^{*i}$	$\bar{u}_R^i$	$-$	$\bar{3}$	1	$-2/3$	$-1/3$	0
$(\hat{d}^c)^i$	$\tilde{d}_R^{*i}$	$\bar{d}_R^i$	$-$	$\bar{3}$	1	$1/3$	$-1/3$	0
$\hat{l}^i$	$\tilde{\nu}_L^i,\ \tilde{e}_L^i$	$\nu_L^i,\ e_L^i$	$-$	1	2	$-1/2$	0	1
$(\hat{e}^c)^i$	$\tilde{e}_R^{*i}$	$\bar{e}_R^i$	$-$	1	1	1	0	-1
$\hat{H}_u$	$H_u^+,\ H_u^0$	$\tilde{H}_u^+,\ \tilde{H}_u^0$	$-$	1	2	$1/2$	0	0
$\hat{H}_d$	$H_d^0,\ H_d^-$	$\tilde{H}_d^0,\ \tilde{H}_d^-$	$-$	1	2	$-1/2$	0	0
$\hat{G}^A$	$-$	$\tilde{g}$	g	8	1	0	0	0
$\hat{W}^a$	$-$	$\tilde{W}^{\pm},\ \tilde{W}^0$	$W^{\pm},\ W^0$	1	3	0	0	0
$\hat{B}$	$-$	$\tilde{B}^0$	B^0	1	1	0	0	0

Table 1.4: Chiral and gauge superfields of the minimal supersymmetric standard model. The quantum numbers of the fields under the gauge groups are listed. Quarks, squarks, leptons, and sleptons come in three generations as denoted by the index i.

Supersymmetry relates masses and couplings of particles with different spins, combining them into chiral superfields. Within a given superfield, the particles are described by the same quantum numbers and have equal masses, but their spins differ by a half. It is obvious that supersymmetry must be broken at some scale in the real world, since we do not observe any equal-mass partners of the standard model particles.

The MSSM is based on the same $SU(3)_c \times SU(2)_L \times U(1)_Y$ gauge group as the standard model. The spin zero partners of quarks and leptons are the squarks and sleptons. The spin $1/2$ partner of the Higgs is the higgsino. Finally, the spin $1/2$ partners of the

gauge bosons, G^A_μ, W^a_μ, and B_μ, are the gluinos, winos, and bino, respectively. A second Higgs doublet with its supersymmetric partner is needed to cancel the $SU(2)^2_L \times U(1)_Y$ and $U(1)^3_Y$ gauge anomalies and to give masses to both the up- and down-type quarks. The complete particle content of the MSSM, including both the chiral and gauge superfields, is presented in Table 1.4. After electroweak symmetry breaking, the bino and neutral wino mix to give a zino ($\tilde{Z}^0$) and photino ($\tilde{\gamma}$).

The Lagrangian of a supersymmetric theory with supersymmetry broken below some scale can be written as

$$\mathcal{L} = \mathcal{L}_{\rm kin} + \mathcal{L}_{\rm int} + \mathcal{L}_W + \mathcal{L}_{\rm SB} \; . \tag{1.37}$$

Assuming the theory is described by the superpotential

$$W = \frac{1}{2} m^{ij} \hat{\Phi}_i \hat{\Phi}_j + \frac{1}{6} \lambda^{ijk} \hat{\Phi}_i \hat{\Phi}_j \hat{\Phi}_k \; , \tag{1.38}$$

where the chiral superfields $\hat{\Phi}_i$ have scalar components ϕ_i and fermion components ψ_i, the terms in the Lagrangian (1.37) have the following form:

$$\mathcal{L}_{\rm kin} = D^\mu \phi^{*i} D_\mu \phi_i + i\, \bar{\psi}^i\, \bar{\sigma}^\mu D_\mu \psi_i - \frac{1}{4} F^a_{\mu\nu} F^{\mu\nu a} + i\, \bar{\lambda}^a \bar{\sigma}^\mu D_\mu \lambda^a \; , \tag{1.39}$$

$$\mathcal{L}_{\rm int} = -\sqrt{2} g_a \left(\phi^* T^a \psi\right) \lambda^a - \sqrt{2} g_a \bar{\lambda}^a \left(\bar{\psi} T^a \phi\right) , \tag{1.40}$$

$$\begin{aligned} \mathcal{L}_W = & -m^*_{ik} m^{kj} \phi^{*i} \phi_j - \frac{1}{2} m^{in} \lambda^*_{jkn} \phi_i \phi^{*j} \phi^{*k} - \frac{1}{2} m^*_{in} \lambda^{jkn} \phi^{*i} \phi_j \phi_k \\ & - \frac{1}{4} \lambda^{ijn} \lambda^*_{kln} \phi_i \phi_j \phi^{*k} \phi^{*l} - \frac{1}{2} g_a^2 \left(\phi^* T^a \phi\right)^2 \\ & - \frac{1}{2} m^{ij} \psi_i \psi_j - \frac{1}{2} m^*_{ij} \bar{\psi}^i \bar{\psi}^j - \frac{1}{2} \lambda^{ijk} \phi_i \psi_j \psi_k - \frac{1}{2} \lambda^*_{ijk} \phi^{*i} \bar{\psi}^j \bar{\psi}^k \; , \end{aligned} \tag{1.41}$$

$$\mathcal{L}_{\rm SB} = -\left(\frac{1}{2} m_a \lambda^a \lambda^a + \frac{1}{6} a^{ijk} \phi_i \phi_j \phi_k + \frac{1}{2} b^{ij} \phi_i \phi_j + t^i \phi_i\right) + \text{c.c.} - (m^2)^i_j \phi^{j*} \phi_i \; . \tag{1.42}$$

In the expressions above the sums extend over all scalars ϕ_i, chiral fermions ψ_i, gauginos λ^a and vector bosons A^a_μ in the spectrum of the theory, and D_μ is the covariant derivative. The first part of the Lagrangian (1.39) consists of kinetic terms for all the fields and includes the Yang-Mills term for the gauge fields. The second piece (1.40) describes the interactions between the scalar and fermion components of the chiral superfields and the gauginos. There

are no adjustable parameters in those two parts of the Lagrangian. The third part (1.41) contains the supersymmetric contribution to the scalar potential and Yukawa interactions between the scalar and fermion components of the chiral superfields. The last part (1.42) is responsible for supersymmetry breaking and consists of the gaugino mass terms, trilinear scalar interactions, scalar mass terms, as well as terms linear and bilinear in the scalar fields.

The minimal superpotential for the MSSM is

$$W_{\rm MSSM} = \epsilon_{ab}\left[y_u^{ij}\hat{Q}_i^a(\hat{u}^c)_j\hat{H}_u^b + y_d^{ij}\hat{Q}_i^b(\hat{d}^c)_j\hat{H}_d^a + y_e^{ij}\hat{L}_i^b(\hat{e}^c)_j\hat{H}_d^a - \mu\hat{H}_u^a\hat{H}_d^b\right] . \quad (1.43)$$

With this superpotential, it is straightforward to write down the full supersymmetric sector of the MSSM Lagrangian using the relations (1.38)−(1.41). In order for the MSSM to solve the hierarchy problem, we expect the characteristic mass scale of the supersymmetry breaking sector to be on the order of $m_{\rm soft} \approx 1\ {\rm TeV}$. Therefore, it is reasonable to expect that masses of the few lightest sparticles are approximately at the TeV scale. A more detailed review of the MSSM is given in Ref. [44].

The superpotential (1.43) is sufficient for the MSSM to be a phenomenologically viable model. However, apart from the terms included in (1.43), it is possible to construct four other Lagrangian terms which are also gauge invariant and consistent with supersymmetry:

$$\mathcal{L}_{\rm RP} = \frac{1}{2}\lambda_1^{ijk}\hat{L}_i\hat{L}_j\hat{e}_k^c + \lambda_2^{ijk}\hat{L}_i\hat{Q}_j\hat{d}_k^c + \frac{1}{2}\lambda_3^{ijk}\hat{u}_i^c\hat{d}_j^c\hat{d}_k^c + \mu'^i\hat{L}_i\hat{H}_u\ . \quad (1.44)$$

Those operators violate baryon and lepton number, and result in proton decay at a rate

$$\Gamma(p \to e^+\,\pi^0) \approx |\lambda_2^{11i}\lambda_3^{11i}|^2\frac{m_p^5}{m_{\tilde{d}_i}^4}\ . \quad (1.45)$$

The experimental limit [25] gives

$$|\lambda_2^{11i}\lambda_3^{11i}| < 10^{-25}\left(\frac{m_{\tilde{d}_i}}{1\ {\rm TeV}}\right)^2, \quad (1.46)$$

which requires a huge fine-tuning of the couplings.

One possible way to avoid this naturalness problem is to impose a discrete symmetry called R-parity,

$$R \equiv (-1)^{3(B-L)+2s} \,, \tag{1.47}$$

where s is the spin of the particle. This symmetry forbids all the Lagrangian terms in (1.44). Of course, this was not necessary in the standard model, where gauge invariance itself did not allow for interactions violating baryon or lepton number. Apart from forbidding proton decay, R-parity plays another extremely important role in the MSSM: it assures the stability of the lightest supersymmetric particle, making it a good dark matter candidate.

However, even after imposing R-parity, there still exist nonrenormalizable operators in the MSSM which mediate proton decay:

$$\frac{\hat{Q}\hat{Q}\hat{Q}\hat{L}}{\Lambda} \quad \text{and} \quad \frac{\hat{u}^c\hat{u}^c\hat{d}^c\hat{e}^c}{\Lambda} \,, \tag{1.48}$$

suppressed only by the supersymmetry breaking mass scale compared to ordinary dimension-five operators. Due to tightening experimental bounds on proton decay, a mechanism for suppressing those nonrenormalizable operators is needed as well.

In Chapter 4 we propose an extension of the MSSM with gauged baryon and lepton numbers, which naturally solves all the problems related to proton decay without imposing any *ad hoc* discrete symmetry.

Chapter 2

Simplified models with baryon number violation but no proton decay

We enumerate the simplest models that have baryon number violation at the classical level but do not give rise to proton decay. These models have scalar fields in two representations of $SU(3) \times SU(2) \times U(1)$ and violate baryon number by two units. Some of the models give rise to $n\bar{n}$ (neutron-antineutron) oscillations, while some also violate lepton number by two units. We discuss the range of scalar masses for which $n\bar{n}$ oscillations are measurable in the next generation of experiments. We give a brief overview of the phenomenology of these models and then focus on one of them for a more quantitative discussion of $n\bar{n}$ oscillations, the generation of the cosmological baryon number, the electric dipole moment of the neutron, and neutral kaon mixing.

The contents of this chapter were written in collaboration with Mark Wise and Jonathan Arnold, and have been published in Ref. [1].

2.1 Introduction

The standard model has nonperturbative violation of baryon number (B). This source of baryon number nonconservation also violates lepton number (L); however, it conserves baryon number minus lepton number ($B - L$). The violation of baryon number by nonperturbative weak interactions is important at high temperatures in the early universe, but it has negligible impact on laboratory experiments that search for baryon number violation and thus we neglect it in this paper. If we add massive right-handed neutrinos that have a

Majorana mass term and Yukawa couple to the standard model left-handed neutrinos, then lepton number is violated by two units, $|\Delta L| = 2$, at tree level in the standard model.

Motivated by grand unified theories (GUT), there has been an ongoing search for proton decay (and bound neutron decay). The limits on possible decay modes are very strong. For example, the lower limit on the partial mean lifetime for the mode $p \to e^+\pi^0$ is 8.2×10^{33} yrs [25]. All proton decays violate baryon number by one unit and lepton number by an odd number of units. See Ref. [28] for a review of proton decay in extensions of the standard model.

There are models where baryon number is violated but proton (and bound neutron) decay does not occur. This paper is devoted to finding the simplest models of this type and discussing some of their phenomenology. We include all renormalizable interactions allowed by the $SU(3) \times SU(2) \times U(1)$ gauge symmetry. In addition to standard model fields, these models have scalar fields $X_{1,2}$ that couple to quark bilinear terms or lepton bilinear terms. Baryon number violation occurs either through trilinear scalar interactions of the type (i) $X_2 X_1 X_1$ or quartic scalar terms of the type (ii) $X_2 X_1 X_1 X_1$. The cubic scalar interaction in (i) is similar in structure to renormalizable terms in the superpotential that give rise to baryon number violation in supersymmetric extensions of the standard model. However, in our case the operator is dimension three and is in the scalar potential. Without adding right-handed neutrinos to the standard model spectrum there are four models of type (i) where each of the X's couples to quark bilinears and has baryon number $-2/3$. Hence, in this case the X's are either color $\mathbf{3}$ or $\bar{\mathbf{6}}$. There are also five models of type (ii) where X_1 is a color $\mathbf{3}$ or $\bar{\mathbf{6}}$ with baryon number $-2/3$ that couples to quark bilinears, and X_2 is a color singlet with lepton number -2 that couples to lepton bilinears.

We analyze one of the models in more detail. In that model the $SU(3) \times SU(2) \times U(1)$ quantum numbers of the new colored scalars are $X_1 = (\bar{6}, 1, -1/3)$ and $X_2 = (\bar{6}, 1, 2/3)$. The $n\bar{n}$ oscillation frequency is calculated using the vacuum insertion approximation for the required hadronic matrix element and lattice QCD results. For dimensionless coupling constants equal to unity and all mass parameters equal, the present absence of observed $n\bar{n}$ oscillations provides a lower limit on the scalar masses of around 500 TeV. If we consider the limit $M_1 \ll M_2$ then for $M_1 = 5$ TeV, the next generation of $n\bar{n}$ oscillation

experiments will be sensitive to M_2 masses at the GUT scale.

There are three models that have $n\bar{n}$ mixing at tree level without proton decay. In these models, constraints on flavor changing neutral currents and the electric dipole moment (edm) of the neutron require some very small dimensionless coupling constants if we are to have both observable $n\bar{n}$ oscillations and one of the scalar masses approaching the GUT scale.

In the next section we enumerate the models and discuss their basic features. The phenomenology of one of the models is discussed in more detail in Section 2.3. Some concluding remarks are given in Section 2.4.

2.2 The models

We are looking for the simplest models which violate baryon number but do not induce proton decay. We do not impose any global symmetries. Hence, all local renormalizable interactions permitted by Lorentz and gauge invariance are assumed to be present. We begin by considering renormalizable scalar couplings with all possible standard model fermion bilinears. A similar philosophy can be used to construct models involving proton decay [45] or baryon number violating interactions in general [46, 47]. We first eliminate any scalars which produce proton decay via tree-level scalar exchange as in Fig. 2.1. In particular, this eliminates the scalars with $SU(3) \times SU(2) \times U(1)$ quantum numbers $(3, 1, -1/3)$, $(3, 3, -1/3)$, and $(3, 1, -4/3)$. Note that in the case of $(3, 1, -4/3)$ we need an additional W-boson exchange to get proton decay (Fig. 2.2), since the Yukawa coupling to right-handed charge 2/3 quarks is antisymmetric (for a detailed discussion see Ref. [48]). The remaining possible scalar representations and Yukawa couplings are listed in Table 2.1. We have assumed there are no right-handed neutrinos (ν_R) in the theory.

None of these scalars induce baryon number violation on their own, so we consider minimal models with the requirement that only two unique sets of scalar quantum numbers from Table 2.1 are included, though a given set of quantum numbers may come with multiple scalars.

Baryon number violation will arise from terms in the scalar potential, so we need to

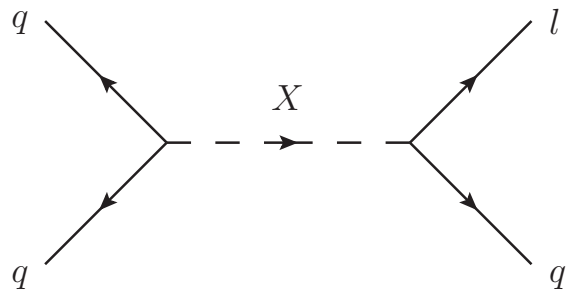

Figure 2.1: $\Delta B = 1$ and $\Delta L = 1$ scalar exchange.

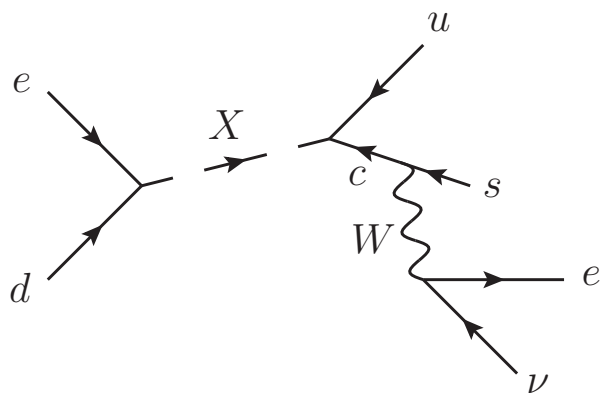

Figure 2.2: Feynman diagram that contributes to tree level $p \rightarrow K^+e^+e^-\bar{\nu}$ from $(3, 1, -4/3)$ scalar exchange.

take into account just the models whose scalar quantum numbers are compatible in the sense that they allow scalar interactions that violate baryon number. For scalars coupling to standard model fermion bilinears, there are three types of scalar interactions which may violate baryon number: 3-scalar $X_1X_1X_2$, 4-scalar $X_1X_1X_1X_2$, and 3-scalar with a Higgs $X_1X_1X_1H$ or $X_1X_1X_2H$, where the Higgs gets a vacuum expectation value (Fig. 2.3).

Actually, the simplest possible model violating baryon number through the interaction $X_1X_1X_1H$ includes just one new scalar $(\bar{3}, 2, -1/6)$, but it gives proton decay via $p \rightarrow \pi^+\pi^+e^-\nu\nu$ (Fig. 2.4). Note that a similar diagram with $\langle H \rangle$ replaced by X_2 allows us to ignore scalars with the same electroweak quantum numbers as the Higgs and coupling to $\bar{Q}u$ and $\bar{Q}d$, $X_2 = (1, 2, 1/2)$ and $(8, 2, 1/2)$, as these will produce tree-level proton decay as well. The other two baryon number violating models with an interaction term $X_1X_1X_2H$

Operator	$SU(3) \times SU(2) \times U(1)$ representation of X	B	L
XQQ, Xud	$(\bar{6}, 1, -1/3)\,, (3, 1, -1/3)_{\rm PD}$	$-2/3$	0
XQQ	$(\bar{6}, 3, -1/3)\,, (3, 3, -1/3)_{\rm PD}$	$-2/3$	0
Xdd	$(3, 1, 2/3)$, $(\bar{6}, 1, 2/3)$	$-2/3$	0
Xuu	$(\bar{6}, 1, -4/3)\,, (3, 1, -4/3)_{\rm PD}$	$-2/3$	0
$X\bar{Q}\bar{L}$	$(3, 1, -1/3)_{\rm PD}\,, (3, 3, -1/3)_{\rm PD}$	$1/3$	1
$X\bar{u}\bar{e}$	$(3, 1, -1/3)_{\rm PD}$	$1/3$	1
$X\bar{d}\bar{e}$	$(3, 1, -4/3)_{\rm PD}$	$1/3$	1
$X\bar{Q}e, XL\bar{u}$	$(3, 2, 7/6)$	$1/3$	-1
$X\bar{L}d$	$(\bar{3}, 2, -1/6)_{\rm PD}$	$-1/3$	1
XLL	$(1, 1, 1)$, $(1, 3, 1)$	0	-2
Xee	$(1, 1, 2)$	0	-2

Table 2.1: Possible interaction terms between the scalars and fermion bilinears along with the corresponding quantum numbers and B and L charges of the X field. Representations labeled with the subscript "PD" allow for proton decay via either tree-level scalar exchange (Fig. 2.1) or 3-scalar interactions involving the Higgs vacuum expectation value (Fig. 2.4).

are $X_1^* = (3, 1, -1/3)$, $X_2 = (\bar{3}, 2, -7/6)$ and $X_1 = (3, 1, -1/3)$, $X_2^* = (\bar{3}, 2, -1/6)$. As argued earlier, such quantum numbers for X_1 also induce tree-level proton decay, so we disregard them.

We now consider models with a 3-scalar interaction $X_1 X_1 X_2$. A straightforward analysis shows that there are only four models which generate baryon number violation via a 3-scalar interaction without proton decay. We enumerate them and give the corresponding Lagrangians below. All of these models give rise to processes with $\Delta B = 2$ and $\Delta L = 0$, but only the first three models contribute to $n\bar{n}$ oscillations at tree level due to the symmetry

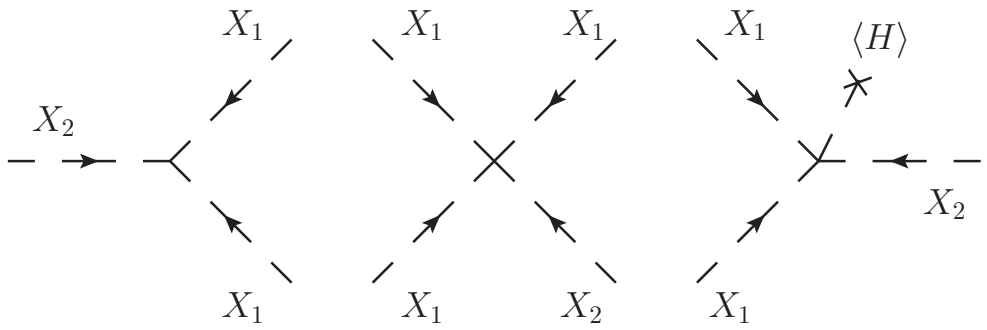

Figure 2.3: Scalar interactions which may generate baryon number violation.

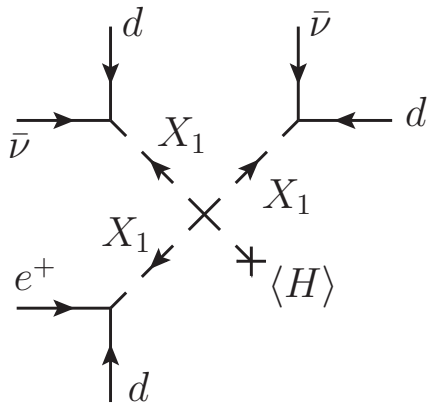

Figure 2.4: Interaction which leads to proton decay, $p \to \pi^+\pi^+e^-\nu\nu$, for $X_1 = (\bar{3}, 2, -1/6)$.

properties of the Yukawas. Note that a choice of normalization for the sextet given by

$$(X^{\alpha\beta}) = \begin{pmatrix} \tilde{X}^{11} & \tilde{X}^{12}/\sqrt{2} & \tilde{X}^{13}/\sqrt{2} \\ \tilde{X}^{12}/\sqrt{2} & \tilde{X}^{22} & \tilde{X}^{23}/\sqrt{2} \\ \tilde{X}^{13}/\sqrt{2} & \tilde{X}^{23}/\sqrt{2} & \tilde{X}^{33} \end{pmatrix} \tag{2.1}$$

leads to canonically normalized kinetic terms for the elements $\tilde{X}^{\alpha\beta}$ and the usual form of the scalar propagator with symmetrized color indices. Unless otherwise stated, we will be using two-component spinor notation. Parentheses indicate contraction of two-component spinor indices to form a Lorentz singlet.

Model 1. $X_1 = (\bar{6}, 1, -1/3),\ X_2 = (\bar{6}, 1, 2/3)$,

$$\begin{aligned}\mathcal{L} \;=\; & -\, g_1^{ab} X_1^{\alpha\beta} \left(Q_{L\alpha}^a \epsilon\, Q_{L\beta}^b\right) - g_2^{ab} X_2^{\alpha\beta} (d_{R\alpha}^a d_{R\beta}^b) -\; g_1'^{ab} X_1^{\alpha\beta} (u_{R\alpha}^a d_{R\beta}^b) \\ & + \lambda\, X_1^{\alpha\alpha'} X_1^{\beta\beta'} X_2^{\gamma\gamma'} \epsilon_{\alpha\beta\gamma} \epsilon_{\alpha'\beta'\gamma'}\ . \end{aligned} \tag{2.2}$$

By virtue of the symmetric color structure of the $\bar{\mathbf{6}}$ representation and the antisymmetric weak structure of the QQ bilinear in the first term, g_1 must be antisymmetric in flavor. However, this antisymmetry is not retained upon rotation into the mass eigenstate basis. Similarly, g_2 must be symmetric because of the symmetric color structure in the second term. In this case, the symmetry character of g_2 will be retained upon rotation into the mass eigenstate basis because it involves quarks of the same charge. Therefore, the interaction involving the Yukawa coupling g_2 gives rise to (and is thus constrained by) K^0-$\bar{K}^0$ mixing through tree-level X_2 exchange. The coupling g_1' has no particular flavor symmetry.

Model 2. $X_1 = (\bar{6}, 3, -1/3),\ X_2 = (\bar{6}, 1, 2/3)$,

$$\begin{aligned}\mathcal{L} \;=\; & -\, g_1^{ab} X_1^{\alpha\beta A} (Q_{L\alpha}^a \epsilon\, \tau^A\, Q_{L\beta}^b) - g_2^{ab} X_2^{\alpha\beta} (d_{R\alpha}^a d_{R\beta}^b) \\ & + \lambda\, X_1^{\alpha\alpha' A} X_1^{\beta\beta' A} X_2^{\gamma\gamma'} \epsilon_{\alpha\beta\gamma} \epsilon_{\alpha'\beta'\gamma'}\ . \end{aligned} \tag{2.3}$$

Here the matrix $\epsilon\,\tau^A$ is symmetric. Because the first and second terms have symmetric color structures, g_1 and g_2 must be symmetric in flavor. The weak triplet X_1 has components which introduce both K^0-$\bar{K}^0$ and D^0-$\bar{D}^0$ mixing. As in model 1, the interaction involving g_2 will introduce K^0-$\bar{K}^0$ mixing via X_2 exchange.

Model 3. $X_1 = (\bar{6}, 1, 2/3),\ X_2 = (\bar{6}, 1, -4/3)$,

$$\mathcal{L} \;=\; -\, g_1^{ab} X_1^{\alpha\beta} (d_{R\alpha}^a d_{R\beta}^b) -\; g_2^{ab} X_2^{\alpha\beta} (u_{R\alpha}^a u_{R\beta}^b) + \lambda\, X_1^{\alpha\alpha'} X_1^{\beta\beta'} X_2^{\gamma\gamma'} \epsilon_{\alpha\beta\gamma} \epsilon_{\alpha'\beta'\gamma'}\ . \tag{2.4}$$

Both terms have symmetric color structures and no weak structure, so g_1 and g_2 must be symmetric in flavor. In this model, the interactions involving g_1 and g_2 each have the po-

tential to introduce neutral meson-antimeson mixing. For example, the g_1 interaction will induce K^0-$\bar{K}^0$ mixing while g_2 will induce D^0-$\bar{D}^0$ mixing.

Model 4. $X_1 = (3, 1, 2/3),\ X_2 = (\bar{6}, 1, -4/3)$,

$$\mathcal{L} \;=\; -\, g_1^{ab} X_{1\alpha} \left(d^a_{R\beta}\, d^b_{R\gamma}\right) \epsilon^{\alpha\beta\gamma} - g_2^{ab} X_2^{\alpha\beta} (u^a_{R\alpha} u^b_{R\beta}) + \lambda\, X_{1\alpha} X_{1\beta} X_2^{\alpha\beta}\,. \tag{2.5}$$

Because of the antisymmetric color structure in the first term, g_1 must be antisymmetric in flavor, which prevents it from introducing meson-antimeson mixing. The antisymmetric structure of g_1 also prevents the existence of six-quark operators involving all first-generation quarks, and thus prevents $n\bar{n}$ oscillations. As in previous models, g_2 is symmetric and so we will get D^0-$\bar{D}^0$ mixing as in model 3. Although this model does not have $n\bar{n}$ oscillations, there are still baryon number violating processes which would constrain this model – for example, the process $pp \to K^+K^+$. This has been searched using the Super-Kamiokande detector looking for the nucleus decay $^{16}O \to\ ^{14}CK^+K^+$ [49]. Had we included ν_R, model 4 would have been excluded by tree-level scalar exchange.

Now, a similar line of reasoning applies to the case where we have a quartic scalar interaction term $X_1X_1X_1X_2$. The only models violating baryon number which do not generate proton decay (or bound neutron decay) are discussed briefly below. These last five models have dinucleon decay to leptons, but do not contribute to tree-level $n\bar{n}$ oscillations by virtue of their coupling to leptons.

Model 5. $X_1 = (\bar{6}, 1, -1/3),\ X_2 = (1, 1, 1)$,

$$\begin{aligned}\mathcal{L} \;=\; & -\, g_1^{ab} X_1^{\alpha\beta} \left(Q^a_{L\alpha} \epsilon\, Q^b_{L\beta}\right) - g_2^{ab} X_2 (L^a_L \epsilon L^b_L) - \; g_1'^{ab} X_1^{\alpha\beta} (u^a_{R\alpha} d^b_{R\beta}) \\ & + \lambda\, X_1^{\alpha\alpha'} X_1^{\beta\beta'} X_1^{\gamma\gamma'} X_2\, \epsilon_{\alpha\beta\gamma} \epsilon_{\alpha'\beta'\gamma'}\,. \end{aligned} \tag{2.6}$$

Similar arguments to those for the previous models tell us that g_1 and g_2 must be antisymmetric in flavor.

Model 6. $X_1 = (\bar{6}, 3, -1/3),\ X_2 = (1, 1, 1)$,

$$\begin{aligned}\mathcal{L} \;=\; & - g_1^{ab} X_1^{\alpha\beta A} (Q^a_{L\alpha} \epsilon\, \tau^A\, Q^b_{L\beta}) - \; g_2^{ab} X_2 (L^a_L \epsilon L^b_L) \\ & + \lambda\, X_1^{\alpha\alpha' A} X_1^{\beta\beta' B} X_1^{\gamma\gamma' C} X_2\, \epsilon^{ABC} \epsilon_{\alpha\beta\gamma} \epsilon_{\alpha'\beta'\gamma'}\ . \end{aligned} \tag{2.7}$$

In comparison with model 2, we see that g_1 is symmetric in flavor, while g_2 is antisymmetric.

Model 7. $X_1 = (\bar{6}, 3, -1/3),\ X_2 = (1, 3, 1)$,

$$\begin{aligned}\mathcal{L} \;=\; & - g_1^{ab} X_1^{\alpha\beta A} (Q^a_{L\alpha} \epsilon\, \tau^A\, Q^b_{L\beta}) - g_2^{ab} X_2^A (L^a_L \epsilon \tau^A L^b_L) \\ & + \lambda\, X_1^{\alpha\alpha' A} X_1^{\beta\beta' B} X_1^{\gamma\gamma' C} X_2^D\, \epsilon_{\alpha\beta\gamma} \epsilon_{\alpha'\beta'\gamma'}\, (\delta^{AB}\delta^{CD} + \delta^{AC}\delta^{BD} + \delta^{AD}\delta^{BC})\ . \end{aligned} \tag{2.8}$$

Once again, as in model 2, we have a symmetric g_1, thus the coupling g_2 must be symmetric in flavor as well.

Model 8. $X_1 = (\bar{6}, 1, 2/3),\ X_2 = (1, 1, -2)$,

$$\mathcal{L} \;=\; - g_1^{ab} X_1^{\alpha\beta} (d^a_{R\alpha} d^b_{R\beta}) - g_2^{ab} X_2 (e^a_R e^b_R) + \; \lambda\, X_1^{\alpha\alpha'} X_1^{\beta\beta'} X_1^{\gamma\gamma'} X_2\, \epsilon_{\alpha\beta\gamma}\, \epsilon_{\alpha'\beta'\gamma'}\ . \tag{2.9}$$

As in model 1, g_1 must be symmetric. The coupling g_2 must also be symmetric in flavor.

Model 9. $X_1 = (3, 1, 2/3),\ X_2 = (1, 1, -2)$,

$$\mathcal{L} \;=\; - g_1^{ab} X_{1\alpha} (d^a_{R\beta} d^b_{R\gamma}) \epsilon^{\alpha\beta\gamma} - g_2^{ab} X_2 (e^a_R e^b_R) + \; \lambda\, X_{1\alpha} X_{1\beta} X_{1\gamma} X_2\, \epsilon^{\alpha\beta\gamma}\ . \tag{2.10}$$

By comparison with model 4, we see that g_1 must be antisymmetric in flavor. The coupling g_2 is symmetric. Note that the antisymmetric color structure of the scalar interaction requires the existence of at least three different kinds of X_1 scalars for this coupling to exist. Including ν_R would eliminate model 9 for the same reason as model 4.

2.3 Phenomenology of model 1

In this section we present a detailed analysis of model 1. The corresponding calculations for the other models can be performed in a similar manner. Our work is partly motivated by the recently proposed $n\bar{n}$ oscillation experiment with increased sensitivity [33]. In addition to $n\bar{n}$ oscillations, we also analyze the cosmological baryon asymmetry generation in model 1 as well as flavor and electric dipole moment constraints. A brief comment on LHC phenomenology is made.

2.3.1 Neutron-antineutron oscillations

The topic of $n\bar{n}$ oscillations has been explored in the literature in various contexts. For some of the early works on the subject, see Refs. [50, 51, 52, 53]. Recently, a preliminary study of the required hadronic matrix elements using lattice QCD has been carried out [54]. Ref. [55] claims that a signal of $n\bar{n}$ oscillations has been observed.

The scalar content of model 1 we are considering is similar to the content of a unified model explored in Ref. [56]. The transition matrix element

$$\Delta m = \langle \bar{n}|\mathcal{H}_{\rm eff}|n\rangle \ , \tag{2.11}$$

leads to a transition probability for a neutron at rest to change into an antineutron after time t equal to $P_{n\to\bar{n}}(t) = \sin^2(|\Delta m|\, t)$.

Neglecting the coupling g_1 in the Lagrangian (2.2) (for simplicity) the effective $|\Delta B| = 2$ Hamiltonian that causes $n\bar{n}$ oscillations is (see Appendix A)

$$\begin{aligned}\mathcal{H}_{\rm eff} \ = \ & -\frac{(g_1'^{11})^2 g_2^{11}\lambda}{4M_1^4 M_2^2} d^{\dot{\alpha}}_{Ri} d^{\dot{\beta}}_{Ri'} u^{\dot{\gamma}}_{Rj} d^{\dot{\delta}}_{Rj'} u^{\dot{\lambda}}_{Rk} d^{\dot{\chi}}_{Rk'} \epsilon_{\dot{\alpha}\dot{\beta}}\epsilon_{\dot{\gamma}\dot{\delta}}\epsilon_{\dot{\lambda}\dot{\chi}} \\ & \times\Big(\epsilon_{ijk}\epsilon_{i'j'k'} + \epsilon_{i'jk}\epsilon_{ij'k'} + \epsilon_{ij'k}\epsilon_{i'jk'} + \epsilon_{ijk'}\epsilon_{i'j'k}\Big) + \text{h.c.} \ ,\end{aligned} \tag{2.12}$$

where Latin indices are color and Greek indices are spinor. It arises from the tree-level diagram in Fig. 2.5 (see, for example Ref. [57]). We have rotated the couplings g_1' and g_2 to the quark mass eigenstate basis and adopted a phase convention where λ is real and

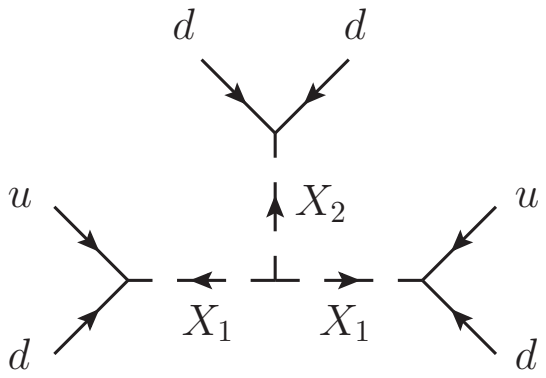

Figure 2.5: Interaction which leads to neutron-antineutron oscillations.

positive. We estimate Δm using the vacuum insertion approximation [58]. This relates the required $n\bar{n}$ six-quark matrix element to a matrix element from the neutron to the vacuum of a three-quark operator. The later matrix element is relevant for proton decay and has been determined using lattice QCD methods. The general form of the required hadronic matrix elements is

$$\langle 0|d^{\dot{\alpha}}_{Ri} d^{\dot{\beta}}_{Rj} u^{\dot{\gamma}}_{Rk}|n(p,s)\rangle = -\frac{1}{18}\beta\,\epsilon_{ijk}\left(\epsilon^{\dot{\alpha}\dot{\gamma}} u^{\dot{\beta}}_R(p,s) + \epsilon^{\dot{\beta}\dot{\gamma}} u^{\dot{\alpha}}_R(p,s)\right) . \tag{2.13}$$

Here u_R is the right-handed neutron two-component spinor and the Dirac equation was used to remove the term proportional to the left-handed neutron spinor. The constant β was determined using lattice methods in Ref. [59] to have the value $\beta \simeq 0.01\ \mathrm{GeV}^3$. In the vacuum insertion approximation to Eq. (2.11) we find (see Appendix B)

$$|\Delta m| = 2\lambda\beta^2 \frac{|(g_1'^{11})^2 g_2^{11}|}{3M_1^4 M_2^2} . \tag{2.14}$$

We note that an analogous calculation using the MIT bag model was performed in Ref. [60] and yields a similar result. The current experimental limit on Δm is [30]

$$|\Delta m| < 2 \times 10^{-33}\ \mathrm{GeV} . \tag{2.15}$$

For scalars of equal mass, $M_1 = M_2 \equiv M$, and the values of the couplings $g_1'^{11} = g_2^{11} = 1$,

$\lambda = M$, one obtains

$$M \gtrsim 500 \text{ TeV} . \tag{2.16}$$

If, instead, the masses form a hierarchy, the effect on $n\bar{n}$ oscillations is maximized if we choose $M_2 > M_1$. Assuming $M_1 = 5$ TeV (above the current LHC reach) and $\lambda = M_2$, this yields

$$M_2 \gtrsim 5 \times 10^{13} \text{ GeV} . \tag{2.17}$$

Note that $\lambda = M_2$ is a reasonable value for this coupling, since integrating out M_2 then gives a quartic X_1 interaction term with a coupling on the order of one. Of course, this model does have a hierarchy problem, so having the Higgs scalar and the X_1 light compared with X_2 requires fine-tuning.

Experiments in the future [33] may be able to probe $n\bar{n}$ oscillations with increased sensitivity of $|\Delta m| \simeq 7 \times 10^{-35}$ GeV. If no oscillations are observed, the new limit in the case of equal masses will be

$$M \gtrsim 1000 \text{ TeV} . \tag{2.18}$$

On the other hand, having $M_1 = 5$ TeV would push the mass of the heavier scalar up to the GUT scale, leading to the following constraint on the second scalar mass:

$$M_2 \gtrsim 1.5 \times 10^{15} \text{ GeV} . \tag{2.19}$$

We note, however, that in Section 2.3.2 we show that M_1 on the order of a few TeV is disfavored by the electric dipole moment constraints.

2.3.2 LHC, flavor and electric dipole moment constraints

If the mass of the scalar X_1 is small enough, it can be produced at the LHC through both single and pair production. Detailed analyses have been performed setting limits on the

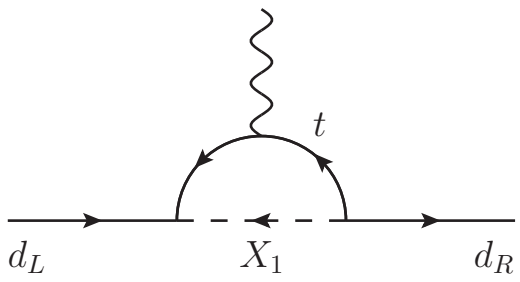

Figure 2.6: Diagram contributing to the electric dipole moment of the down quark.

mass of X_1 from such processes [61, 62, 63]. A recent simulation [61] shows that 100 fb^{-1} of data from the LHC running at 14 TeV center of mass energy can be used to rule out or claim a discovery of X_1 scalars with masses only up to approximately 1 TeV, even when the couplings to quarks are of order one. Our earlier choice of $M_1 = 5$ TeV used to estimate the constraint on M_2 from $n\bar{n}$ oscillations lies well within the allowed mass region.

Some of the most stringent flavor constraints on new scalars come from neutral meson mixing and electric dipole moments. Since in model 1 X_1 couples directly to both left- and right-handed quarks, this means that at one loop the top quark mass can induce the chirality flip necessary to give a light quark edm, putting strong constraints on this model even when X_1 is at the 100 TeV scale. The diagram contributing to the edm of the down quark is given in Fig. 2.6. We find

$$|d_d| \simeq \frac{m_t}{6\pi^2 M_1^2} \log\left(\frac{M_1^2}{m_t^2}\right) \left|\mathrm{Im}[g_1^{31}(g'^{31}_1)^*]\right| \ e \ \mathrm{cm} \,. \tag{2.20}$$

Here we have neglected pieces not logarithmically enhanced. This will give the largest contribution to the neutron edm because of the top quark mass factor. All Yukawa couplings in this section are in the mass eigenstate basis.

Using $SU(6)$ wavefunctions, this can be related to the neutron edm via $d_n = \frac{4}{3}d_d - \frac{1}{3}d_u \simeq \frac{4}{3}d_d$. The present experimental limit is [64]

$$d_n^{\mathrm{exp}} < 2.9 \times 10^{-26} \ e \ \mathrm{cm} \,. \tag{2.21}$$

Assuming $M_1 = 500$ TeV, neutron edm measurements imply the bound $\left|\mathrm{Im}[g_1^{31}(g'^{31}_1)^*]\right| \lesssim$

6×10^{-3}. Furthermore, for observable $n\bar{n}$ oscillation effects, with M_2 being close to the GUT scale, we need $M_1 \approx 5$ TeV. In such a scenario the edm constraint requires $\left|\mathrm{Im}[g_1^{31}(g'^{31}_1)^*]\right| \lesssim 10^{-6}$.

Another important constraint on the parameters of model 1 is provided by K^0-$\bar{K}^0$ mixing. Integrating out X_2 generates an effective Hamiltonian,

$$\mathcal{H}_{\text{eff}} = \frac{g_2^{22}\left(g_2^{11}\right)^*}{M_2^2}(s_{R\alpha}s_{R\beta})(d_R^{*\alpha}d_R^{*\beta}) \;\rightarrow\; \frac{g_2^{22}\left(g_2^{11}\right)^*}{2M_2^2}(\bar{d}_R^{\alpha}\gamma^{\mu}s_{R\alpha})(\bar{d}_R^{\alpha}\gamma_{\mu}s_{R\alpha}), \tag{2.22}$$

where in the second line we have gone from two- to four-component spinor notation. This gives the following constraints on the couplings [65]:

$$\left|\mathrm{Re}\left[g_2^{22}\left(g_2^{11}\right)^*\right]\right| < 1.8 \times 10^{-6}\left(\frac{M_2}{1\text{ TeV}}\right)^2, \tag{2.23}$$

$$\left|\mathrm{Im}\left[g_2^{22}\left(g_2^{11}\right)^*\right]\right| < 6.8 \times 10^{-9}\left(\frac{M_2}{1\text{ TeV}}\right)^2. \tag{2.24}$$

If we set M_2 to 500 TeV, this corresponds to an upper bound on the real and imaginary parts of $g_2^{22}(g_2^{11})^*$ of 0.45 and 1.7×10^{-3}, respectively.

2.3.3 Baryon asymmetry

We now investigate baryon number generation in model 1. B and L violating processes in cosmology have been studied in the literature in great detail (for early works, see Refs. [66, 67]). We treat X_2 as much heavier than X_1, and use two different X_2's to get a CP violating phase in the one-loop diagrams that generate the baryon asymmetry. For this calculation X_1 is treated as stable with baryon number $-2/3$, as each will eventually decay via baryon number conserving processes to two antiquarks. To simplify our discussion, let us consider the case in which the couplings satisfy the hierarchy $\lambda, \tilde{\lambda} \ll g_2, \tilde{g}_2$. The top line of Fig. 2.7 shows the dominant tree-level and one-loop diagrams contributing to the baryon number violating decays of X_2. Rotating the X fields to make the couplings λ and $\tilde{\lambda}$ real, we find

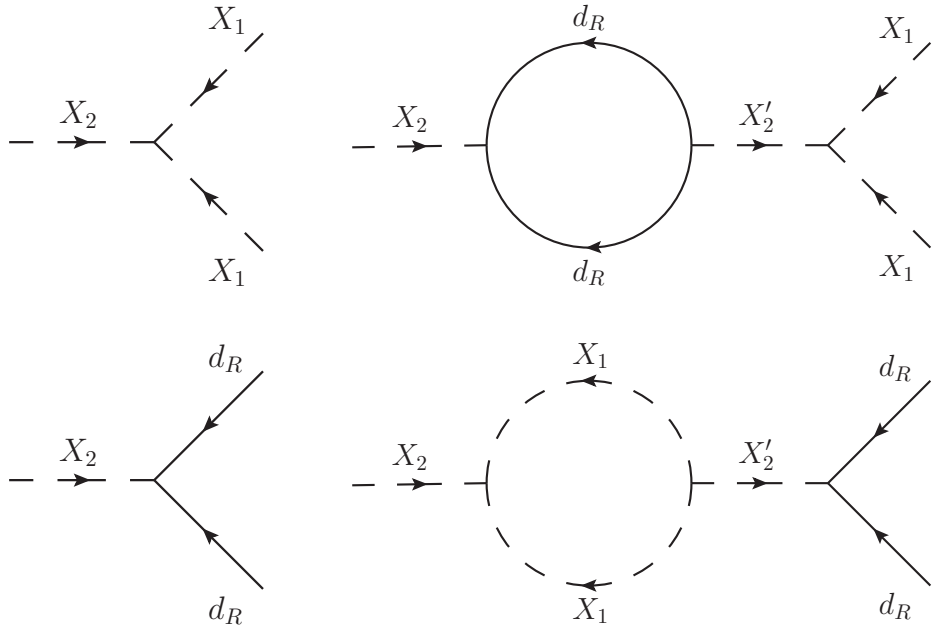

Figure 2.7: Diagrams corresponding to the decay of X_2. The diagrams on top contribute to the $\Delta B = 2$ decays, while the diagrams on bottom contribute to $\Delta B = 0$.

(see Appendix C)

$$\Gamma(X_2 \to \overline{X}_1 \overline{X}_1) = \frac{3\lambda}{8\pi M_2}\left[\lambda - \tilde{\lambda}\frac{M_2^2}{4\pi(M_2^2 - \tilde{M}_2^2)}\mathrm{Im}(\mathrm{Tr}(g_2^\dagger\, \tilde{g}_2))\right],$$
$$\Gamma(\overline{X}_2 \to X_1 X_1) = \frac{3\lambda}{8\pi M_2}\left[\lambda + \tilde{\lambda}\frac{M_2^2}{4\pi(M_2^2 - \tilde{M}_2^2)}\mathrm{Im}(\mathrm{Tr}(g_2^\dagger\, \tilde{g}_2))\right]. \qquad (2.25)$$

The net baryon number produced per $X_2\overline{X}_2$ pair is (see, Table 2.2)

$$\Delta n_B = 2(r - \bar{r}) = \frac{6}{\pi\,\mathrm{Tr}(g_2^\dagger g_2)}\frac{1}{\tilde{M}_2^2 - M_2^2}\,\mathrm{Im}\left[\lambda\,\tilde{\lambda}^*\,\mathrm{Tr}(g_2^\dagger\,\tilde{g}_2)\right], \qquad (2.26)$$

where we have used the fact that CPT invariance guarantees that the total width of X_2 and $\bar{X}_2$ are the same. Given our choice of hierarchy for the couplings, we have approximated the total width as coming from the tree-level decay of X_2 to antiquarks. A similar result in the context of $SO(10)$ models was obtained in Ref. [56].

Even with just one generation of quarks, the CP violating phase cannot be removed from the couplings λ, $\tilde{\lambda}$, g_2, $\tilde{g}_2$ and a baryon asymmetry can be generated at one loop. At

Decay	Br	B_f
$X_2 \to \overline{X}_1\overline{X}_1$	r	$4/3$
$X_2 \to \bar{d}_R\bar{d}_R$	$1-r$	$-2/3$
$\overline{X}_2 \to X_1X_1$	$\bar{r}$	$-4/3$
$\overline{X}_2 \to d_Rd_R$	$1-\bar{r}$	$2/3$

Table 2.2: Branching ratios and final state baryon numbers for the decays of X_2 and $\overline{X}_2$ which contribute to the baryon asymmetry in the coupling hierarchy $\lambda, \tilde{\lambda} \ll g_2, \tilde{g}_2$.

first glance this is surprising since there are four fields (X_2, $\tilde{X}_2$, X_1, and d_R) whose phases can be redefined and four relevant couplings. However, this can be understood by looking at the relevant Lagrangian terms, g_2X_2dd, $\tilde{g}_2\tilde{X}_2dd$, $\lambda X_1X_1X_2$ and $\tilde{\lambda}X_1X_1\tilde{X}_2$. The problem reduces to finding solutions to the following matrix equation:

$$\begin{pmatrix} 2 & 1 & 0 & 0 \\ 2 & 0 & 1 & 0 \\ 0 & 1 & 0 & 2 \\ 0 & 0 & 1 & 2 \end{pmatrix} \begin{pmatrix} \phi_{X_1} \\ \phi_{X_2} \\ \phi_{\tilde{X}_2} \\ \phi_d \end{pmatrix} = \begin{pmatrix} \phi_\lambda \\ \phi_{\tilde{\lambda}} \\ \phi_{g_2} \\ \phi_{\tilde{g}_2} \end{pmatrix} , \tag{2.27}$$

where the phases on the right-hand side are arbitrary. Let us take the difference of the first two equations to remove phases for the couplings λ and $\tilde{\lambda}$, and the difference of the last two equations to remove phases for the couplings $g_2, \tilde{g}_2$. We therefore obtain $\phi_{\tilde{\lambda}_2} - \phi_{\lambda_2} = \phi_{\tilde{X}_2} - \phi_{X_2}$ and $\phi_{\tilde{g}_2} - \phi_{g_2} = \phi_{\tilde{X}_2} - \phi_{X_2}$. Those two equations cannot be simultaneously fulfilled for arbitrary ϕ_λ, $\phi_{\tilde{\lambda}}$, ϕ_{g_2}, $\phi_{\tilde{g}_2}$.

The baryon number generated in the early universe can be calculated from Eq. (2.26) by following the usual steps (see, for example, Ref. [68]). Out of equilibrium decay of X_2 and $\bar{X}_2$ is most plausible if they are very heavy (e.g., $\sim 10^{12}$ GeV). However, to get measurable $n\bar{n}$ oscillation in this case, X_1 would have to be light – a case that is disfavored by neutron edm constraints, since it requires some very small dimensionless couplings.

2.4 Conclusions

We have investigated a set of minimal models which violate baryon number at tree level without inducing proton decay. We have looked in detail at the phenomenological aspects of one of these models (model 1) which can have $n\bar{n}$ oscillations within the reach of future experiments. When all the mass parameters in model 1 have the same value, M, and the magnitudes of the Yukawa couplings $g_1'^{11}$ and g_2^{11} are unity, the present limit on $n\bar{n}$ oscillations implies that M is greater than 500 TeV. For $M = 500$ TeV, the neutron edm and flavor constraints give $\mathrm{Im}[g_1^{31}(g_1'^{31})^*] < 6 \times 10^{-6}$, $\mathrm{Re}[g_2^{22}(g_2^{11})^*] < 0.45$, and $\mathrm{Im}[g_2^{22}(g_2^{11})^*] < 1.7 \times 10^{-3}$, which indicates that some of the Yukawa couplings and/or their phases must be small if $n\bar{n}$ oscillations are to be observed in the next generation of experiments. Of course, even in the standard model some of the Yukawa couplings are small.

There are two other models (model 2 and model 3) that have $n\bar{n}$ oscillations at tree level. Similar conclusions can be drawn for them, although the details are different. In models 2 and 3, exchange of a single X_1 does not give rise to a one-loop edm of the neutron. However, K^0-$\bar{K}^0$ mixing can occur from tree-level X_1 exchange.

Observable $n\bar{n}$ oscillations can occur for $M_2 \gg M_1$ with M_2 at/near the GUT scale. This requires $M_1 \simeq 5$ TeV, and flavor and electric dipole constraints require some very small Yukawa couplings in that case.

Chapter 3

Phenomenology of scalar leptoquarks

We study the simplest renormalizable scalar leptoquark models where the standard model is augmented only by one additional scalar representation of $SU(3) \times SU(2) \times U(1)$. The requirement that there be no proton decay from renormalizable interactions singles out two such models, one of which exhibits an unusual top mass enhancement of the $\mu \to e\gamma$ decay rate. We analyze the phenomenology of the model with the unusual top mass enhancement of loop level chirality changing charged lepton processes in the light of existing and upcoming experiments. Both of the models that do not allow proton decay from renormalizable interactions have dimension-five operators that, even if suppressed by the Planck scale, can give rise to an unacceptably high level of baryon number violation. We discuss symmetries that can forbid these dimension-five operators.

The contents of this chapter were written in collaboration with Mark Wise and Jonathan Arnold, and have been published in Ref. [2].

3.1 Introduction

Currently, the standard model describes most aspects of nature with remarkable precision. If there is new physics at the multi-TeV scale (perhaps associated with the hierarchy puzzle), it is reasonable to expect measurable deviations from the predictions of the standard model in the flavor sector. Among the experiments with very high reach in the mass scale associated with beyond the standard model physics are those that look for flavor violation in the charged lepton sector through measurements of the processes, $\mu \to e\gamma$ [69] and $\mu \to e$

conversion [41, 42], and the search for electric dipole moments of the neutron, proton, and electron. For a recent discussion of the reach provided by the data from K and B meson decays, see, for example, Ref. [70].

Models with scalar leptoquarks can modify the rates for these processes. Simple models of this type have been studied previously in the literature, including their classification and phenomenology [71, 72, 73, 74, 75, 76, 77, 78].

Our approach is to first identify the minimal renormalizable scalar leptoquark models containing one single additional representation of $SU(3) \times SU(2) \times U(1)$ and construct the most general renormalizable model without any additional constraints on the couplings apart from the usual ones, i.e., gauge invariance, Poincaré invariance, and locality. Given the strong experimental constraints on baryon number violating processes like $p \to \pi^0 e^+$, we concentrate only on those scalar leptoquark models which do not have baryon number violation in perturbation theory. Of course, there is baryon number violation through nonperturbative quantum effects, since it is an anomalous symmetry. But this is a very small effect at zero temperature. Only two models fulfill this requirement. One of those two models gives a top mass enhanced $\mu \to e\gamma$ decay rate. We perform an analysis of the phenomenology of this specific model, including the $\mu \to e\gamma$ decay rate, $\mu \to e$ conversion rate, as well as electric dipole moment constraints, focusing mostly on the regions of parameter space where the impact of the top quark mass enhancement is most important. For lepton flavor violating processes at higher energies such as $\tau \to \mu\gamma$, deep inelastic scattering $e + p \to \mu(\tau) + X$, etc., the impact on the phenomenology of the top quark mass enhancement of charged lepton chirality flip is less dramatic, and that is why we focus in this paper on low energy processes involving the lightest charged leptons.

There is also an m_t enhancement of the one-loop contribution to the charged lepton mass matrix. We explore the region of parameter space where this contribution does not necessitate a fine-tuning of parameters.

We also consider the effects of dimension-five operators that can cause baryon number violation. We find that the two models without renormalizable baryon number violation can have such operators, and even if the operators are suppressed by the Planck scale, they may (depending on the values of coupling constants and masses) give rise to an unaccept-

able level of baryon number violation. We discuss a way to forbid these dimension-five operators.

This paper is not a broad survey of the phenomenology of leptoquark models. Rather, we focus on two issues that have not been discussed adequately in the previous literature: first, whether the chirality flip by the top quark mass results in much greater experimental reach in leptoquark mass when one takes into account a naturalness constraint on the lepton mass matrix, and second, the nature of baryon number violation in these models.

3.2 Models

A general classification of renormalizable leptoquark models can be found in Refs. [71, 72]. However, in the spirit of our approach, in which we are interested in models with no proton decay, a more useful list of possible interaction terms between the scalar leptoquarks and fermion bilinears is presented in Ref. [1], where those models that have tree-level proton decay are highlighted. The relevant models are listed in Table 3.1. The only two models fulfilling our requirement are $X = (3, 2, 7/6)$ and $X = (3, 2, 1/6)$.

Model I: $X = (3, 2, 7/6)$.

The Lagrangian for the scalar leptoquark couplings to the fermion bilinears in this model is

$$\mathcal{L} \;=\; -\lambda_u^{ij}\bar{u}_R^i X^T \epsilon L_L^j - \lambda_e^{ij}\bar{e}_R^i X^\dagger Q_L^j + \text{h.c.}\,, \tag{3.1}$$

where

$$X = \begin{pmatrix} V_\alpha \\ Y_\alpha \end{pmatrix}, \quad \epsilon = \begin{pmatrix} 0 & 1 \\ -1 & 0 \end{pmatrix}, \quad L_L = \begin{pmatrix} \nu_L \\ e_L \end{pmatrix}. \tag{3.2}$$

After expanding the $SU(2)$ indices, it takes the form

$$\mathcal{L} \;=\; -\lambda_u^{ij}\bar{u}_{\alpha R}^i (V_\alpha e_L^j - Y_\alpha \nu_L^j) - \lambda_e^{ij}\bar{e}_R^i (V_\alpha^\dagger u_{\alpha L}^j + Y_\alpha^\dagger d_{\alpha L}^j) + \text{h.c.}\,. \tag{3.3}$$

Note that in this model the left-handed charged lepton fields couple to right-handed top

Leptoquark couplings	Diquark couplings	$SU(3) \times SU(2) \times U(1)$ representation of X
$X\bar{Q}e$, $XL\bar{u}$	–	$(3, 2, 7/6)$
$XL\bar{d}$	–	$(3, 2, 1/6)$
$X\bar{Q}\bar{L}$, $X\bar{u}\bar{e}$	XQQ, Xud	$(3, 1, -1/3)_{\rm PD}$
$X\bar{Q}\bar{L}$	XQQ	$(3, 3, -1/3)_{\rm PD}$
$X\bar{d}\,\bar{e}$	Xuu	$(3, 1, -4/3)_{\rm PD}$

Table 3.1: Possible interaction terms between the scalar leptoquarks and fermion bilinears along with the corresponding quantum numbers. Representations labeled with the subscript "PD" allow for proton decay via tree-level scalar exchange.

quarks, and the right-handed charged lepton fields couple to left-handed top quarks. So a charged lepton chirality flip can be caused by the top mass at one loop.

Model II: $X = (3, 2, 1/6)$.

The corresponding Lagrangian is

$$\mathcal{L} \;=\; -\lambda_d^{ij}\bar{d}_R^i X^T \epsilon L_L^j + \text{h.c.}\,, \tag{3.4}$$

where we have used the same notation as in the previous case. Expanding the $SU(2)$ indices yields

$$\mathcal{L} \;=\; -\lambda_d^{ij}\bar{d}_{\alpha R}^i (V_\alpha e_L^j - Y_\alpha \nu_L^j) + \text{h.c.}\,. \tag{3.5}$$

In model II the leptoquark cannot couple to the top quark, so there is no m_t enhancement in the $\mu \to e\gamma$ decay rate. There is also no m_b enhancement, and the one-loop effective Hamiltonian for $\mu \to e\gamma$ (after integrating out the massive scalars and the heavy quarks) is proportional to the muon mass. For this reason, in the remainder of the paper we will focus entirely on model I.

3.3 Phenomenology

In this section we analyze some of the phenomenology of model I, i.e., $X = (3, 2, 7/6)$. We concentrate only on those constraints which are most restrictive for the model and potentially most sensitive to the unusual top mass enhancement of the charged lepton chirality change, i.e., the ones coming from the following processes: muon decay to an electron and a photon, muon to electron conversion, and electric dipole moment of the electron.

3.3.1 Naturalness

There is a logarithmically divergent contribution to the charged lepton mass matrix that is enhanced by m_t. This contribution to the mass matrix, coming from momenta between Λ (the cutoff) and m_V, is

$$\Delta m_{ij} \simeq \tilde{\lambda}_u^{3i} \tilde{\lambda}_e^{j3} \frac{3\, m_t}{16\pi^2} \log\left(\frac{\Lambda^2}{m_V^2}\right) \ . \tag{3.6}$$

To avoid unnatural cancellations between this loop contribution to the lepton mass matrix and the tree-level lepton mass matrix, we require

$$|\Delta m_{ij}| \lesssim \sqrt{m_i m_j} \ . \tag{3.7}$$

For example, for a scalar of mass $m_V = 50$ TeV and a cutoff set at the GUT scale, Eq. (3.6) gives

$$\Delta m_{ij} \simeq \tilde{\lambda}_u^{3i} \tilde{\lambda}_e^{j3} \times 170 \text{ GeV} \ , \tag{3.8}$$

which, combined with Eq. (3.7), yields the following constraint on the couplings:

$$|\tilde{\lambda}_e^{13} \tilde{\lambda}_u^{32}|, |\tilde{\lambda}_e^{23} \tilde{\lambda}_u^{31}| \lesssim 4.3 \times 10^{-5} \ . \tag{3.9}$$

In the subsequent analysis, we will include the constraint imposed by Eq. (3.7) by indicating which regions of the plots are not favored by the naturalness considerations. A more

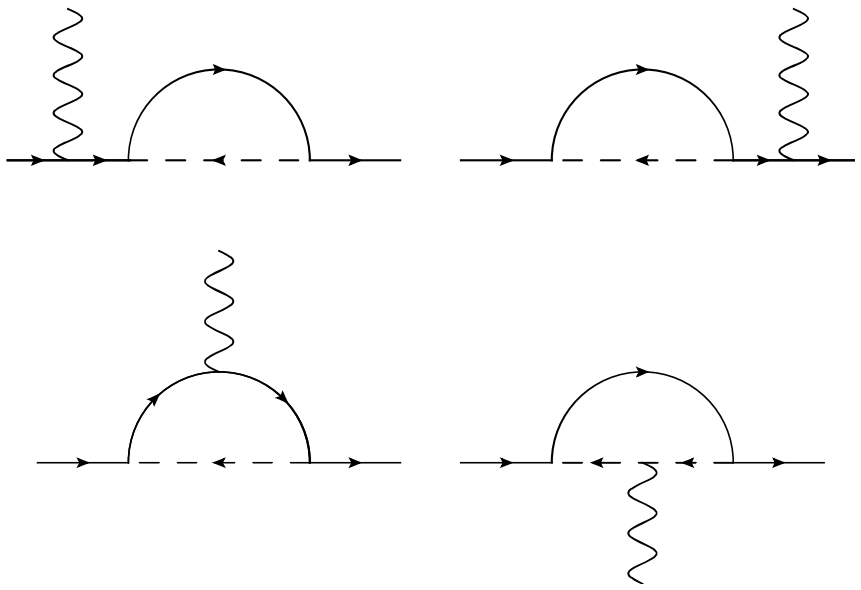

Figure 3.1: Feynman diagrams contributing to the process $\mu \to e\gamma$.

precise analysis would involve solving renormalization group equations for the couplings in the model.

3.3.2 $\mu \to e\gamma$ decay

The relevant Feynman diagrams for this process are presented in Fig. 3.1. The uniqueness of model I is that, apart from the fact there is no tree-level proton decay, the $\mu \to e\gamma$ rate is enhanced by the top quark mass. To our knowledge, such an enhancement of $\mu \to e\gamma$ was observed previously only in Ref. [75] in the context of an $SU(2)$ singlet scalar leptoquark model. However, that model suffers from perturbative proton decay, and the impact of the m_t enhancement was not focused on.

Keeping only the piece enhanced by m_t, the sum of amplitudes corresponding to the diagrams in Fig. 3.1 (neglecting the terms proportional to m_e) is given by (see Appendix D for a detailed calculation)

$$\begin{aligned} i\mathcal{M} \;=\; & -\frac{3\,e\,m_t}{16\,\pi^2 m_V^2} f\left(\frac{m_t^2}{m_V^2}\right)\, k_\nu\, \epsilon_\mu(k) \\ & \times\Big[\tilde{\lambda}_e^{13}\tilde{\lambda}_u^{32}\,\bar{e}_R(p-k)\,\sigma^{\mu\nu}\mu_L(p) + (\tilde{\lambda}_u^{31})^*(\tilde{\lambda}_e^{23})^*\,\bar{e}_L(p-k)\,\sigma^{\mu\nu}\mu_R(p)\Big], \end{aligned} \tag{3.10}$$

where k is the photon four-momentum and ϵ is the photon polarization. The function $f(m_t^2/m_V^2)$ is given by

$$f(x) = \frac{1 - x^2 + 2x\log x}{2(1-x)^3} + \frac{2}{3}\left(\frac{1 - x + \log x}{(1-x)^2}\right), \tag{3.11}$$

and the tilde over the couplings denotes that they are related by transformations that take the quarks and leptons to their mass eigenstate basis through the following 3×3 matrix transformations:

$$\tilde{\lambda}_u = U(u,R)^\dagger \lambda_u U(e,L)\ , \quad \tilde{\lambda}_e = U(e,R)^\dagger \lambda_e U(u,L)\ , \tag{3.12}$$

where the right-handed up quarks in the Lagrangian are related to the right-handed mass eigenstate up-type quarks by the matrix $U(u,R)$, the left-handed up quarks in the Lagrangian are related to the left-handed mass eigenstate up-type quarks by the matrix $U(u,L)$, etc.

The $\mu \to e\gamma$ decay rate is

$$\Gamma(\mu \to e\gamma) = \frac{9\, e^2 \lambda^2 m_t^2 m_\mu^3}{2048\, \pi^5 m_V^4}\, f\left(\frac{m_t^2}{m_V^2}\right)^2, \tag{3.13}$$

where

$$\lambda \equiv \sqrt{\frac{1}{2}\left|\tilde{\lambda}_e^{13}\tilde{\lambda}_u^{32}\right|^2 + \frac{1}{2}\left|\tilde{\lambda}_u^{31}\tilde{\lambda}_e^{23}\right|^2}\ . \tag{3.14}$$

Fig. 3.2 shows the relation between λ and the scalar leptoquark mass. This dependence was plotted for the $\mu \to e\gamma$ branching ratio equal to the current upper limit of $\mathrm{Br}(\mu \to e\gamma) \simeq 2.4 \times 10^{-12}$ reported by the MEG experiment and the prospective MEG sensitivity of $\mathrm{Br}(\mu \to e\gamma) \simeq 5.0 \times 10^{-13}$. It shows that the experiment will be sensitive to scalar leptoquark masses at the hundred TeV scale for small values of the couplings.

For very small x, $f(x) \to \tilde{f}(x) = \frac{2}{3}\log x$. This is a reasonable approximation in the range of x we are interested in. For example, $\tilde{f}(10^{-8})/f(10^{-8}) \simeq 1.1$.

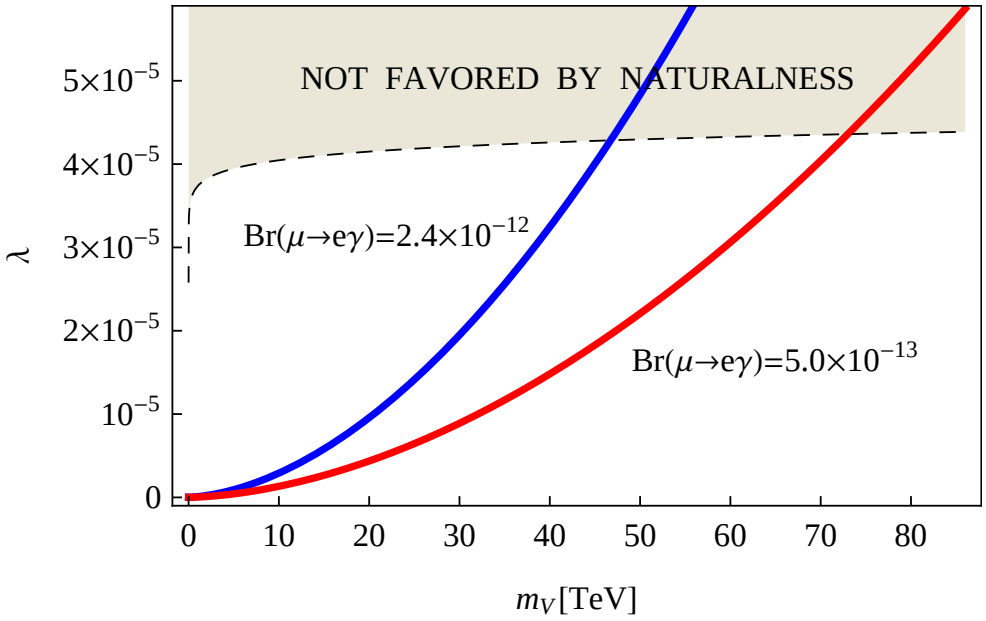

Figure 3.2: The combination of couplings λ from Eq. (3.14) as a function of the scalar leptoquark mass for two values of the $\mu \to e\gamma$ branching ratio relevant for the MEG experiment. The shaded region consists of points which do not satisfy Eq. (3.7).

3.3.3 $\mu \to e$ conversion

The effective Hamiltonian for the $\mu \to e$ conversion arises from two sources,

$$\mathcal{H}_{\text{eff}} = \mathcal{H}_{\text{eff}}^{(\text{a})} + \mathcal{H}_{\text{eff}}^{(\text{b})} \,. \tag{3.15}$$

The first is the dipole transition operator that comes from the loop diagrams, which are responsible for the $\mu \to e\gamma$ decay, given by

$$\mathcal{H}_{\text{eff}}^{(\text{a})} = \frac{3\, e\, m_t}{32\pi^2 m_V^2} f(m_t^2/m_V^2) \left[\tilde{\lambda}_e^{13} \tilde{\lambda}_u^{32}\, \bar{e}_R \sigma_{\mu\nu} \mu_L F^{\mu\nu} + (\tilde{\lambda}_u^{31})^* (\tilde{\lambda}_e^{23})^*\, \bar{e}_L \sigma_{\mu\nu} \mu_R F^{\mu\nu} \right] . \tag{3.16}$$

Using the following Fierz identities for spinors (see Appendix E),

$$\begin{aligned} (\bar{u}_{1L} u_{2R})(\bar{u}_{3R} u_{4L}) &= \frac{1}{2} (\bar{u}_{1L} \gamma^\mu u_{4L})(\bar{u}_{3R} \gamma_\mu u_{2R}) \,, \\ (\bar{u}_{1L} u_{2R})(\bar{u}_{3L} u_{4R}) &= \frac{1}{2} (\bar{u}_{1L} u_{4R})(\bar{u}_{3L} u_{2R}) + \frac{1}{8} (\bar{u}_{1L} \sigma^{\mu\nu} u_{4R})(\bar{u}_{3L} \sigma_{\mu\nu} u_{2R}) \,, \end{aligned} \tag{3.17}$$

we arrive, after integrating out the heavy scalar leptoquarks (at tree level), at the second part of the effective Hamiltonian:

$$\begin{aligned}\mathcal{H}_{\rm eff}^{\rm (b)} &= \frac{1}{2m_V^2}\Big\{\tilde{\lambda}_u^{12}(\tilde{\lambda}_u^{11})^*(\bar{e}_L\gamma^\mu\mu_L)(\bar{u}_{\alpha R}\gamma_\mu u_{\alpha R}) \\ &+ \tilde{\lambda}_e^{11}\tilde{\lambda}_u^{12}\Big[C_S(\mu)(\bar{e}_R\mu_L)(\bar{u}_{\alpha R}u_{\alpha L}) + \frac{1}{4}C_T(\mu)(\bar{e}_R\sigma^{\mu\nu}\mu_L)(\bar{u}_{\alpha R}\sigma_{\mu\nu}u_{\alpha L})\Big] \\ &+ \tilde{\lambda}_e^{11}(\tilde{\lambda}_e^{21})^*(\bar{e}_R\gamma^\mu\mu_R)(\bar{u}_{\alpha L}\gamma_\mu u_{\alpha L}) \\ &+ (\tilde{\lambda}_e^{21})^*(\tilde{\lambda}_u^{11})^*\Big[C_S(\mu)(\bar{e}_L\mu_R)(\bar{u}_{\alpha L}u_{\alpha R}) + \frac{1}{4}C_T(\mu)(\bar{e}_L\sigma^{\mu\nu}\mu_R)(\bar{u}_{\alpha L}\sigma_{\mu\nu}u_{\alpha R})\Big]\Big\} \\ &+ \frac{1}{2m_Y^2}(\tilde{\lambda}_e V_{CKM})^{11}\left((\tilde{\lambda}_e V_{CKM})^{21}\right)^*(\bar{e}_R\gamma^\mu\mu_R)(\bar{d}_{\alpha L}\gamma_\mu d_{\alpha L}) + \dots . \end{aligned} \tag{3.18}$$

The Cabibbo-Kobayashi-Maskawa matrix arises whenever a coupling to the left-handed down-type quark appears. In Eq. (3.18) the contribution of the heavy quarks, as well as the contribution of the strange quark, is in the ellipses. Since the operators $\bar{q}q$ and $\bar{q}\sigma^{\mu\nu}q$ do require renormalization, their matrix elements develop subtraction point dependence that is cancelled in the leading logarithmic approximation by that of the coefficients $C_{S,T}$. Including strong interaction leading logarithms, we get

$$C_S(\mu) = \left[\frac{\alpha_s(m_V)}{\alpha_s(\mu)}\right]^{-12/(33-2N_q)} \tag{3.19}$$

and

$$C_T(\mu) = \left[\frac{\alpha_s(m_V)}{\alpha_s(\mu)}\right]^{4/(33-2N_q)} , \tag{3.20}$$

where $N_q = 6$ is the number of quarks with mass below m_V. In order to match the effective Hamiltonian (3.18) to the Hamiltonian at the nucleon level and use this to compute the conversion rate, we follow the steps outlined in Refs. [79, 80].

Our results, taking into account only the contribution from $\mathcal{H}_{\rm eff}^{\rm (a)}$, are shown in Fig. 3.3. The current experimental limit is $\mathrm{Br}(\mu \to e \text{ conversion in Au}) < 7.0 \times 10^{-13}$ [81]. However, here we focus on the prospective Mu2e experiment [42], which has a sensitivity goal of 5×10^{-17}. The COMET experiment [41] aims for comparable sensitivity in later stages. We use the total capture rate for $^{27}_{13}\mathrm{Al}$ of $\omega_{\rm capture} = 0.7054 \times 10^6\ \mathrm{s}^{-1}$ [82] to switch from the $\mu \to e$ conversion rate to a branching ratio.

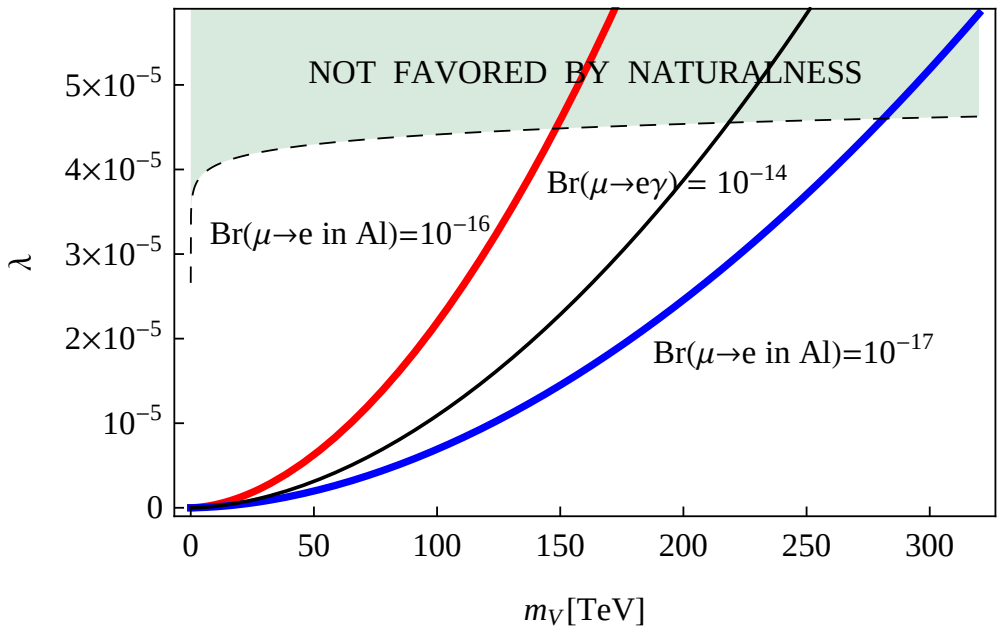

Figure 3.3: The combination of couplings λ from Eq. (3.14) as a function of the scalar leptoquark mass for two values of the $\mathrm{Br}(\mu \to e \text{ conversion in Al})$ relevant for the Mu2e experiment. The thin solid line, corresponding to $\mathrm{Br}(\mu \to e\gamma) = 10^{-14}$, is included for reference. The shaded region consists of points which do not satisfy Eq. (3.7).

Apart from coupling constant factors, the contribution to the $\mu \to e$ conversion amplitude from $\mathcal{H}_{\text{eff}}^{(\text{a})}$ is enhanced over the contribution to the amplitude from $\mathcal{H}_{\text{eff}}^{(\text{b})}$ roughly by $(m_t/m_\mu)(3e^2/32\pi^2)\log(m_V^2/m_t^2) \sim 10$ for m_V in the hundred TeV range.

Our results show that in some regions of parameter space, the Mu2e experiment will be able to constrain leptoquark couplings with similar precision to that which can be done with an experiment which is sensitive to a branching ratio for $\mu \to e\gamma$ of around 10^{-14}. In other regions the Mu2e experiment is likely to give a more powerful constraint for such a $\mu \to e\gamma$ branching ratio, as, for example, when the Yukawa couplings are strongly hierarchical and the top quark loop is very suppressed.

To show graphically the contributions to the branching ratio originating from terms in the effective Hamiltonian with different structures, we set all the couplings to zero apart from $\tilde{\lambda}_e^{13}, \tilde{\lambda}_e^{23}, \tilde{\lambda}_u^{31}, \tilde{\lambda}_u^{32}, \tilde{\lambda}_u^{11}, \tilde{\lambda}_u^{12}$ for simplicity; i.e., we leave only the couplings relevant for the $\mu \to e\gamma$ decay and one of the vector contributions to $\mathcal{H}_{\text{eff}}^{(\text{b})}$.

Note that the heavy quark contributions are suppressed by Λ_{QCD}/m_Q; low energy phe-

nomenology suggests that the strange quark contribution is small, and furthermore the tensor contributions are not enhanced by the atomic number of the target.

In addition, we consider only real couplings and define $\kappa \equiv \tilde{\lambda}_u^{11}\tilde{\lambda}_u^{12}$. We also assume $\tilde{\lambda}_e^{13}\tilde{\lambda}_u^{32} = \tilde{\lambda}_u^{31}\tilde{\lambda}_e^{23} = \lambda$, so that we can plot λ as a function of the scalar leptoquark mass m_V for a given value of the ratio,

$$r \equiv \frac{\kappa}{\lambda} = \frac{\tilde{\lambda}_u^{11}\tilde{\lambda}_u^{12}}{\sqrt{\frac{1}{2}(\tilde{\lambda}_e^{13}\tilde{\lambda}_u^{32})^2 + \frac{1}{2}(\tilde{\lambda}_u^{31}\tilde{\lambda}_e^{23})^2}} \,. \tag{3.21}$$

Figs. 3.4 – 3.7 show our results for a few values of $r = \pm 1, \pm 10, \pm 100, \pm 200$, and two values of the branching ratio $\mathrm{Br}(\mu \to e \text{ conversion in Al}) = 10^{-16}, 10^{-17}$.

For $r \lesssim 1$ the branching ratio is dominated by the $\mathcal{H}_{\text{eff}}^{(\text{a})}$ contribution, and in this parameter region all curves look like the ones in Fig. 3.3. For larger values of r, depending on the relative sign between the contributions from $\mathcal{H}_{\text{eff}}^{(\text{a})}$ and $\mathcal{H}_{\text{eff}}^{(\text{b})}$, there are two possibilities. If the interference is constructive, the curve moves down with increasing r, since a smaller value of the coupling λ is required to achieve a given branching ratio (Figs. 3.5 and 3.7). In the case of a destructive interference, the curves move up until a value of r is reached for which the two contributions are the same (Figs. 3.4 and 3.6). As estimated before, this occurs for $r \approx 10$. Increasing r further brings the curves back down, since the $\mathcal{H}_{\text{eff}}^{(\text{b})}$ contribution becomes dominant.

Large values of r are expected if the Yukawa couplings of X exhibit a hierarchical pattern like what is observed in the quark sector; κ changes generations by one unit, while the product of couplings in λ involves changing generations by three units. Finally, we note that for all the curves in the plots above, the Yukawa couplings are well within the perturbative regime.

3.3.4 Electron EDM

Another flavor constraint on the couplings of model I comes from the electric dipole moment (EDM) of the electron. As mentioned earlier, the fact that X couples directly to both left- and right-handed quarks means that at one loop the top quark mass can induce the

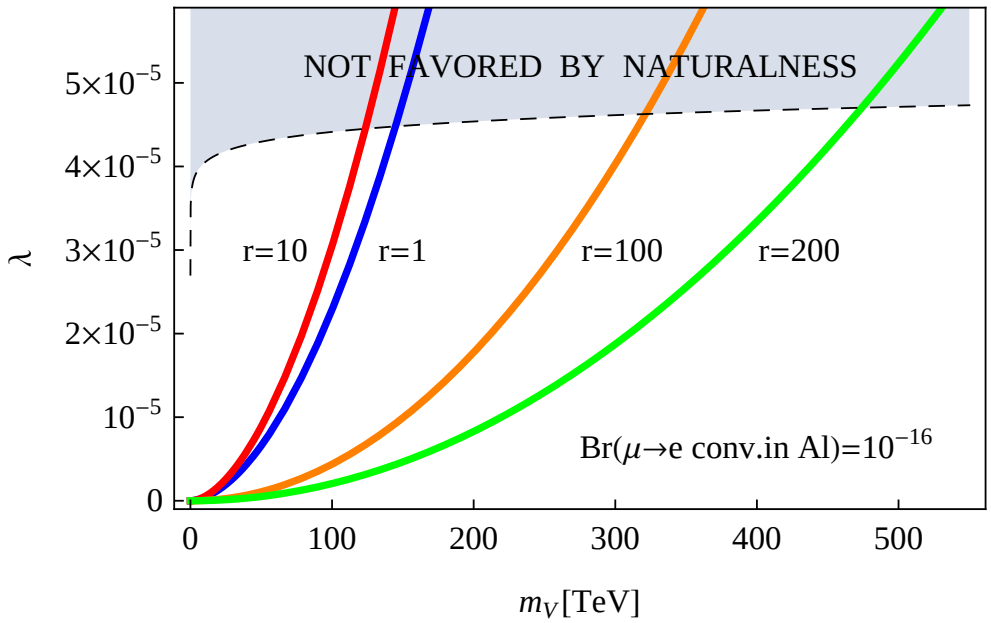

Figure 3.4: The combination of couplings λ from Eq. (3.14) as a function of the scalar leptoquark mass for a branching ratio $\mathrm{Br}(\mu \to e \text{ conversion in Al}) = 10^{-16}$ and four different positive values of the ratio of the couplings r from Eq. (3.21). The shaded region consists of points which do not satisfy Eq. (3.7).

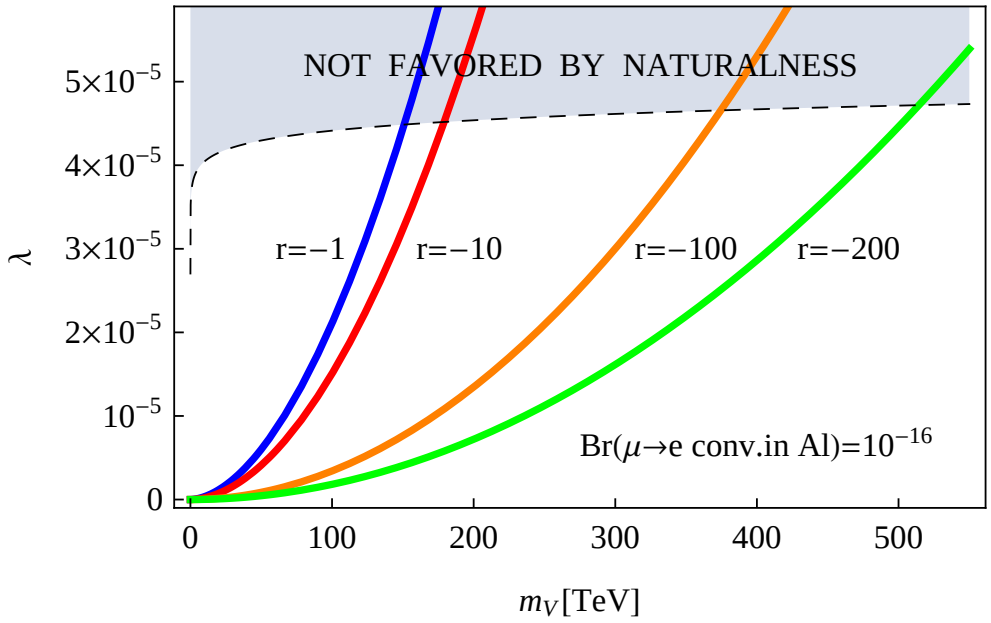

Figure 3.5: Same as Fig. 3.4 but for negative values of r.

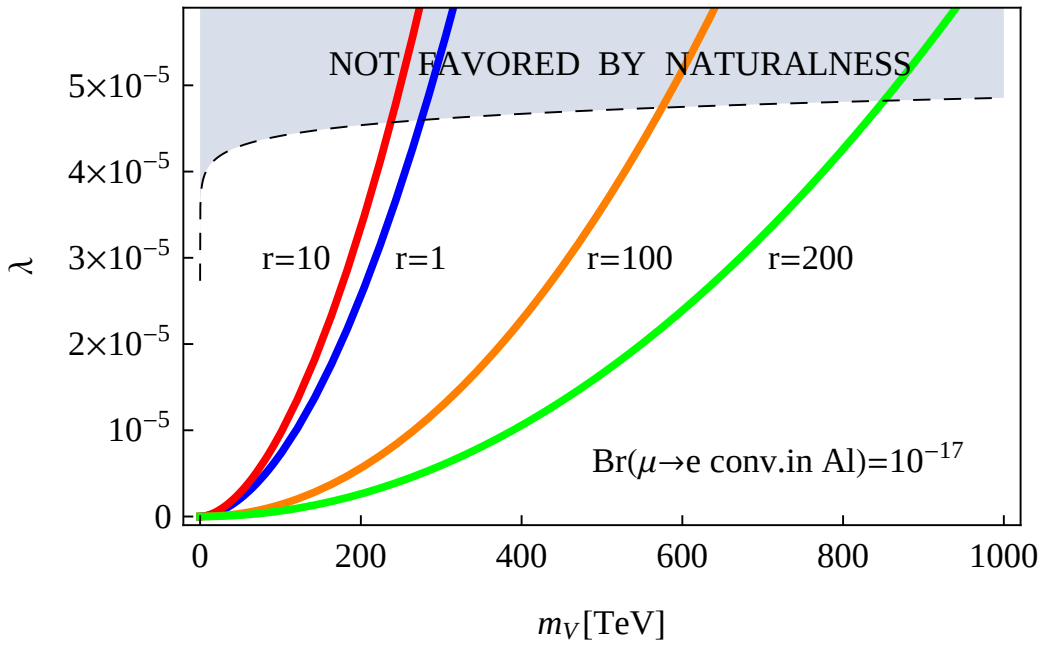

Figure 3.6: Same as Fig. 3.4 but for a branching ratio $\mathrm{Br}(\mu \to e \text{ conversion in Al}) = 10^{-17}$.

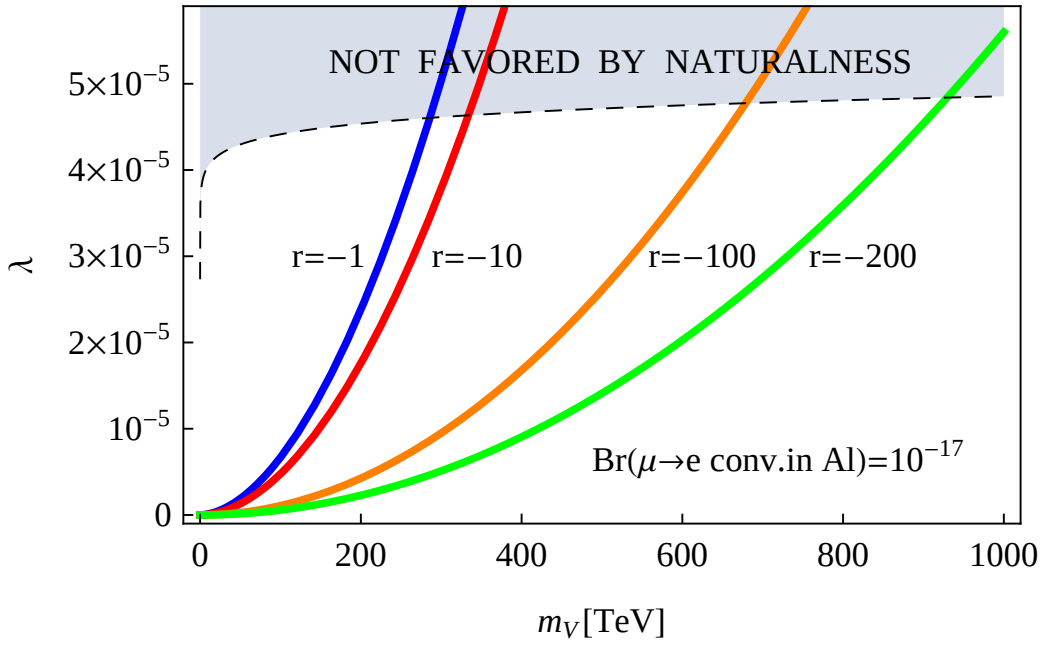

Figure 3.7: Same as Fig. 3.5 but for a branching ratio $\mathrm{Br}(\mu \to e \text{ conversion in Al}) = 10^{-17}$.

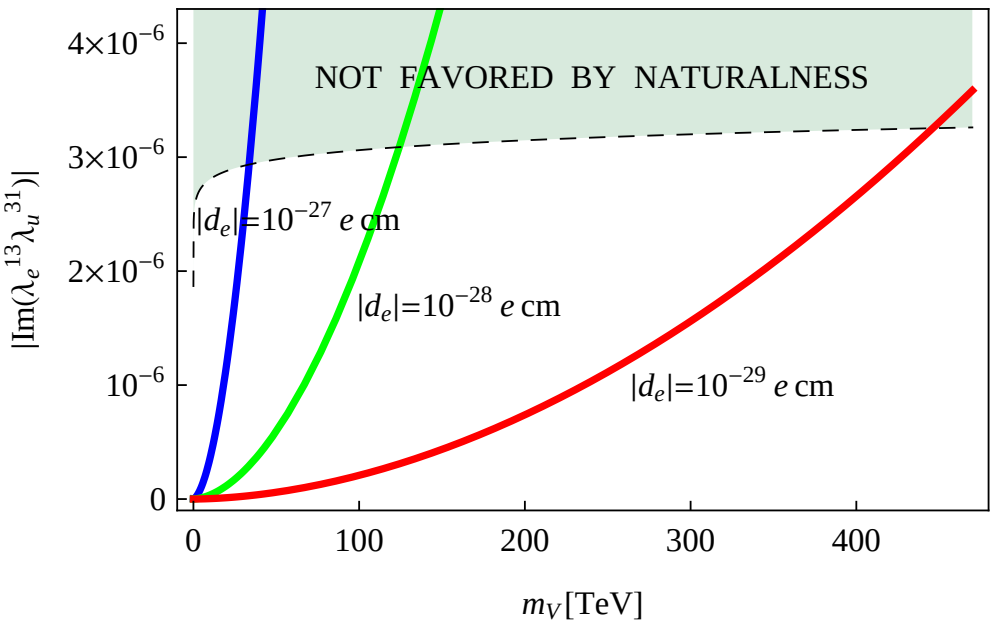

Figure 3.8: The combination of couplings $\left|\mathrm{Im}[\tilde{\lambda}_e^{13}\tilde{\lambda}_u^{31}]\right|$ as a function of the scalar leptoquark mass for three different values of the electron EDM. The shaded region consists of points which do not satisfy Eq. (3.7).

chirality flip necessary to give an electron EDM. We find that

$$|d_e| \simeq \frac{3\,e\,m_t}{16\,\pi^2 m_V^2}\, f\left(\frac{m_t^2}{m_V^2}\right) \left|\mathrm{Im}[\tilde{\lambda}_e^{13}\tilde{\lambda}_u^{31}]\right| . \tag{3.22}$$

The present electron EDM experimental limit [83] is

$$|d_e| < 10.5 \times 10^{-28}\ e\ \mathrm{cm} . \tag{3.23}$$

We can write the dipole moment in terms of the branching ratio, $\mathrm{Br}(\mu \to e\gamma)$, giving the constraint

$$\frac{\left|\mathrm{Im}[\tilde{\lambda}_e^{13}\tilde{\lambda}_u^{31}]\right|}{\lambda}\sqrt{\mathrm{Br}(\mu \to e\gamma)} < 2.0 \times 10^{-7} . \tag{3.24}$$

For example, if model I gave a branching ratio equal to the current experimental bound of $\mathrm{Br}(\mu \to e\gamma) < 2.4 \times 10^{-12}$, this would correspond to the constraint on the couplings of $\left|\mathrm{Im}[\tilde{\lambda}_e^{13}\tilde{\lambda}_u^{31}]\right|/\lambda < 0.13$. Fig. 3.8 shows the relation between the parameters $\left|\mathrm{Im}[\tilde{\lambda}_e^{13}\tilde{\lambda}_u^{31}]\right|$ and m_V for the electron EDM equal to $|d_e| = 10^{-27},\ 10^{-28},$ and $10^{-29}\ e$ cm.

3.4 Baryon number violation and dimension-five operators

Tree-level renormalizable interactions are not the only possible source of baryon number violation. It might also occur through higher-dimensional nonrenormalizable operators. In the standard model, proton decay is restricted to operators of mass dimension six or higher. However, the scalar leptoquark models we consider exhibit proton decay through dimension-five operators.

Let us first consider model I, in which $X = (3, 2, 7/6)$. Although it does not give proton decay at tree level, one can construct the following dimension-five operator:

$$\mathcal{O}_I = \frac{1}{\Lambda}\, g^{ab} d^a_{R\alpha} d^b_{R\beta} (H^\dagger X_\gamma) \epsilon^{\alpha\beta\gamma} \ . \tag{3.25}$$

The coupling constant matrix g is antisymmetric in flavor space. Because of the tree-level leptoquark couplings (see Table 3.1), baryon number violating decay occurs here through the process shown in Fig. 3.9 , resulting in $n \to e^- K^+$ and $p \to K^+ \nu$. Setting the coupling constants to unity, we estimate the baryon number violating nucleon decay rate caused by this operator to be

$$\Gamma_p \approx 2 \times 10^{-57} \left(\frac{50 \text{ TeV}}{m_V} \right)^4 \left(\frac{M_{\rm PL}}{\Lambda} \right)^2 \text{GeV} \ . \tag{3.26}$$

Since the current experimental limit is $\Gamma_p^{\rm exp} < 2.7 \times 10^{-66}$ GeV [25], even if the scale of new physics Λ is equal to the Planck mass $M_{\rm PL}$ when the coupling constants are unity, this operator causes too large a proton decay rate for $m_V \lesssim 10\,000$ TeV.

In the case of model II, where $X = (3, 2, 1/6)$, there are two dimension-five baryon number violating operators:

$$\begin{aligned} \mathcal{O}^{(1)}_{II} &= \frac{1}{\Lambda}\, g^{ab} u^a_{R\alpha} d^b_{R\beta} (H^\dagger X_\gamma) \epsilon^{\alpha\beta\gamma} \ , \\ \mathcal{O}^{(2)}_{II} &= \frac{1}{\Lambda}\, g^{ab} u^a_{R\alpha} e^b_R (X_\beta \epsilon X_\gamma) \epsilon^{\alpha\beta\gamma} \ . \end{aligned} \tag{3.27}$$

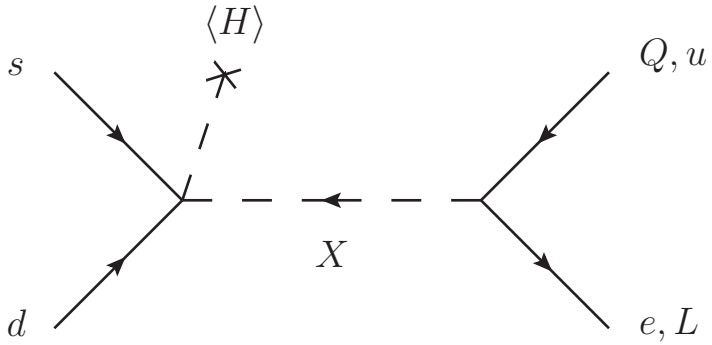

Figure 3.9: Feynman diagram representing proton decay in model I.

The operator $\mathcal{O}_{II}^{(1)}$ permits a nucleon decay pattern similar to the previous case, e.g., $n \to e^- \pi^+$ and $p \to \pi^+ \nu$. Proton decay through the operator $\mathcal{O}_{II}^{(2)}$ is much more suppressed.

In order to prevent proton decay through dimension-five operators, one could introduce a discrete gauge symmetry that forbids the baryon number violating nonrenormalizable couplings. Since $B - L$ is the only anomaly-free global symmetry in the standard model, we chose to impose a discrete subgroup of $B-L$. In models I and II, the leptoquark has $B-L = 4/3$. The usual Z_2, where the nontrivial transformation is $(-1)^{B-L}$, does not work, as the operators $\mathcal{O}_I$, $\mathcal{O}_{II}^{(1)}$, and $\mathcal{O}_{II}^{(2)}$ are invariant under this transformation. However, we find that imposing a Z_3 discrete symmetry, with elements that are powers of $\exp[2\pi i(B-L)/3]$, forbids these dimension-five operators, and thus, prevents the proton from decaying in this class of models. Note that gauging $B - L$ and spontaneously breaking the symmetry with a charge three scalar (at some high scale) leaves this unbroken discrete Z_3 gauge symmetry. It is not possible to use any discrete subgroup of $B - L$ to forbid proton decays in the models from Table 3.1 which exhibit proton decay at tree level since all the interactions conserve $B - L$.

Finally, we would like to comment on the relation between this work and that of Ref. [1], where renormalizable models that have additional scalars and have baryon number violation at tree level, but not proton decay, were enumerated and discussed. In these models, none of the scalars were leptoquarks (they could rather be called diquarks or dileptons). However, if we permit higher dimension operators, then models 4 and 9 presented

in Ref. [1] containing the scalar $X = (3, 1, 2/3)$ (which has renormalizable diquark couplings) have dimension-five leptoquark-type couplings,

$$\mathcal{O}_{III} \;=\; \frac{1}{\Lambda}\, g^{ab}(\bar{Q}_L^{\alpha a} H) e_R^b X_\alpha \,. \tag{3.28}$$

This operator, combined with the renormalizable couplings of X to two quarks, gives proton decay with the rate estimated in Eq. (3.26). This observation restricts the parameter space of models 4 and 9 to the one in which either the color triplet scalar X is very heavy or its Yukawa couplings are small.

3.5 Conclusions

We have investigated the minimal set of renormalizable models in which a single scalar leptoquark is added to the standard model with the requirement that proton decay not be induced in perturbation theory. We have looked in detail at the model which gives an unusual top quark mass enhancement of the branching ratio of $\mu \to e\gamma$, and studied whether this enhancement results in greater experimental reach given a naturalness constraint on the lepton mass matrix.

For this model, we have considered the $\mu \to e\gamma$ branching ratio, the $\mu \to e$ conversion rate, and the electric dipole moment of the electron, in light of current constraints and future experiments. We have shown the potential limits that the MEG, Mu2e, and the electron EDM experiments could place on some of the couplings of the scalar leptoquark to the $\bar{Q}e$ and $L\bar{u}$ bilinears. We have explored the region of parameter space for which the loop contribution to the charged lepton mass matrix does not overwhelm the tree-level part. Given this naturalness constraint, and focusing on the contribution enhanced by m_t, we have found that current experiments are sensitive to leptoquark masses on the order of a hundred TeV, whereas future experiments may push the sensitivity into the several hundred TeV mass region. Without the naturalness constraint, taking the relevant Yukawa couplings to unity, the experimental reach would be $10\,000$ TeV.

We have commented on the existence of nonrenormalizable operators in these minimal

models, which can give an unacceptably large proton decay rate for $m_V \lesssim 10\,000$ TeV, as well as provided a simple mechanism for avoiding them.

Since there are only two scalar leptoquark models where at the renormalizable level baryon number is automatically conserved, it would be interesting to examine a more extensive range of phenomena and address, over a wide range of parameter space, how to distinguish experimentally between these two models.

Chapter 4

B and *L* at the supersymmetry scale, dark matter and *R*-parity violation

We present a simple theory where baryon and lepton numbers are spontaneously broken at the supersymmetry scale. In this context R-parity must be spontaneously broken, but the theory still contains a stable field which can play the role of the cold dark matter of the universe. We discuss the spectrum of the theory, the properties of the dark matter candidate, and the predictions for direct detection experiments. This theory provides a concrete example of exotic supersymmetric signatures associated with having the simultaneous presence of R-parity violating and missing energy signals at the Large Hadron Collider.

The contents of this chapter were written in collaboration with Pavel Fileviez Pérez, Sogee Spinner and Jonathan Arnold, and have been published in Ref. [3].

4.1 Introduction

The minimal supersymmetric standard model (MSSM) is considered one of the most appealing candidates for physics beyond the standard model. While the recent results from the Large Hadron Collider (LHC) have set serious constraints on the masses of the supersymmetric particles, if one suspects that new physics exists at an LHC accessible scale, an MSSM-like theory still highly recommends itself as a candidate theory.

Despite its various appealing properties, the MSSM poses a challenge for proton stability. This is because it introduces two separate sets of operators which induce proton decay: tree-level terms, which separately violate baryon and lepton number, and nonrenormaliz-

able terms which individually violate both baryon and lepton number. The first of these are

$$\hat{L}\hat{H}_u,\ \hat{L}\hat{L}\hat{e}^c,\ \hat{Q}\hat{L}\hat{d}^c,\ \text{and}\ \ \hat{u}^c\hat{d}^c\hat{d}^c,$$

where the first three operators violate lepton number and the last baryon number. Any combination of the first three operators with the last one leads to rapid proton decay. Their absence is typically explained by invoking R-parity, an *ad hoc* discrete symmetry defined as $R = (-1)^{3(B-L)+2S}$, which forbids all of these terms. However, the fate of such operators is most simply divined from models of gauged $B - L$. The most minimal of such models lead to lepton number violating R-parity violation (and therefore no tree-level proton decay) [84] but R-parity conserving models are also possible [85, 86, 87]. Regardless of the type of $B - L$ model, the second type of proton decay inducing operators exists. These are nonrenormalizable operators which conserve $B - L$ but violate B and L separately, e.g.,

$$\frac{\hat{Q}\hat{Q}\hat{Q}\hat{L}}{\Lambda}\ \ \text{and}\ \ \frac{\hat{u}^c\hat{u}^c\hat{d}^c\hat{e}^c}{\Lambda}\ .$$

Despite the suppression in these terms due to the scale of new physics, the bounds on proton decay are strong enough to motivate a mechanism for suppressing them. See Ref. [28] for a review of proton decay.

Recently, a simple theory for the spontaneous breaking of local baryon and lepton numbers has been proposed in Ref. [88]. In this context one can define an anomaly-free theory using fermionic leptobaryons which have both baryon and lepton number charges. Furthermore, even after symmetry breaking, the lightest leptobaryon is stable due to a remnant Z_2 symmetry and can therefore be a dark matter candidate (see also Refs. [89, 90, 91] for similar studies). This idea can be applied in the context of supersymmetric theories to establish not only the origin of the R-parity violating terms, as in the $B - L$ models, but also determine the fate of the nonrenormalizable terms which violate B and L separately.

In this paper we investigate an extension of the MSSM where the local baryonic and leptonic symmetries are spontaneously broken at the supersymmetry scale. We find that the minimal model predicts that R-parity must be spontaneously broken in the MSSM sector (leading only to lepton number violation). Despite the breaking of R-parity, the

remnant Z_2 symmetry from the breaking of the baryonic and leptonic symmetries ensures that the lightest leptobaryon is stable and may be a candidate for the cold dark matter of the Universe. We investigate the spectrum of the theory and the predictions for dark matter direct detection. This article is organized as follows: in Section 4.2 we discuss the model with local B and L symmetries, and in Section 4.3 we discuss the possible dark matter candidates and the predictions for dark matter experiments; finally, we summarize our results in Section 4.4.

4.2 Spontaneous breaking of *B* and *L*

In order to define a theory for local baryon and lepton numbers, we use the gauge group

$$SU(3)_C \times SU(2)_L \times U(1)_Y \times U(1)_B \times U(1)_L \, .$$

An anomaly-free theory can be achieved by adding the following new leptobaryonic fields with B and L numbers [88]:

$$\begin{aligned}
\hat{\Psi} &\sim (1, 2, -1/2, B_1, L_1) \, , \;\; \hat{\Psi}^c \sim (1, 2, 1/2, B_2, L_2) \, , \\
\hat{\eta}^c &\sim (1, 1, 1, -B_1, -L_1) \, , \;\; \hat{\eta} \sim (1, 1, -1, -B_2, -L_2) \, , \\
\hat{X}^c &\sim (1, 1, 0, -B_1, -L_1) \, , \text{ and } \; \hat{X} \sim (1, 1, 0, -B_2, -L_2) \, .
\end{aligned}$$

Notice that these fields are vector-like with respect to the SM transformations. The anomalies can be canceled for any values of B_i and L_i $(i = 1, 2)$, which satisfy the conditions (see Appendix F)

$$B_1 + B_2 = -3 \quad \text{and} \quad L_1 + L_2 = -3 \, . \tag{4.1}$$

In order to generate masses for the new fields and for symmetry breaking, we need the chiral superfields

$$\hat{S}_1 \sim (1, 1, 0, 3, 3) \quad \text{and} \quad \hat{S}_2 \sim (1, 1, 0, -3, -3) \, .$$

Therefore, the superpotential of this theory is given by

$$\mathcal{W}_{\rm BL} \;=\; \mathcal{W}_{\rm RpC} \,+\, \mathcal{W}_{\rm LB}\,, \tag{4.2}$$

where

$$\mathcal{W}_{\rm RpC} \;=\; Y_u\hat{Q}\hat{H}_u\hat{u}^c + Y_d\hat{Q}\hat{H}_d\hat{d}^c + Y_e\hat{L}\hat{H}_d\hat{e}^c + Y_\nu\hat{L}\hat{H}_u\hat{\nu}^c + \mu\hat{H}_u\hat{H}_d \tag{4.3}$$

contains the R-parity conserving terms present in the MSSM (plus a Yukawa coupling for the neutrinos, Y_ν) and

$$\begin{aligned}\mathcal{W}_{\rm LB} \;=\;& Y_1\hat{\Psi}\hat{H}_d\hat{\eta}^c + Y_2\hat{\Psi}\hat{H}_u\hat{X}^c + Y_3\hat{\Psi}^c\hat{H}_u\hat{\eta} + Y_4\hat{\Psi}^c\hat{H}_d\hat{X} \\ &+ \lambda_1\hat{\Psi}\hat{\Psi}^c\hat{S}_1 + \lambda_2\hat{\eta}\hat{\eta}^c\hat{S}_2 + \lambda_3\hat{X}\hat{X}^c\hat{S}_2 + \mu_{BL}\hat{S}_1\hat{S}_2\end{aligned} \tag{4.4}$$

is the superpotential of the leptobaryonic sector needed for anomaly cancelation. Of course, because of the conservation of B and L, both the R-parity violating terms and the non-renormalizable terms leading to proton decay are forbidden. Notice that when $B_1 = B_2$ and $L_1 = L_2$ we can have Majorana masses for the $\hat{X}$ and $\hat{X}^c$, but we stick to the general case where $B_1 \neq B_2$ and $L_1 \neq L_2$.

An interesting consequence of the leptobaryonic sector is the presence of a Z_2 symmetry once S_1 and S_2 acquire a vacuum expectation value (VEV). Under this symmetry, all leptobaryons are odd: $\Psi \to -\Psi$, $\Psi^c \to -\Psi^c$, $\eta \to -\eta$, $\eta^c \to -\eta^c$, $X \to -X$ and $X^c \to -X^c$. The consequence of this is that the lightest leptobaryon is stable (must be neutral) and therefore a dark matter candidate.

4.2.1 Symmetry breaking and gauge boson masses

Symmetry breaking in the baryon and lepton number sector proceeds through the following scalar potential:

$$\begin{aligned} V \;=\; & \left(M_1^2+|\mu_{BL}|^2\right)|S_1|^2+\left(M_2^2+|\mu_{BL}|^2\right)|S_2|^2+M_{\tilde{\nu}^c}^2|\tilde{\nu}^c|^2+\frac{9}{2}g_B^2\left(|S_1|^2-|S_2|^2\right)^2 \\ & +\frac{1}{2}g_L^2\left(3|S_1|^2-3|S_2|^2-|\tilde{\nu}^c|^2\right)^2-\left(b_{BL}S_1S_2+\text{h.c.}\right), \end{aligned} \tag{4.5}$$

where M_1, M_2 and $M_{\tilde{\nu}^c}$ are the soft terms for the scalar fields S_1, S_2 and $\tilde{\nu}^c$, respectively. Here b_{BL} is the bilinear term between S_1 and S_2, and we define the VEVs as

$$\sqrt{2}\,S_1 \;=\; v_1+h_1+ia_1\,, \tag{4.6}$$

$$\sqrt{2}\,S_2 \;=\; v_2+h_2+ia_2\,, \tag{4.7}$$

$$\sqrt{2}\,\tilde{\nu}^c \;=\; v_R+h_R+ia_R\,. \tag{4.8}$$

The squared mass matrix for the new gauge bosons can be written as

$$\mathcal{M}_{Z'}^2=\begin{pmatrix} 9g_B^2(v_1^2+v_2^2) & 9g_Bg_L(v_1^2+v_2^2) \\ 9g_Bg_L(v_1^2+v_2^2) & 9g_L^2(v_1^2+v_2^2)+g_L^2v_R^2 \end{pmatrix}, \tag{4.9}$$

which has a zero determinant if $v_R = 0$; note that this cannot be modified even in the case where $\langle X\rangle \neq 0$ when $B_i = L_i$. We stick to these scenarios for simplicity. This is a consequence of the fact that when S_1 and S_2 acquire VEVs the symmetry group $U(1)_B \times U(1)_L$ is broken to $U(1)_{B-L}$. The $B-L$ symmetry can only be broken by the VEV of the right-handed sneutrino, as in Ref. [84]. Therefore, we conclude that *R-parity must be spontaneously broken in this theory.* However, it is only lepton number violating R-parity violation and therefore the proton remains safe.

The minimization conditions read as

$$
\begin{aligned}
0 &= \left(M_1^2 + |\mu_{BL}|^2\right) - b_{BL}\frac{v_2}{v_1} + \frac{9}{2}g_B^2(v_1^2 - v_2^2) + \frac{3}{2}g_L^2(3v_1^2 - 3v_2^2 - v_R^2)\,, \quad (4.10)\\
0 &= \left(M_2^2 + |\mu_{BL}|^2\right) - b_{BL}\frac{v_1}{v_2} - \frac{9}{2}g_B^2(v_1^2 - v_2^2) - \frac{3}{2}g_L^2(3v_1^2 - 3v_2^2 - v_R^2)\,, \quad (4.11)\\
0 &= M_{\tilde{\nu}^c}^2 - \frac{1}{2}g_L^2\left(3v_1^2 - 3v_2^2 - v_R^2\right), \quad (4.12)
\end{aligned}
$$

and can be reformulated as

$$
\begin{aligned}
v_R^2 &= \frac{2}{g_L^2}\left[-M_{\tilde{\nu}^c}^2 + \frac{3}{2}g_L^2\left(v_1^2 - v_2^2\right)\right], \quad (4.13)\\
\sin(2\gamma) &= \frac{2b_{BL}}{M_1^2 + M_2^2 + 2|\mu_{BL}|^2}\,, \quad (4.14)
\end{aligned}
$$

where we have defined

$$
\tan\gamma = \frac{v_2}{v_1}\,. \quad (4.15)
$$

One can easily prove that there is no symmetry breaking in the supersymmetry (SUSY) limit. Therefore, the B and L breaking scales are determined by the SUSY scale. In order to have a potential bounded from below, we must satisfy the condition

$$
2b_{BL} < M_1^2 + M_2^2 + 2|\mu_{BL}|^2, \quad (4.16)
$$

and in order to break the symmetry we need the condition

$$
b_{BL}^2 > \left(M_1^2 + |\mu_{BL}|^2 - \frac{3}{2}g_L^2 v_R^2\right)\left(M_2^2 + |\mu_{BL}|^2 + \frac{3}{2}g_L^2 v_R^2\right). \quad (4.17)
$$

The mixing angle between Z_1 and Z_2 is defined by

$$
\begin{pmatrix} Z_B \\ Z_L \end{pmatrix} = \begin{pmatrix} \cos\theta_{BL} & \sin\theta_{BL} \\ -\sin\theta_{BL} & \cos\theta_{BL} \end{pmatrix}\begin{pmatrix} Z_1 \\ Z_2 \end{pmatrix}, \quad (4.18)
$$

where $M_{Z_1} < M_{Z_2}$. The eigenvalues for the new neutral gauge bosons are

$$M^2_{Z_{1,2}} = \frac{1}{2}\left(M^2_{Z_L} + M^2_{Z_B} \pm \sqrt{\left(M^2_{Z_L} - M^2_{Z_B}\right)^2 + 4\tfrac{g_L^2}{g_B^2} M^4_{Z_B}} \right), \tag{4.19}$$

where

$$M^2_{Z_B} \equiv 9g_B^2(v_1^2 + v_2^2)\,, \tag{4.20}$$

$$M^2_{Z_L} \equiv g_L^2\left(9v_1^2 + 9v_2^2 + v_R^2\right)\,, \tag{4.21}$$

and the mixing angle is given by

$$\sin(2\theta_{BL}) = \frac{2g_B g_L(v_1^2 + v_2^2)}{M^2_{Z_2} - M^2_{Z_1}}\,. \tag{4.22}$$

Note that this produces a Z_1 lighter than Z_2 only for $M_{Z_B} < M_{Z_L}$. For the opposite case take $\theta_{BL} \to -\theta_{BL}$ and $Z_1 \leftrightarrow Z_2$. In the limit $v_R^2 \gg v_1^2 + v_2^2$ the eigenvalues are

$$M_{Z_1} \sim 9g_B^2\left(v_1^2 + v_2^2\right)(1 - 9\epsilon)\,, \tag{4.23}$$

$$M_{Z_2} \sim g_L^2 v_R^2\,(1 + 9\epsilon)\,, \tag{4.24}$$

where $\epsilon \equiv (v_1^2 + v_2^2)/v_R^2$ and the mass eigenstates are

$$Z_1 = \left(1 - \frac{81}{2}\frac{g_B^2}{g_L^2}\epsilon^2\right) Z_B - 9\frac{g_B}{g_L}\,\epsilon\, Z_L\,, \tag{4.25}$$

$$Z_2 = 9\frac{g_B}{g_L}\,\epsilon\, Z_B + \left(1 - \frac{81}{2}\frac{g_B^2}{g_L^2}\epsilon^2\right) Z_L\,. \tag{4.26}$$

This is an interesting limit, since the lighter Z_1 eigenstate is predominately Z_B-like and therefore has lower collider bounds [92, 93] compared to a Z' that significantly couples to leptons [94].

Finally, we note that when baryon and lepton numbers are broken at the SUSY scale, one expects operators mediating proton decay. However, in this theory, the proton is stable because baryon number is broken by three units. The least suppressed nonrenormalizable

terms which generate baryon and lepton number violating interactions occur at dimension fourteen, e.g.,

$$W_{14} \;=\; \frac{1}{\Lambda^{10}}\Big[c_1\hat{S}_1(\hat{u}^c\hat{u}^c\hat{d}^c\hat{e}^c)^3 + c_2\hat{S}_1(\hat{u}^c\hat{d}^c\hat{d}^c\hat{\nu}^c)^3 + c_3\hat{S}_2(\hat{Q}\hat{Q}\hat{Q}\hat{L})^3\Big]\,. \qquad (4.27)$$

Because of this large suppression, there is no need to assume a large scale to be in agreement with experiments.

4.2.2 Spontaneous *R*-parity violation

As we saw earlier, in order to avoid a long range $B-L$ force, the sneutrino must acquire a VEV. The consequences of this are very similar to those in the minimal supersymmetric $B-L$ model [84] and we briefly review them here.

The first and most obvious of these consequences is that R-parity is spontaneously broken. This induces a mixing between SUSY and non-SUSY fields with the same quantum numbers: neutralinos with neutrinos, charginos with charged leptons, sneutrinos with neutral Higgs, and charged sleptons with charged Higgs. Typically, the most important of these mixings proceeds through the neutrino Yukawa coupling in the superpotential once the right-handed sneutrino acquires a VEV, and one obtains

$$W \supset \frac{1}{\sqrt{2}}Y_\nu v_R \hat{L}\,\hat{H}_u, \qquad (4.28)$$

which is the so-called bilinear R-parity violating term usually referred to as μ'. This term also induces a VEV for the left-handed sneutrino which leads to various mixing terms of gauge coupling strength such as $\frac{1}{2}g_1\tilde{B}\nu v_L$ and $g_L\tilde{B}_L\nu v_L$, where $\tilde{B}$ and $\tilde{B}_L$ are the hypercharge and lepton number gauginos, respectively. The size of R-parity violation is related to the neutrino sector and is therefore small. Phenomenologically, this means that SUSY processes proceed as if R-parity is conserved except for the decay of the lightest supersymmetric particle (LSP), which can now decay into SM states. More specifically, SUSY particles are still pair produced. For specific decay channels for a given LSP, see Ref. [95].

A further interesting consequence is that a sizable VEV can only be realized for one

generation of right-handed sneutrinos. This means that lepton number is broken by one unit only in one generation, and it is only the corresponding generation of right-handed neutrinos which attains a TeV scale mass; the other two right-handed, or sterile, neutrinos attain sub-eV masses [96, 97, 98]. This has important consequences for cosmology in the form of dark radiation in the early universe and for neutrino oscillation anomalies.

4.3 Dark matter candidates

After symmetry breaking, the lightest leptobaryon is stable due to the remnant Z_2 symmetry, as discussed earlier. This particle must be neutral and could play the role of dark matter. Furthermore, unlike in R-parity conservation, the lightest leptobaryon can be either a fermion or a scalar. The best candidates are the $\hat{X}$ and $\hat{X}^c$ superfields since they do not couple to the Z. In this study, we assume the lightest leptobaryon is the fermionic component of $\hat{X}$ and $\hat{X}^c$, whose Dirac spinor we refer to as $\tilde{X}$, and focus on its properties. It is also interesting to note that because the mass of $\tilde{X}$ is given by the VEV of S_2, it is automatically at the SUSY scale, and therefore like a weakly interacting massive particle. This would not be true if its mass was simply a parameter in the superpotential whose magnitude would be arbitrary. Of course, there is a trade-off here with the μ-type problem associated with the μ_{BL} parameter.

The fermionic dark matter candidate can annihilate into two fermions through the neutral gauge bosons present in the theory:

$$\bar{\tilde{X}}\tilde{X} \;\rightarrow\; Z_i \;\rightarrow\; \bar{f}f \,. \tag{4.29}$$

The relevant interactions in this case are

$$-\mathcal{L} = g_B \bar{\tilde{X}}\gamma^\mu \left(-B_2 P_L + B_1 P_R\right) Z_{B\mu}\tilde{X} + g_L \bar{\tilde{X}}\gamma^\mu \left(-L_2 P_L + L_1 P_R\right) Z_{L\mu}\tilde{X} \,, \tag{4.30}$$

which in the physical basis reads as

$$-\mathcal{L} = g_B \bar{\tilde{X}}\gamma^\mu \left(C_{11} P_L + C_{12} P_R\right) Z_{1\mu}\tilde{X} + g_B \bar{\tilde{X}}\gamma^\mu \left(C_{21} P_L + C_{22} P_R\right) Z_{2\mu}\tilde{X} \,, \tag{4.31}$$

where

$$C_{11} = -B_2 \cos\theta_{BL} + \frac{g_L}{g_B} L_2 \sin\theta_{BL} \,, \tag{4.32}$$

$$C_{12} = B_1 \cos\theta_{BL} - \frac{g_L}{g_B} L_1 \sin\theta_{BL} \,, \tag{4.33}$$

$$C_{21} = -B_2 \sin\theta_{BL} - \frac{g_L}{g_B} L_2 \cos\theta_{BL} \,, \tag{4.34}$$

$$C_{22} = B_1 \sin\theta_{BL} + \frac{g_L}{g_B} L_1 \cos\theta_{BL} \,. \tag{4.35}$$

Assuming the contribution from Z_1 dominates, we find an annihilation cross section (see Appendix G)

$$\sigma v = \sum_q \frac{1}{36\pi s} \sqrt{1 - \frac{4m_q^2}{s}} \frac{g_B^4 \tilde{C}}{(s - M_{Z_1}^2)^2 + \Gamma_{Z_1}^2 M_{Z_1}^2} \,, \tag{4.36}$$

where

$$\tilde{C} = \left[(C_{11}^2 + C_{12}^2)(s + 2m_q^2)(s - M_{\tilde{X}}^2) + 6\, C_{11} C_{12} M_{\tilde{X}}^2 (s + 2m_q^2) \right] \cos^2\theta_{BL} \,. \tag{4.37}$$

In the nonrelativistic limit, the cross section is given by

$$(\sigma v)_{NR} = \sum_q \frac{1}{24\pi} \sqrt{1 - \frac{m_q^2}{M_{\tilde{X}}^2}} \frac{g_B^4 C^2 (2M_{\tilde{X}}^2 + m_q^2)}{(4M_{\tilde{X}}^2 - M_{Z_1}^2)^2 + \Gamma_{Z_1}^2 M_{Z_1}^2} \,, \tag{4.38}$$

where we have denoted

$$C = (C_{11} + C_{12}) \cos\theta_{BL} \,. \tag{4.39}$$

In the present epoch the energy density of the relic dark matter particles $\tilde{X}$ would be

$$\Omega_{\tilde{X}} h^2 \simeq \frac{x_f}{\sqrt{g_*}\, \sigma_0 M_P} \frac{(1.07 \times 10^9)}{\mathrm{GeV}} \,. \tag{4.40}$$

We adopt the value $\Omega_{DM}^{\mathrm{obs}} h^2 = 0.1199 \pm 0.0027$ [99]. The freeze-out temperature $x_f =$

$M_{\tilde{X}}/T_f$ is then given by

$$x_f = \ln\left(\frac{0.038\, g\, M_P M_{\tilde{X}} \sigma_0}{\sqrt{g_*}}\right) - \frac{1}{2}\ln\left[\ln\left(\frac{0.038\, g\, M_P M_{\tilde{X}} \sigma_0}{\sqrt{g_*}}\right)\right], \tag{4.41}$$

where g is the number of internal degrees of freedom (in our case $g = 4$), g_* is the effective number of relativistic degrees of freedom evaluated around the freeze-out temperature, M_P is the Planck mass, and $\sigma v = \sigma_0 + \sigma_1 v^2$.

The direct detection also proceeds through the Z_i:

$$\tilde{X}N \;\rightarrow\; Z_i \;\rightarrow\; \tilde{X}N\,, \tag{4.42}$$

and the spin-independent nucleon-dark matter cross section is then given by

$$\sigma_{\rm SI} = \frac{1}{4\pi}\frac{M_{\tilde{X}}^2 M_N^2}{(M_{\tilde{X}} + M_N)^2}\frac{g_B^4}{M_{Z_1}^4} C^2\,, \tag{4.43}$$

assuming that the dominant contribution comes from the Z_1 gauge boson. Because both the dark matter annihilation and direct detection proceed through Z_1, they are intimately related to each other. Specifically, once one determines the parameters that yield the correct relic density for a given dark matter mass, there are no free parameters left to hide it from direct detection. Keeping this in mind, we present the predictions for the direct detection experiments.

In Fig. 4.1 we show the values for the spin-independent cross section versus the dark matter mass when $C = 1$, $0.1 \leq g_B \leq 0.3$, $2.5\ \text{TeV} \leq M_{Z_1} \leq 5\ \text{TeV}$, and assuming that the relic density is in the range $0.11 < \Omega_{\tilde{X}} h^2 < 0.13$. One can appreciate in Fig. 4.1 that the allowed solutions are below the XENON100 bounds [100], but could be tested in future dark matter experiments such as XENON1T or LUX.

In Fig. 4.2 we show some solutions when the mass of the new lightest neutral gauge boson is 2, 3, or 4 TeV. One can see that there is no need to be very close to the resonance to achieve the required cross section for the relic density.

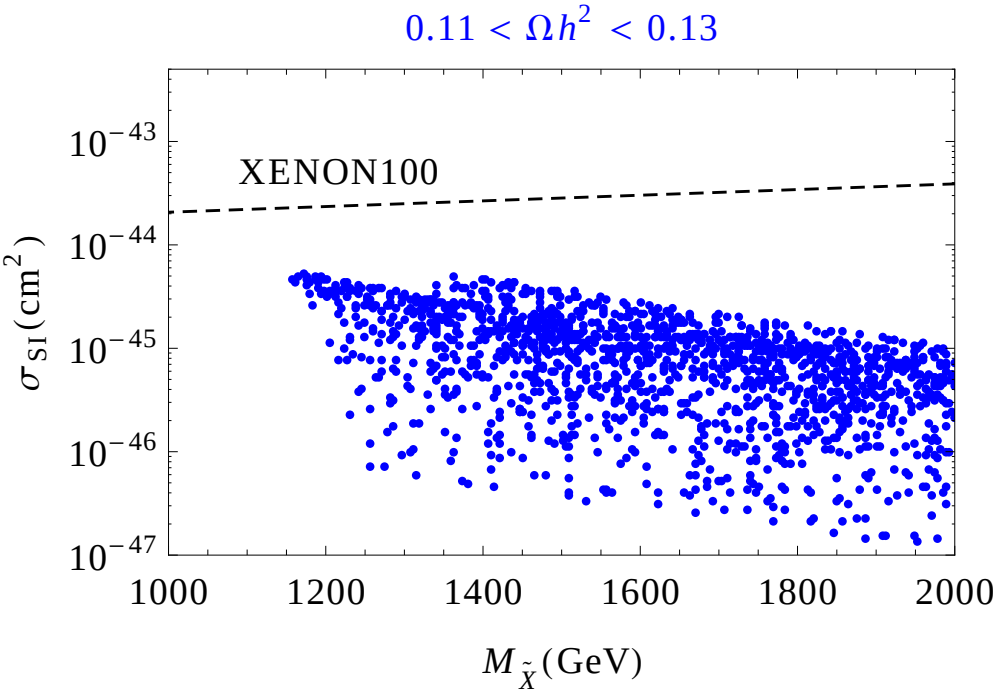

Figure 4.1: Predictions for the elastic nucleon-dark matter cross section for different values of the dark matter mass when $0.11 < \Omega_{\tilde{X}} h^2 < 0.13$.

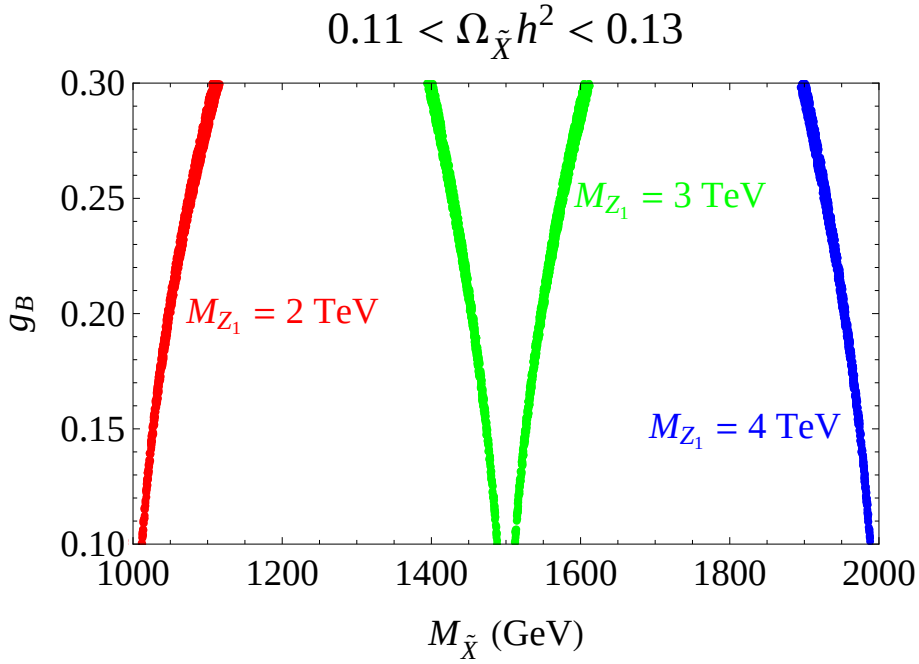

Figure 4.2: Allowed values for the gauge coupling and the dark matter mass when $0.11 < \Omega_{\tilde{X}} h^2 < 0.13$ and $M_{Z_1} = 2, 3, 4$ TeV.

4.4 Summary and discussions

In this article we have presented the simplest supersymmetric extension of the model proposed in Ref. [88] where baryon and lepton number are local symmetries. In this context, the baryonic and leptonic gauge symmetries are broken at the SUSY scale and the proton is stable.

One of the main predictions of this theory is that R-parity must be spontaneously broken in the MSSM sector because the right-handed sneutrino VEVs are needed to break the remnant local $U(1)_{B-L}$ that results from the VEVs of S_1 and S_2. Even though R-parity is broken, the lightest leptobaryon is stable and can be a cold dark matter candidate. The dark matter candidate can either be the spin one-half or spin zero SM singlet leptobaryon; we have focused on the former in this paper. It furthermore has baryon and lepton number, and therefore couples to the two Z's in the model.

There are many interesting predictions for the Large Hadron Collider searches in this theory. Since R-parity is broken in the MSSM sector, we will have lepton number violating signatures at the LHC. For example, one can have exotic channels with four leptons and four jets where three of the leptons have the same electric charge [95, 101]. On the other hand, there is a stable dark matter candidate in the theory which can be produced through the new neutral gauge bosons. Therefore, one can also expect signatures with missing energy at the LHC. This theory provides a simple example of very exotic supersymmetric signatures at colliders, since one can have the simultaneous presence of R-parity violating and missing energy signatures at the LHC.

Chapter 5

Standard model with gauged baryon, lepton and flavor symmetries

We propose an extension of the standard model in which baryon number, lepton number, and the flavor group are spontaneously broken local gauge symmetries. The anomalies are cancelled by including leptobaryonic and flavor-triplet fields with appropriate quantum numbers. The model contains a dark matter candidate, generates masses for the neutrinos, and does not suffer from dangerous low-dimensional baryon number violating operators inducing proton decay. It also has the potential to solve the flavor puzzle. We discuss the Lagrangian of the theory, the symmetry breaking mechanism, experimental constraints, and possible signatures at the LHC.

5.1 Introduction

The standard model has been providing an extremely successful description of our world. However, despite its undisputable virtues, it suffers from a variety of issues enumerated in Chapter 1. Apart from experiencing the hierarchy problem, it does not explain the existence of dark matter and neutrino masses, requires a desert between the electroweak scale and the GUT scale to be consistent with experimental limits on proton decay, exhibits the strong CP problem, provides no explanation for the hierarchical pattern of Yukawas, and much more. All this suggests that the standard model by itself is incomplete. Many extensions have been proposed, each having its advantages, but so far none of the new physics models have been able to successfully explain all issues simultaneously.

It has recently been shown that theories with gauged baryon and lepton numbers are not plagued with dimension four and five baryon number violating operators responsible for proton decay [88, 89, 90, 102]. Anomaly cancellation in those theories requires introducing a set of new fields: a sequential fourth generation [89, 102], vector-like fourth generation [90], or vector-like leptobaryons [88]. The models with a fourth generation are in tension with experiments either because of the nonperturbativity of the Yukawa couplings [89], or because of the suppression in the $H \to \gamma\gamma$ decay rate [103, 104]. This leaves the model presented in [88] as the most appealing non-supersymmetric extension of the standard model with baryon and lepton numbers gauged.

At the same time, much progress has been made in understanding flavor symmetries. In particular, models with gauged flavor symmetries were brought back into attention in [105] by constructing a minimal anomaly-free extension of the standard model of this type. The cancellation of anomalies was obtained by introducing a set of fermionic fields which are vector-like with respect to the flavor gauge group. A more detailed phenomenological study of this model was carried out in [106]. An interesting property of such theories is that spontaneous flavor symmetry breaking, driven by the flavon fields, is capable of explaining the hierarchy of the standard model Yukawas through the appropriate shape of the flavon potential [107].

In this thesis we propose a model in which all the baryon, lepton, and flavor symmetries are gauged. We call this model the BLFSM. Our motivation is to construct a consistent theory which has an appealing dark matter candidate, contains a mechanism for generating neutrino masses, does not exhibit proton decay, and within which the hierarchical pattern of Yukawas can be understood. We are not concerned with the hierarchy problem, since it can be alleviated by supersymmetrizing our model, which itself would be an extension of the model presented in [108], but with baryon and lepton numbers gauged in addition to the flavor group.

5.2 The model

Our model is based on the gauge group

$$SU(3)_c \times SU(2)_L \times U(1)_Y \times U(1)_B \times U(1)_L$$
$$\times\, SU(3)_{Q_L} \times SU(3)_{u_R} \times SU(3)_{d_R} \times\ SU(3)_{l_L} \times SU(3)_{\nu_R} \times SU(3)_{e_R}\ ,$$

where the second line represents the gauged flavor symmetries of the standard model augmented by a right-handed neutrino. The minimal particle content of the model, along with the quantum numbers of the fields, is presented in Table 5.1.

The leptobaryonic fermion fields Ψ_L, Ψ_R, η_R, η_L, X_R, X_L are introduced in order to cancel the gauge anomalies involving $U(1)_B$ and $U(1)_L$. The requirement of anomaly cancellation imposes the following conditions on the baryon and lepton charges of the new fields:

$$B_2 - B_1 = 3\ , \quad L_2 - L_1 = 3\ . \tag{5.1}$$

We note that a similar particle content was introduced in Ref. [88] when gauging only baryon and lepton numbers. For consistency, we stick to their notation for some of the fields and couplings, but we do not make the simplifying assumption that $B_1 = -B_2$ and $L_1 = -L_2$. On the contrary, we focus specifically on the case $B_1 \neq -B_2$ and $L_1 \neq -L_2$ in order to avoid Majorana mass terms for X_R and X_L. The new Higgs field S_{BL} has to have baryon and lepton number equal to -3 in order to generate vector-like masses for the new fermions. An additional Higgs field S_L is required to realize the type I seesaw mechanism for neutrino masses.

The simplest way to cancel gauge flavor anomalies in the quark sector is to add the fermionic fields Ψ^u_R, Ψ^d_R, Ψ^u_L, Ψ^d_L. This unique choice of fields (chiral with respect to the standard model gauge group and vector-like with respect to the flavor gauge symmetry) was proposed in Ref. [105]. We include an additional set of fields (Ψ^ν_R, Ψ^e_R, Ψ^ν_L, Ψ^e_L) to cancel the gauge anomalies in the lepton sector.

The flavor symmetry breaking occurs through the scalar potential. The quark flavor gauge group $SU(3)_{Q_L} \times SU(3)_{u_R} \times SU(3)_{d_R}$ is broken spontaneously by the vacuum

Field	$SU(3)_c$	$SU(2)_L$	$U(1)_Y$	$U(1)_B$	$U(1)_L$	**3** under	$\bar{\mathbf{3}}$ under
Q_L	3	2	$1/6$	$1/3$	0	$SU(3)_{Q_L}$	–
u_R	3	1	$2/3$	$1/3$	0	$SU(3)_{u_R}$	–
d_R	3	1	$-1/3$	$1/3$	0	$SU(3)_{d_R}$	–
l_L	1	2	$-1/2$	0	1	$SU(3)_{l_L}$	–
ν_R	1	1	0	0	1	$SU(3)_{\nu_R}$	–
e_R	1	1	-1	0	1	$SU(3)_{e_R}$	–
H	1	2	$1/2$	0	0	–	–
Ψ_L	1	2	$1/2$	B_1	L_1	–	–
Ψ_R	1	2	$1/2$	B_2	L_2	–	–
η_R	1	1	1	B_1	L_1	–	–
η_L	1	1	1	B_2	L_2	–	–
X_R	1	1	0	B_1	L_1	–	–
X_L	1	1	0	B_2	L_2	–	–
S_{BL}	1	1	0	-3	-3	–	–
S_L	1	1	0	0	-2	–	–
Ψ_R^u	3	1	$2/3$	$1/3$	0	$SU(3)_{Q_L}$	–
Ψ_R^d	3	1	$-1/3$	$1/3$	0	$SU(3)_{Q_L}$	–
Ψ_L^u	3	1	$2/3$	$1/3$	0	$SU(3)_{u_R}$	–
Ψ_L^d	3	1	$-1/3$	$1/3$	0	$SU(3)_{d_R}$	–
Ψ_R^ν	3	1	$2/3$	0	1	$SU(3)_{l_L}$	–
Ψ_R^e	3	1	$-1/3$	0	1	$SU(3)_{l_L}$	–
Ψ_L^ν	3	1	$2/3$	0	1	$SU(3)_{\nu_R}$	–
Ψ_L^e	3	1	$-1/3$	0	1	$SU(3)_{e_R}$	–
Y_u	1	1	0	0	0	$SU(3)_{u_R}$	$SU(3)_{Q_L}$
Y_d	1	1	0	0	0	$SU(3)_{d_R}$	$SU(3)_{Q_L}$
Y_ν	1	1	0	0	0	$SU(3)_{\nu_R}$	$SU(3)_{l_L}$
Y_e	1	1	0	0	0	$SU(3)_{e_R}$	$SU(3)_{l_L}$

Table 5.1: Matter fields of the minimal BLFSM.

expectation values (VEVs) of the scalar fields Y_u and Y_d, while the lepton flavor gauge symmetry $SU(3)_{l_L} \times SU(3)_{\nu_R} \times SU(3)_{e_R}$ is broken by the VEVs of Y_ν and Y_e. In order for the model to explain the hierarchy of standard model Yukawas one needs to include in the flavon potential, in addition to the Higgs and Yukawa fields, additional scalar fields Z being triplets under each of the individual flavor groups, as discussed in Section 5.3.

The Lagrangian of the theory is given by

$$\mathcal{L} = \mathcal{L}_{\text{kin}} + \mathcal{L}_{\text{int}}^{BL} + \mathcal{L}_{\text{int}}^{Y} - V(H, Y, Z) \ , \tag{5.2}$$

where $\mathcal{L}_{\text{kin}}$ describes the dynamics of the fields, $\mathcal{L}_{\text{int}}^{BL}$ corresponds to the interactions in the leptobaryonic sector with the additional Majorana mass term for the right-handed neutrino, $\mathcal{L}_{\text{int}}^{Y}$ consists of Yukawa interactions and mass terms, and $V(H, Y, Z)$ is the scalar potential. In particular:

$$\begin{aligned} \mathcal{L}_{\text{int}}^{BL} &= h_1 \bar{\Psi}_L H \eta_R + h_2 \bar{\Psi}_L \tilde{H} X_R + h_3 \bar{\Psi}_R H \eta_L + \ h_4 \bar{\Psi}_R \tilde{H} X_L \\ &\quad + \lambda_1 \bar{\Psi}_L \Psi_R S_{BL} + \lambda_2 \bar{\eta}_R \eta_L S_{BL} + \ \lambda_3 \bar{X}_R X_L S_{BL} + \lambda_4 \nu_R \nu_R S_L + \text{h.c.} \ , \end{aligned} \tag{5.3}$$

$$\begin{aligned} \mathcal{L}_{\text{int}}^{Y} &= \lambda_u \bar{Q}_L \tilde{H} \Psi_R^u + \lambda_u' \bar{\Psi}_L^u Y_u \Psi_R^u + M_u \bar{\Psi}_L^u u_R + \lambda_d \bar{Q}_L H \Psi_R^d \\ &\quad + \lambda_d' \bar{\Psi}_L^d Y_d \Psi_R^d + M_d \bar{\Psi}_L^d d_R + \lambda_\nu \bar{l}_L \tilde{H} \Psi_R^\nu + \lambda_\nu' \bar{\Psi}_L^\nu Y_\nu \Psi_R^\nu \\ &\quad + M_\nu \bar{\Psi}_L^\nu \nu_R + \lambda_e \bar{l}_L H \Psi_R^e + \lambda_e' \bar{\Psi}_L^e Y_e \Psi_R^e + M_e \bar{\Psi}_L^e e_R + \text{h.c.} \ , \end{aligned} \tag{5.4}$$

and the potential $V(H, Y, Z)$, invariant under the flavor group, is a function of the Higgs and Yukawa fields, as well as other scalar fields in some representations of the flavor group needed to produce a hierarchical pattern of the standard model Yukawa couplings.

5.3 Symmetry breaking

As mentioned in the previous section, the VEVs of the Yukawa fields, $\langle Y \rangle$, spontaneously break the flavor symmetry. The values of those VEVs are governed by the shape of the flavor invariant potential $V(H, Y, Z)$. The standard model Yukawa interactions are obtained

by integrating out the new fermions from the Lagrangian (5.4):

$$y_u = V_q^\dagger \frac{\lambda_u M_u}{\lambda'_u \langle Y_u \rangle} \ , \quad y_d = \frac{\lambda_d M_d}{\lambda'_d \langle Y_d \rangle} \ , \quad y_\nu = V_l^\dagger \frac{\lambda_\nu M_\nu}{\lambda'_\nu \langle Y_\nu \rangle} \ , \quad y_e = \frac{\lambda_e M_e}{\lambda'_e \langle Y_e \rangle} \tag{5.5}$$

and follow an inverted hierarchy pattern [105]. In Eq. (5.5) the unitary matrices V_q and V_l arise after a flavor transformation diagonalizing Y_d and Y_e, respectively. This seesaw-like mechanism for the standard model Yukawa couplings results in the suppression of flavor and electroweak precision constraints. The mass scale for the flavor gauge bosons can be as low as the TeV scale.

Most of the literature regarding dynamical flavor symmetry breaking concentrates only on the case of a global flavor symmetry and is confined to the quark sector. In those models the standard model Yukawa couplings are generated from dimension-five operators and follow the same hierarchy pattern as the VEVs of the Yukawa fields. It was shown in Ref. [109] that the most general renormalizable flavor invariant potential built from Y_u and Y_d after spontaneous symmetry breaking can only give the tree-level vacuum configuration $\langle Y_q \rangle \sim \mathrm{diag}(0, 0, v_q)$, where $q = u, d$. This was proven to hold to all orders in perturbation theory, also at the nonrenormalizable level, in Ref. [110]. The same paper shows that adding new scalar fields in nontrivial representations of the flavor group can yield a hierarchical Yukawa structure of the form $\langle Y_q \rangle \sim v_q \, \mathrm{diag}(\epsilon_1, \epsilon_2, 1)$, where $\epsilon_1 \ll \epsilon_2 \ll 1$. Those ideas were extended to the full quark sector in Ref. [107], explaining not only the quark mass hierarchy, but also the Cabibbo-Kobayashi-Maskawa mixing and the weak CP violating phase. All this was accomplished at the cost of introducing four new scalar fields in the following representations of $SU(3)_{Q_L} \times SU(3)_{u_R} \times SU(3)_{d_R}$: $Z_{Q_1} \sim (3, 1, 1)$, $Z_{Q_2} \sim (3, 1, 1)$, $Z_u \sim (1, 3, 1)$, and $Z_d \sim (1, 1, 3)$.

In our model, and in the case of spontaneously broken gauged flavor symmetries in general, the construction of a flavor invariant potential providing a given Yukawa pattern proceeds along similar lines. However, contrary to models with a global flavor symmetry, for which a hierarchical pattern of the Yukawa VEVs corresponds to a hierarchical pattern of standard model Yukawas, we require an inverted hierarchy of the Yukawa VEVs to emerge.

The first step to explaining the inverted hierarchy of the Yukawa VEVs in models with gauged flavor symmetry in the quark sector was provided in Ref. [111], where an explicit formula for the flavor part of the scalar potential $V(Y)$ is given:

$$\begin{aligned} V(Y) \;=\; & -m_u^2\,\mathrm{Tr}\left(Y_u^\dagger Y_u\right) + \lambda_1^u\,\mathrm{Tr}\left(Y_u^\dagger Y_u\right)^2 + \lambda_2^u\,\mathrm{Tr}\left(Y_u^\dagger Y_u Y_u^\dagger Y_u\right) + \det\left(Y_u\right) \\ & -m_d^2\,\mathrm{Tr}\left(Y_d^\dagger Y_d\right) + \lambda_1^d\,\mathrm{Tr}\left(Y_d^\dagger Y_d\right)^2 + \lambda_2^d\,\mathrm{Tr}\left(Y_d^\dagger Y_d Y_d^\dagger Y_d\right) + \det\left(Y_d\right) \\ & + \Big[m_{ud}^2\,\mathrm{Tr}\left(Y_u^\dagger Y_d\right) + \lambda^{ijkl}\,\mathrm{Tr}\left(Y_i^\dagger Y_j Y_k^\dagger Y_l\right) \\ & + \lambda'^{ijkl}\,\mathrm{Tr}\left(Y_i^\dagger Y_j\right)\mathrm{Tr}\left(Y_k^\dagger Y_l\right) + \epsilon^{ijk} Y_i Y_j Y_k + \mathrm{h.c.}\Big]\,. \end{aligned} \tag{5.6}$$

This potential has a minimum at $\langle Y_q\rangle = \mathrm{diag}(m_q, 0, 0)$, where $q = u, d$. The authors suggest that an inverse hierarchy pattern with all diagonal elements nonzero might be accomplished after including contributions from higher dimensional operators.

Their speculation seems very well-founded. Taking into account dimension-six operators would correspond, at the renormalizable level, to including new scalar fields in the potential involving appropriate interactions with the Yukawa fields. One could use the known results from spontaneous breaking of global flavor symmetry and construct a potential which would give an inverted hierarchy of the Yukawa VEVs in the case of our model. In order to accomplish this, one most likely needs six new scalar fields, three in nontrivial representations of $SU(3)_{Q_L} \times SU(3)_{u_R} \times SU(3)_{d_R}$: $Z_Q \sim (3,1,1)$, $Z_u \sim (1,3,1)$, $Z_d \sim (1,1,3)$, and the other three in the following representations of $SU(3)_{l_L} \times SU(3)_{\nu_R} \times SU(3)_{e_R}$: $Z_l \sim (3,1,1)$, $Z_\nu \sim (1,3,1)$, $Z_e \sim (1,1,3)$. Furthermore, to reproduce not only the standard model Yukawa hierarchy, but also the nonzero mixing and phases in the CKM matrix, additional fields would have to be included. We leave a detailed investigation of this aspect for future work.

5.4 Leptobaryonic dark matter

The dark matter candidate in our model is the fermionic particle X. The calculations of the relic density and direct detection cross section are analogous to those in Ref. [3], assuming that X couples dominantly to the Z_B gauge boson. This analysis was the subject of Section 4.3 of this thesis. The updated limits from the LUX experiment [112] are more

constraining, but there is still a large potion of parameter space available. We recall that in the dark matter analysis we strongly rely on the assumption $B_1 \neq -B_2$. Otherwise, the annihilation cross section would be velocity suppressed and it would not be possible to keep it in agreement with observational constraints in a non-fine-tuned way.

5.5 Phenomenology and constraints

The phenomenology of the quark flavor sector in models with just the flavor symmetry gauged was analyzed in great detail in Refs. [105, 106]. Their results are applicable to our model with the additionally gauged baryon and lepton numbers without any substantial modifications, since the quantum numbers B and L we chose for the flavor-triplet fields in order to cancel the gauge anomalies allow for the same couplings to quarks as in Ref. [105]. The bounds originate mainly from mixing effects between the standard model and new fermions. Although the flavor and electroweak precision constraints are greatly reduced by the seesaw-like mechanism for the standard model Yukawas, they are not absent, especially for the third generation. The relevant processes and precision observables considered in Ref. [105] affected by the mixing are $Z \to b_L \bar{b}_L$, electroweak oblique parameters, $b \to s\gamma$, and V_{tb}. Other bounds come from direct searches. One of the most striking signatures of the model consists of six bottom quarks in the final state. Ref. [106] completes this study by concentrating on a precise analysis of flavor constraints, including those coming from tree-level heavy gauge boson exchanges. The lepton flavor sector still needs to be analyzed.

A phenomenological investigation of the leptobaryonic sector has not been carried out yet as well, even in models with only baryon and lepton numbers gauged. However, we note that for an extension of the standard model with just lepton number gauged such an analysis was performed in Ref. [113]. The authors study the phenomenology of the exotic lepton sector and its effects on Higgs decay rates. One of the unique signatures of their model is a four-lepton final state with the new gauge boson resonance in two of the leptons. It would be interesting to extend their results to the case in which baryon number is gauged as well. We leave such an investigation for future work.

5.6 Conclusions

We have constructed a model (BLFSM) based on the standard model gauge group extended by gauging baryon and lepton numbers, as well as flavor symmetries. The BLFSM provides solutions to some of the most important problems of the standard model, while at the same time not being heavily constrained by experiments. Some of its appealing features are the following:

- → The BLFSM contains a natural dark matter candidate required for the theory to be anomaly-free. A large region of parameter space is consistent with current dark matter experimental constraints.
- → The model incorporates the type I seesaw mechanism for neutrino masses.
- → Proton decay is forbidden by gauge symmetry. Processes violating baryon and lepton number are strongly suppressed.
- → Spontaneous breaking of gauged flavor symmetry through the appropriate shape of the scalar potential can provide a dynamical mechanism generating the hierarchy of standard model Yukawa couplings.

Future work on this model includes constructing the flavor invariant scalar potential which, after spontaneous breaking of the flavor symmetry, yields an inverted hierarchy for the vacuum expectation values of the Yukawa fields, thus explaining the standard model Yukawa hierarchy. It would also be interesting to analyze the LHC constraints on the leptobaryonic and lepton flavor sectors of the theory and propose other specific signatures to look for in experimental searches.

Chapter 6

Thesis summary

This thesis investigates models beyond the standard model which contain new processes violating baryon number but are not plagued by tree-level proton decay. The main body of the thesis is composed of three published papers: Refs. [1], [2], and [3], which constitute Chapters 2, 3, and 4, respectively. Chapter 5 discusses an unpublished idea involving an extension of the standard model with gauged baryon number, lepton number, and flavor symmetry.

In Chapter 2 we consider simple renormalizable models containing new scalars responsible for baryon number violation, in which proton decay does not occur at tree level. We investigate models where the new scalar fields couple to quark or lepton bilinear terms in a gauge invariant way. The sources of baryon number violation are the trilinear and quartic scalar interactions. We identify nine such models and briefly discuss their properties, but concentrate our analysis on the phenomenological aspects of the model containing scalars in the following representations of the standard model gauge group: $X_1 = (\bar{6}, 1, -1/3)$ and $X_2 = (\bar{6}, 1, 2/3)$. We calculate the neutron-antineutron oscillation frequency in this model using the vacuum insertion approximation, discuss the generation of cosmological baryon number, compute the electric dipole moment of the neutron, and analyze constraints from neutral kaon mixing. We show that in this model the neutron-antineutron oscillation signal is potentially detectable by present day experiments, with the mass of the lighter scalar at the TeV scale and the mass of the heavier scalar being as high as at the grand unification scale. Nevertheless, in such a case the constraints on flavor changing neutral currents and the electric dipole moment of the neutron require some very small Yukawa couplings.

In Chapter 3 we concentrate on finding the minimal renormalizable models with just a single scalar leptoquark added to the standard model particle spectrum. As in the previous case, we impose the condition that proton decay not be induced in perturbation theory. There are only two models that fulfill our requirements and contain the scalar leptoquark in the following gauge representations: $X = (3, 2, 7/6)$ and $X = (3, 2, 1/6)$. We perform a detailed analysis of the phenomenology of the first model since it exhibits a top quark mass enhancement of the $\mu \to e\gamma$ branching ratio. Our study includes the calculation of the $\mu \to e\gamma$ decay rate, the $\mu \to e$ conversion rate, and the electric dipole moment of the electron. We show the potential limits which current and future experiments could place on some of the couplings involving the scalar leptoquark. We concentrate on the region of parameter space for which the loop contribution to the charged lepton mass matrix does not overwhelm the tree-level part. Given this naturalness constraint, we find that current experiments are sensitive to leptoquark masses on the order of a hundred TeV, whereas future experiments may push the sensitivity into the several hundred TeV mass region. The model in its original form also predicts baryon number violating nonrenormalizable dimension-five operators triggering proton decay. We show that imposing an appropriate discrete symmetry forbids these dimension-five operators.

In Chapter 4 we propose a simple extension of the minimal supersymmetric standard model, in which baryon and lepton numbers are local gauge symmetries spontaneously broken at the supersymmetry scale. The gauge anomalies are cancelled by adding a set of leptobaryonic chiral superfields. The theory provides a natural explanation for the absence of proton decay. It also predicts that R-parity must be spontaneously broken. However, despite R-parity nonconservation, the remnant Z_2 symmetry from the breaking of the baryon and lepton symmetries ensures that the lightest leptobaryon is stable and may serve as a good dark matter candidate. We discuss the spectrum of the theory, the properties of the dark matter candidate, and the predictions for direct detection experiments. A large region of parameter space is consistent with current dark matter experimental constraints. This model provides concrete exotic supersymmetric signatures associated with having the simultaneous presence of R-parity violating interactions and missing energy signals at the Large Hadron Collider.

In Chapter 5 we describe a non-supersymmetric extension of the standard model with an even larger gauge sector, which now includes gauged baryon, lepton, and flavor symmetries. New leptobaryonic and flavor-triplet fields are required to cancel the anomalies. This theory has a number of virtues. As the model described in Chapter 4, it contains a natural leptobaryonic dark matter candidate required for the theory to be anomaly-free. It realizes the type I seesaw mechanism for neutrino masses. Baryon and lepton number violating processes are heavily suppressed and proton decay is totally forbidden by gauge symmetry. In addition to inheriting those appealing properties, this theory has the potential to explain the hierarchical structure of the standard model Yukawas through the spontaneous breaking of the gauge flavor symmetry by the vacuum expectation values of the Yukawa fields. A nice feature of the model is that the seesaw-like mechanism for the standard model Yukawa couplings offers a suppression of experimental constraints in the flavor sector. Directions for future work are discussed.

Appendices

Appendix A

Effective Hamiltonian for low energy $|\Delta B| = 2$ processes

The process leading to neutron-antineutron oscillations in model 1 is shown in Fig. 2.5. The relevant Feynman rules derived from the Lagrangian (2.2) are the following:

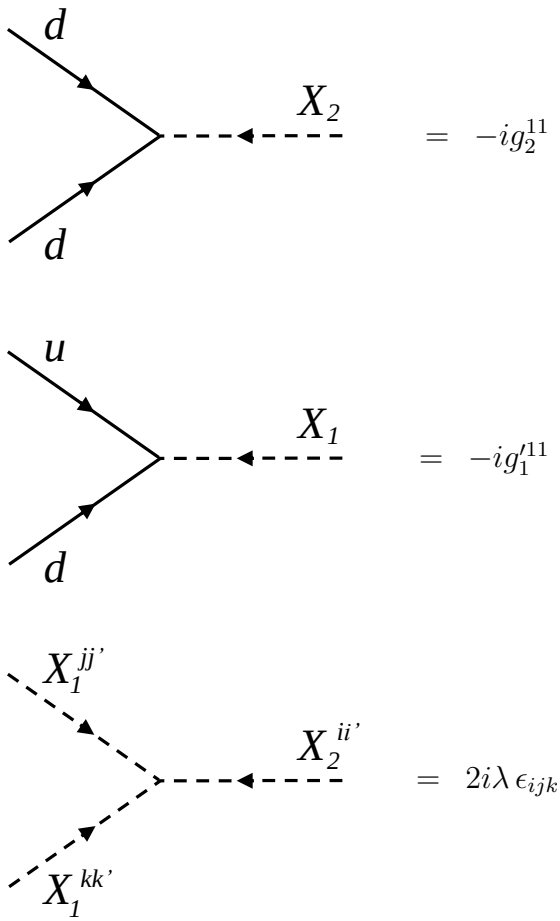

The low energy effective Hamiltonian responsible for the $|\Delta B| = 2$ process is

$$
\begin{aligned}
-i\,\mathcal{H}_{\text{eff}} \;=\; & \frac{-i\,\lambda\,(g_1'^{11})^2\,g_2^{11}}{8(-M_1^2)(-M_1^2)(-M_2^2)}\,\epsilon_{ijk}\epsilon_{i'j'k'}\left(d^{\dot\alpha}_{Ri}d^{\dot\beta}_{Ri'}+d^{\dot\alpha}_{Ri'}d^{\dot\beta}_{Ri}\right)\epsilon_{\dot\alpha\dot\beta} \\
& \times\left(u^{\dot\gamma}_{Rj}d^{\dot\delta}_{Rj'}+u^{\dot\gamma}_{Rj'}d^{\dot\delta}_{Rj}\right)\epsilon_{\dot\gamma\dot\delta}\left(u^{\dot\lambda}_{Rk}d^{\dot\chi}_{Rk'}+u^{\dot\lambda}_{Rk'}d^{\dot\chi}_{Rk}\right)\epsilon_{\dot\lambda\dot\chi}+\text{h.c.}\,, \qquad \text{(A.1)}
\end{aligned}
$$

where Latin letters denote color indices and dotted Greek letters indicate spinor indices. Writing out all the terms in Eq. (A.1) separately, the effective Hamiltonian takes the form

$$
\begin{aligned}
\mathcal{H}_{\text{eff}} \;=\; & -\frac{\lambda\,(g_1'^{11})^2\,g_2^{11}}{8M_1^4M_2^2}\,\epsilon_{ijk}\,\epsilon_{i'j'k'}\,\epsilon_{\dot\alpha\dot\beta}\,\epsilon_{\dot\gamma\dot\delta}\,\epsilon_{\dot\lambda\dot\chi} \\
& \times\Big(d^{\dot\alpha}_{Ri}d^{\dot\beta}_{Ri'}u^{\dot\gamma}_{Rj}d^{\dot\delta}_{Rj'}u^{\dot\lambda}_{Rk}d^{\dot\chi}_{Rk'}+d^{\dot\alpha}_{Ri}d^{\dot\beta}_{Ri'}u^{\dot\gamma}_{Rj}d^{\dot\delta}_{Rj'}u^{\dot\lambda}_{Rk'}d^{\dot\chi}_{Rk}+d^{\dot\alpha}_{Ri}d^{\dot\beta}_{Ri'}u^{\dot\delta}_{Rj'}d^{\dot\gamma}_{Rj}u^{\dot\lambda}_{Rk}d^{\dot\chi}_{Rk'} \\
& +d^{\dot\alpha}_{Ri}d^{\dot\beta}_{Ri'}u^{\dot\delta}_{Rj'}d^{\dot\gamma}_{Rj}u^{\dot\lambda}_{Rk'}d^{\dot\chi}_{Rk}+d^{\dot\alpha}_{Ri'}d^{\dot\beta}_{Ri}u^{\dot\gamma}_{Rj}d^{\dot\delta}_{Rj'}u^{\dot\lambda}_{Rk}d^{\dot\chi}_{Rk'}+d^{\dot\alpha}_{Ri'}d^{\dot\beta}_{Ri}u^{\dot\gamma}_{Rj}d^{\dot\delta}_{Rj'}u^{\dot\lambda}_{Rk'}d^{\dot\chi}_{Rk} \\
& +d^{\dot\alpha}_{Ri'}d^{\dot\beta}_{Ri}u^{\dot\delta}_{Rj'}d^{\dot\gamma}_{Rj}u^{\dot\lambda}_{Rk}d^{\dot\chi}_{Rk'}+d^{\dot\alpha}_{Ri'}d^{\dot\beta}_{Ri}u^{\dot\delta}_{Rj'}d^{\dot\gamma}_{Rj}u^{\dot\lambda}_{Rk'}d^{\dot\chi}_{Rk}\Big)+\text{h.c.}\,. \qquad \text{(A.2)}
\end{aligned}
$$

This expression can be rewritten as

$$
\begin{aligned}
\mathcal{H}_{\text{eff}} \;=\; & -\frac{\lambda\,(g_1'^{11})^2\,g_2^{11}}{4M_1^4M_2^2}\,\epsilon_{ijk}\,\epsilon_{i'j'k'}\,\epsilon_{\dot\alpha\dot\beta}\,\epsilon_{\dot\gamma\dot\delta}\,\epsilon_{\dot\lambda\dot\chi} \\
& \times\Big(d^{\dot\alpha}_{Ri}d^{\dot\beta}_{Ri'}u^{\dot\gamma}_{Rj}d^{\dot\delta}_{Rj'}u^{\dot\lambda}_{Rk}d^{\dot\chi}_{Rk'}+d^{\dot\alpha}_{Ri'}d^{\dot\beta}_{Ri}u^{\dot\gamma}_{Rj}d^{\dot\delta}_{Rj'}u^{\dot\lambda}_{Rk}d^{\dot\chi}_{Rk'} \\
& +d^{\dot\alpha}_{Ri}d^{\dot\beta}_{Ri'}u^{\dot\gamma}_{Rj'}d^{\dot\delta}_{Rj}u^{\dot\lambda}_{Rk}d^{\dot\chi}_{Rk'}+d^{\dot\alpha}_{Ri}d^{\dot\beta}_{Ri'}u^{\dot\gamma}_{Rj}d^{\dot\delta}_{Rj'}u^{\dot\lambda}_{Rk'}d^{\dot\chi}_{Rk}\Big)+\text{h.c.}
\end{aligned}
$$

$$
\begin{aligned}
= \; & -\frac{\lambda\,(g_1'^{11})^2\,g_2^{11}}{4M_1^4M_2^2}d^{\dot\alpha}_{Ri}d^{\dot\beta}_{Ri'}u^{\dot\gamma}_{Rj}d^{\dot\delta}_{Rj'}u^{\dot\lambda}_{Rk}d^{\dot\chi}_{Rk'}\,\epsilon_{\dot\alpha\dot\beta}\,\epsilon_{\dot\gamma\dot\delta}\,\epsilon_{\dot\lambda\dot\chi} \\
& \times\left(\epsilon_{ijk}\,\epsilon_{i'j'k'}+\epsilon_{i'jk}\,\epsilon_{ij'k'}+\epsilon_{ij'k}\,\epsilon_{i'jk'}+\epsilon_{ijk'}\,\epsilon_{i'j'k}\right)+\text{h.c.}\,, \qquad \text{(A.3)}
\end{aligned}
$$

which is equivalent to Eq. (2.12).

Appendix B

$|\Delta m|$ in the vacuum insertion approximation

Using Eq. (2.12), we can write the matrix element (2.11) as

$$\begin{aligned}\langle\bar{n}|\mathcal{H}_{\rm eff}|n\rangle &= -\frac{\lambda\left(g_1'^{11}\right)^2 g_2^{11}}{4M_1^4M_2^2}\epsilon_{\dot\alpha\dot\beta}\,\epsilon_{\dot\gamma\dot\delta}\,\epsilon_{\dot\lambda\dot\chi}\left(\epsilon_{ijk}\,\epsilon_{i'j'k'}+\epsilon_{i'jk}\,\epsilon_{ij'k'}+\epsilon_{ij'k}\,\epsilon_{i'jk'}+\epsilon_{ijk'}\,\epsilon_{i'j'k}\right)\\ &\quad\times\langle\bar{n}|d^{\dot\alpha}_{Ri}d^{\dot\beta}_{Ri'}u^{\dot\gamma}_{Rj}d^{\dot\delta}_{Rj'}u^{\dot\lambda}_{Rk}d^{\dot\chi}_{Rk'}|n\rangle\ . \end{aligned}\tag{B.1}$$

Applying the vacuum insertion approximation and keeping track of the minus signs when interchanging two fermionic fields gives

$$\begin{aligned}\langle\bar{n}|\mathcal{H}_{\rm eff}|n\rangle &= -\frac{\lambda\left(g_1'^{11}\right)^2 g_2^{11}}{4M_1^4M_2^2}\epsilon_{\dot\alpha\dot\beta}\,\epsilon_{\dot\gamma\dot\delta}\,\epsilon_{\dot\lambda\dot\chi}\left(\epsilon_{ijk}\,\epsilon_{i'j'k'}+\epsilon_{i'jk}\,\epsilon_{ij'k'}+\epsilon_{ij'k}\,\epsilon_{i'jk'}+\epsilon_{ijk'}\,\epsilon_{i'j'k}\right)\\ &\times\Big[-\langle\bar{n}|d^{\dot\alpha}_{Ri}d^{\dot\beta}_{Ri'}u^{\dot\gamma}_{Rj}|0\rangle\langle0|d^{\dot\delta}_{Rj'}d^{\dot\chi}_{Rk'}u^{\dot\lambda}_{Rk}|n\rangle+\langle\bar{n}|d^{\dot\alpha}_{Ri}d^{\dot\beta}_{Ri'}u^{\dot\lambda}_{Rk}|0\rangle\langle0|d^{\dot\delta}_{Rj'}d^{\dot\chi}_{Rk'}u^{\dot\gamma}_{Rj}|n\rangle\\ &\quad-\langle\bar{n}|d^{\dot\delta}_{Rj'}d^{\dot\chi}_{Rk'}u^{\dot\gamma}_{Rj}|0\rangle\langle0|d^{\dot\alpha}_{Ri}d^{\dot\beta}_{Ri'}u^{\dot\lambda}_{Rk}|n\rangle+\langle\bar{n}|d^{\dot\delta}_{Rj'}d^{\dot\chi}_{Rk'}u^{\dot\lambda}_{Rk}|0\rangle\langle0|d^{\dot\alpha}_{Ri}d^{\dot\beta}_{Ri'}u^{\dot\gamma}_{Rj}|n\rangle\\ &\quad+\langle\bar{n}|d^{\dot\delta}_{Rj'}d^{\dot\beta}_{Ri'}u^{\dot\gamma}_{Rj}|0\rangle\langle0|d^{\dot\alpha}_{Ri}d^{\dot\chi}_{Rk'}u^{\dot\lambda}_{Rk}|n\rangle-\langle\bar{n}|d^{\dot\delta}_{Rj'}d^{\dot\beta}_{Ri'}u^{\dot\lambda}_{Rk}|0\rangle\langle0|d^{\dot\alpha}_{Ri}d^{\dot\chi}_{Rk'}u^{\dot\gamma}_{Rj}|n\rangle\\ &\quad+\langle\bar{n}|d^{\dot\alpha}_{Ri}d^{\dot\delta}_{Rj'}u^{\dot\gamma}_{Rj}|0\rangle\langle0|d^{\dot\beta}_{Ri'}d^{\dot\chi}_{Rk'}u^{\dot\lambda}_{Rk}|n\rangle-\langle\bar{n}|d^{\dot\alpha}_{Ri}d^{\dot\delta}_{Rj'}u^{\dot\lambda}_{Rk}|0\rangle\langle0|d^{\dot\beta}_{Ri'}d^{\dot\chi}_{Rk'}u^{\dot\gamma}_{Rj}|n\rangle\\ &\quad+\langle\bar{n}|d^{\dot\alpha}_{Ri}d^{\dot\chi}_{Rk'}u^{\dot\gamma}_{Rj}|0\rangle\langle0|d^{\dot\delta}_{Rj'}d^{\dot\beta}_{Ri'}u^{\dot\lambda}_{Rk}|n\rangle-\langle\bar{n}|d^{\dot\alpha}_{Ri}d^{\dot\chi}_{Rk'}u^{\dot\lambda}_{Rk}|0\rangle\langle0|d^{\dot\delta}_{Rj'}d^{\dot\beta}_{Ri'}u^{\dot\gamma}_{Rj}|n\rangle\\ &\quad+\langle\bar{n}|d^{\dot\chi}_{Rk'}d^{\dot\beta}_{Ri'}u^{\dot\gamma}_{Rj}|0\rangle\langle0|d^{\dot\delta}_{Rj'}d^{\dot\alpha}_{Ri}u^{\dot\lambda}_{Rk}|n\rangle-\langle\bar{n}|d^{\dot\chi}_{Rk'}d^{\dot\beta}_{Ri'}u^{\dot\lambda}_{Rk}|0\rangle\langle0|d^{\dot\delta}_{Rj'}d^{\dot\alpha}_{Ri}u^{\dot\gamma}_{Rj}|n\rangle\Big]. \end{aligned}\tag{B.2}$$

Symmetry considerations yield

$$\begin{aligned}\langle 0|d^{\dot\alpha}_{Ri}d^{\dot\beta}_{Rj}u^{\dot\gamma}_{Rk}|n\rangle &= \frac{1}{12}\epsilon_{ijk}\,\xi(p)\left[\epsilon^{\dot\alpha\dot\gamma}u^{\dot\beta}_R(p)+\epsilon^{\dot\beta\dot\gamma}u^{\dot\alpha}_R(p)\right],\\ \langle \bar n|d^{\dot\alpha}_{Ri}d^{\dot\beta}_{Rj}u^{\dot\gamma}_{Rk}|0\rangle &= \frac{1}{12}\epsilon_{ijk}\,\xi(p)^*\left[\epsilon^{\dot\alpha\dot\gamma}v^{\dot\beta}_R(p)+\epsilon^{\dot\beta\dot\gamma}v^{\dot\alpha}_R(p)\right],\end{aligned} \tag{B.3}$$

where p is the momentum of the neutron, while $u_R(p)$ and $v_R(p)$ are spinors. Comparing those formulas with the following relation (see Ref. [59]):

$$\epsilon_{ijk}\epsilon_{\dot\alpha\dot\beta}\langle 0|u^{\dot\alpha}_{Li}u^{\dot\gamma}_{Lk}d^{\dot\beta}_{Lj}|p(k)\rangle = \beta(k)\,u^{\dot\gamma}_L(k) \tag{B.4}$$

(with the value of β calculated using lattice methods), and acting on both sides of Eq. (B.3) with $\epsilon_{ijk}\epsilon_{\dot\alpha\dot\beta}$, gives

$$\xi(p) = -\frac{2}{3}\beta(p)\,. \tag{B.5}$$

Therefore

$$\begin{aligned}&\langle \bar n|d^{\dot\alpha}_{Ri}d^{\dot\beta}_{Ri'}u^{\dot\gamma}_{Rj}|0\rangle\langle 0|d^{\dot\delta}_{Rj'}d^{\dot\chi}_{Rk}u^{\dot\lambda}_{Rk'}|n\rangle\\ &\qquad= \frac{1}{144}\epsilon_{ii'j}\epsilon_{j'kk'}|\xi(p)|^2\left[\epsilon^{\dot\alpha\dot\gamma}v^{\dot\beta}_R(p)+\epsilon^{\dot\beta\dot\gamma}v^{\dot\alpha}_R(p)\right]\left[\epsilon^{\dot\delta\dot\lambda}u^{\dot\chi}_R(p)+\epsilon^{\dot\chi\dot\lambda}u^{\dot\delta}_R(p)\right].\end{aligned} \tag{B.6}$$

The contribution of the first term in Eq. (B.2) contains the following factor:

$$\begin{aligned}&\epsilon_{ii'j}\,\epsilon_{j'k'k}\left(\epsilon_{ijk}\,\epsilon_{i'j'k'}+\epsilon_{i'jk}\,\epsilon_{ij'k'}+\epsilon_{ij'k}\,\epsilon_{i'jk'}+\epsilon_{ijk'}\,\epsilon_{i'j'k}\right)\\ &=\epsilon_{ii'j}\,\epsilon_{ijk}\,\epsilon_{i'j'k'}\,\epsilon_{j'k'k}+\epsilon_{ii'j}\,\epsilon_{i'jk}\,\epsilon_{j'k'k}\,\epsilon_{ij'k'}+\epsilon_{ii'j}\,\epsilon_{i'jk'}\,\epsilon_{j'k'k}\,\epsilon_{ij'k}+\epsilon_{ii'j}\,\epsilon_{ijk'}\,\epsilon_{j'k'k}\,\epsilon_{i'j'k}\\ &=(-2\delta_{i'k})(2\delta_{i'k})+(2\delta_{ik})(2\delta_{ik})+(2\delta_{ik'})(-2\delta_{ik'})+(-2\delta_{i'k'})(-2\delta_{i'k'})=0\,.\end{aligned} \tag{B.7}$$

Similarly, the contributions from all other terms in which a single matrix element contains the pair of indices (i,i'), (j,j'), or (k,k') vanish as well.

This leaves us with

$$\begin{aligned}\langle\bar{n}|\mathcal{H}_{\rm eff}|n\rangle \;=\; & -\frac{\lambda\left(g_1'^{11}\right)^2 g_2^{11}}{4M_1^4M_2^2}\epsilon_{\dot\alpha\dot\beta}\,\epsilon_{\dot\gamma\dot\delta}\,\epsilon_{\dot\lambda\dot\chi}\left(\epsilon_{ijk}\,\epsilon_{i'j'k'}+\epsilon_{i'jk}\,\epsilon_{ij'k'}+\epsilon_{ij'k}\,\epsilon_{i'jk'}+\epsilon_{ijk'}\,\epsilon_{i'j'k}\right)\\ & \times\Big[\langle\bar{n}|d^{\dot\alpha}_{Ri}d^{\dot\chi}_{Rk'}u^{\dot\gamma}_{Rj}|0\rangle\langle 0|d^{\dot\delta}_{Rj'}d^{\dot\beta}_{Ri'}u^{\dot\lambda}_{Rk}|n\rangle-\langle\bar{n}|d^{\dot\delta}_{Rj'}d^{\dot\beta}_{Ri'}u^{\dot\lambda}_{Rk}|0\rangle\langle 0|d^{\dot\alpha}_{Ri}d^{\dot\chi}_{Rk'}u^{\dot\gamma}_{Rj}|n\rangle\\ & +\langle\bar{n}|d^{\dot\chi}_{Rk'}d^{\dot\beta}_{Ri'}u^{\dot\gamma}_{Rj}|0\rangle\langle 0|d^{\dot\delta}_{Rj'}d^{\dot\alpha}_{Ri}u^{\dot\lambda}_{Rk}|n\rangle-\langle\bar{n}|d^{\dot\alpha}_{Ri}d^{\dot\delta}_{Rj'}u^{\dot\lambda}_{Rk}|0\rangle\langle 0|d^{\dot\beta}_{Ri'}d^{\dot\chi}_{Rk'}u^{\dot\gamma}_{Rj}|n\rangle\Big].\end{aligned} \tag{B.8}$$

Using Eq. (B.6), the four terms in Eq. (B.8) can be calculated separately.

$$\begin{aligned}\textbf{(1)}\;\langle\bar{n}|\mathcal{H}_{\rm eff}|n\rangle_1 \;=\; & -\frac{\lambda\left(g_1'^{11}\right)^2 g_2^{11}}{4M_1^4M_2^2}\epsilon_{\dot\alpha\dot\beta}\,\epsilon_{\dot\gamma\dot\delta}\,\epsilon_{\dot\lambda\dot\chi}\left(\epsilon_{ijk}\,\epsilon_{i'j'k'}+\epsilon_{i'jk}\,\epsilon_{ij'k'}+\epsilon_{ij'k}\,\epsilon_{i'jk'}+\epsilon_{ijk'}\,\epsilon_{i'j'k}\right)\\ & \times\langle\bar{n}|d^{\dot\alpha}_{Ri}d^{\dot\chi}_{Rk'}u^{\dot\gamma}_{Rj}|0\rangle\langle 0|d^{\dot\delta}_{Rj'}d^{\dot\beta}_{Ri'}u^{\dot\lambda}_{Rk}|n\rangle\\ = & -\frac{\lambda\left(g_1'^{11}\right)^2 g_2^{11}}{4M_1^4M_2^2}\epsilon_{\dot\alpha\dot\beta}\,\epsilon_{\dot\gamma\dot\delta}\,\epsilon_{\dot\lambda\dot\chi}\left(\epsilon_{ijk}\,\epsilon_{i'j'k'}+\epsilon_{i'jk}\,\epsilon_{ij'k'}+\epsilon_{ij'k}\,\epsilon_{i'jk'}+\epsilon_{ijk'}\,\epsilon_{i'j'k}\right)\\ & \times\frac{1}{144}\epsilon_{ik'j}\epsilon_{j'i'k}|\xi(p)|^2\left[\epsilon^{\dot\alpha\dot\gamma}v_R^{\dot\chi}(p)+\epsilon^{\dot\chi\dot\gamma}v_R^{\dot\alpha}(p)\right]\left[\epsilon^{\dot\delta\dot\lambda}u_R^{\dot\beta}(p)+\epsilon^{\dot\beta\dot\lambda}u_R^{\dot\delta}(p)\right].\end{aligned} \tag{B.9}$$

It is straightforward to show that

$$\epsilon_{ik'j}\epsilon_{j'i'k}\left(\epsilon_{ijk}\,\epsilon_{i'j'k'}+\epsilon_{i'jk}\,\epsilon_{ij'k'}+\epsilon_{ij'k}\,\epsilon_{i'jk'}+\epsilon_{ijk'}\,\epsilon_{i'j'k}\right)=72\,. \tag{B.10}$$

Using the property of the antisymmetric symbols, $\epsilon^{\dot\lambda\dot\alpha}\epsilon_{\dot\lambda\dot\beta}=\delta^{\dot\alpha}_{\dot\beta}$, gives

$$\begin{aligned}&\epsilon^{\dot\alpha\dot\gamma}v_R^{\dot\chi}(p)\epsilon^{\dot\delta\dot\lambda}u_R^{\dot\beta}(p)\epsilon_{\dot\alpha\dot\beta}\epsilon_{\dot\gamma\dot\delta}\epsilon_{\dot\lambda\dot\chi}=-\epsilon^{\dot\alpha\dot\gamma}v_R^{\dot\chi}(p)\epsilon^{\dot\beta\dot\lambda}u_R^{\dot\delta}(p)\epsilon_{\dot\alpha\dot\beta}\epsilon_{\dot\gamma\dot\delta}\epsilon_{\dot\lambda\dot\chi}\\ &=\frac{1}{2}\epsilon^{\dot\chi\dot\gamma}v_R^{\dot\alpha}(p)\epsilon^{\dot\delta\dot\lambda}u_R^{\dot\beta}(p)\epsilon_{\dot\alpha\dot\beta}\epsilon_{\dot\gamma\dot\delta}\epsilon_{\dot\lambda\dot\chi}=\epsilon^{\dot\chi\dot\gamma}v_R^{\dot\alpha}(p)\epsilon^{\dot\beta\dot\lambda}u_R^{\dot\delta}(p)\epsilon_{\dot\alpha\dot\beta}\epsilon_{\dot\gamma\dot\delta}\epsilon_{\dot\lambda\dot\chi}=v_R^{\dot\alpha}(p)\epsilon_{\dot\alpha\dot\beta}u_R^{\dot\beta}(p)\,.\end{aligned} \tag{B.11}$$

All this yields

$$\langle\bar{n}|\mathcal{H}_{\rm eff}|n\rangle_1=-\frac{3\lambda\left(g_1'^{11}\right)^2 g_2^{11}}{8M_1^4M_2^2}|\xi(p)|^2v_R^{\dot\alpha}(p)\epsilon_{\dot\alpha\dot\beta}u_R^{\dot\beta}(p)\,. \tag{B.12}$$

$$\textbf{(2)}\ \langle\bar{n}|\mathcal{H}_{\rm eff}|n\rangle_2 = \frac{\lambda\left(g_1'^{11}\right)^2 g_2^{11}}{4M_1^4M_2^2}\epsilon_{\dot\alpha\dot\beta}\,\epsilon_{\dot\gamma\dot\delta}\,\epsilon_{\dot\lambda\dot\chi}\left(\epsilon_{ijk}\,\epsilon_{i'j'k'}+\epsilon_{i'jk}\,\epsilon_{ij'k'}+\epsilon_{ij'k}\,\epsilon_{i'jk'}+\epsilon_{ijk'}\,\epsilon_{i'j'k}\right)$$
$$\times\frac{1}{144}\epsilon_{j'i'k}\epsilon_{ik'j}|\xi(p)|^2\left[\epsilon^{\dot\delta\dot\lambda}v_R^{\dot\beta}(p)+\epsilon^{\dot\beta\dot\lambda}v_R^{\dot\delta}(p)\right]\left[\epsilon^{\dot\alpha\dot\gamma}u_R^{\dot\chi}(p)+\epsilon^{\dot\chi\dot\gamma}u_R^{\dot\alpha}(p)\right]. \tag{B.13}$$

Using the relations:

$$\epsilon_{j'i'k}\epsilon_{ik'j}\left(\epsilon_{ijk}\,\epsilon_{i'j'k'}+\epsilon_{i'jk}\,\epsilon_{ij'k'}+\epsilon_{ij'k}\,\epsilon_{i'jk'}+\epsilon_{ijk'}\,\epsilon_{i'j'k}\right)=72 \tag{B.14}$$

and

$$-\epsilon^{\dot\delta\dot\lambda}v_R^{\dot\beta}(p)\epsilon^{\dot\alpha\dot\gamma}u_R^{\dot\chi}(p)\epsilon_{\dot\alpha\dot\beta}\epsilon_{\dot\gamma\dot\delta}\epsilon_{\dot\lambda\dot\chi}=-\frac{1}{2}\epsilon^{\dot\delta\dot\lambda}v_R^{\dot\beta}(p)\epsilon^{\dot\chi\dot\gamma}u_R^{\dot\alpha}(p)\epsilon_{\dot\alpha\dot\beta}\epsilon_{\dot\gamma\dot\delta}\epsilon_{\dot\lambda\dot\chi}$$
$$=\epsilon^{\dot\beta\dot\lambda}v_R^{\dot\delta}(p)\epsilon^{\dot\alpha\dot\gamma}u_R^{\dot\chi}(p)\epsilon_{\dot\alpha\dot\beta}\epsilon_{\dot\gamma\dot\delta}\epsilon_{\dot\lambda\dot\chi}=-\epsilon^{\dot\beta\dot\lambda}v_R^{\dot\delta}(p)\epsilon^{\dot\chi\dot\gamma}u_R^{\dot\alpha}(p)\epsilon_{\dot\alpha\dot\beta}\epsilon_{\dot\gamma\dot\delta}\epsilon_{\dot\lambda\dot\chi}=v_R^{\dot\alpha}(p)\epsilon_{\dot\alpha\dot\beta}u_R^{\dot\beta}(p)\,, \tag{B.15}$$

we arrive at

$$\langle\bar{n}|\mathcal{H}_{\rm eff}|n\rangle_2=-\frac{3\lambda\left(g_1'^{11}\right)^2 g_2^{11}}{8M_1^4M_2^2}|\xi(p)|^2v_R^{\dot\alpha}(p)\epsilon_{\dot\alpha\dot\beta}u_R^{\dot\beta}(p)\,. \tag{B.16}$$

$$\textbf{(3)}\ \langle\bar{n}|\mathcal{H}_{\rm eff}|n\rangle_3 = -\frac{\lambda\left(g_1'^{11}\right)^2 g_2^{11}}{4M_1^4M_2^2}\epsilon_{\dot\alpha\dot\beta}\,\epsilon_{\dot\gamma\dot\delta}\,\epsilon_{\dot\lambda\dot\chi}\left(\epsilon_{ijk}\,\epsilon_{i'j'k'}+\epsilon_{i'jk}\,\epsilon_{ij'k'}+\epsilon_{ij'k}\,\epsilon_{i'jk'}+\epsilon_{ijk'}\,\epsilon_{i'j'k}\right)$$
$$\times\frac{1}{144}\epsilon_{k'i'j}\epsilon_{j'ik}|\xi(p)|^2\left[\epsilon^{\dot\chi\dot\gamma}v_R^{\dot\beta}(p)+\epsilon^{\dot\beta\dot\gamma}v_R^{\dot\chi}(p)\right]\left[\epsilon^{\dot\delta\dot\lambda}u_R^{\dot\alpha}(p)+\epsilon^{\dot\alpha\dot\lambda}u_R^{\dot\delta}(p)\right]. \tag{B.17}$$

In this case

$$\epsilon_{k'i'j}\epsilon_{j'ik}\left(\epsilon_{ijk}\,\epsilon_{i'j'k'}+\epsilon_{i'jk}\,\epsilon_{ij'k'}+\epsilon_{ij'k}\,\epsilon_{i'jk'}+\epsilon_{ijk'}\,\epsilon_{i'j'k}\right)=-72 \tag{B.18}$$

and

$$-\frac{1}{2}\epsilon^{\dot\chi\dot\gamma}v_R^{\dot\beta}(p)\epsilon^{\dot\delta\dot\lambda}u_R^{\dot\alpha}(p)\epsilon_{\dot\alpha\dot\beta}\epsilon_{\dot\gamma\dot\delta}\epsilon_{\dot\lambda\dot\chi}=-\epsilon^{\dot\chi\dot\gamma}v_R^{\dot\beta}(p)\epsilon^{\dot\alpha\dot\lambda}u_R^{\dot\delta}(p)\epsilon_{\dot\alpha\dot\beta}\epsilon_{\dot\gamma\dot\delta}\epsilon_{\dot\lambda\dot\chi}$$
$$=-\epsilon^{\dot\beta\dot\gamma}v_R^{\dot\chi}(p)\epsilon^{\dot\delta\dot\lambda}u_R^{\dot\alpha}(p)\epsilon_{\dot\alpha\dot\beta}\epsilon_{\dot\gamma\dot\delta}\epsilon_{\dot\lambda\dot\chi}=\epsilon^{\dot\beta\dot\gamma}v_R^{\dot\chi}(p)\epsilon^{\dot\alpha\dot\lambda}u_R^{\dot\delta}(p)\epsilon_{\dot\alpha\dot\beta}\epsilon_{\dot\gamma\dot\delta}\epsilon_{\dot\lambda\dot\chi}=v_R^{\dot\alpha}(p)\epsilon_{\dot\alpha\dot\beta}u_R^{\dot\beta}(p)\,, \tag{B.19}$$

which gives

$$\langle\bar{n}|\mathcal{H}_{\rm eff}|n\rangle_3=-\frac{3\lambda\left(g_1'^{11}\right)^2 g_2^{11}}{8M_1^4M_2^2}|\xi(p)|^2v_R^{\dot\alpha}(p)\epsilon_{\dot\alpha\dot\beta}u_R^{\dot\beta}(p)\,. \tag{B.20}$$

$$\textbf{(4)}\ \langle\bar{n}|\mathcal{H}_{\rm eff}|n\rangle_4 = \frac{\lambda\left(g_1'^{11}\right)^2 g_2^{11}}{4M_1^4M_2^2}\epsilon_{\dot\alpha\dot\beta}\,\epsilon_{\dot\gamma\dot\delta}\,\epsilon_{\dot\lambda\dot\chi}\left(\epsilon_{ijk}\,\epsilon_{i'j'k'}+\epsilon_{i'jk}\,\epsilon_{ij'k'}+\epsilon_{ij'k}\,\epsilon_{i'jk'}+\epsilon_{ijk'}\,\epsilon_{i'j'k}\right)$$
$$\times\frac{1}{144}\epsilon_{ij'k}\epsilon_{i'k'j}|\xi(p)|^2\left[\epsilon^{\dot\alpha\dot\lambda}v_R^{\dot\delta}(p)+\epsilon^{\dot\delta\dot\lambda}v_R^{\dot\alpha}(p)\right]\left[\epsilon^{\dot\beta\dot\gamma}u_R^{\dot\chi}(p)+\epsilon^{\dot\chi\dot\gamma}u_R^{\dot\beta}(p)\right]. \tag{B.21}$$

Again, it is easy to show that

$$\epsilon_{ij'k}\epsilon_{i'k'j}\left(\epsilon_{ijk}\,\epsilon_{i'j'k'}+\epsilon_{i'jk}\,\epsilon_{ij'k'}+\epsilon_{ij'k}\,\epsilon_{i'jk'}+\epsilon_{ijk'}\,\epsilon_{i'j'k}\right)=-72 \tag{B.22}$$

and

$$-\epsilon^{\dot\alpha\dot\lambda}v_R^{\dot\delta}(p)\epsilon^{\dot\beta\dot\gamma}u_R^{\dot\chi}(p)\epsilon_{\dot\alpha\dot\beta}\epsilon_{\dot\gamma\dot\delta}\epsilon_{\dot\lambda\dot\chi}=\epsilon^{\dot\alpha\dot\lambda}v_R^{\dot\delta}(p)\epsilon^{\dot\chi\dot\gamma}u_R^{\dot\beta}(p)\epsilon_{\dot\alpha\dot\beta}\epsilon_{\dot\gamma\dot\delta}\epsilon_{\dot\lambda\dot\chi}$$
$$=\epsilon^{\dot\delta\dot\lambda}v_R^{\dot\alpha}(p)\epsilon^{\dot\beta\dot\gamma}u_R^{\dot\chi}(p)\epsilon_{\dot\alpha\dot\beta}\epsilon_{\dot\gamma\dot\delta}\epsilon_{\dot\lambda\dot\chi}=\frac{1}{2}\epsilon^{\dot\delta\dot\lambda}v_R^{\dot\alpha}(p)\epsilon^{\dot\chi\dot\gamma}u_R^{\dot\beta}(p)\epsilon_{\dot\alpha\dot\beta}\epsilon_{\dot\gamma\dot\delta}\epsilon_{\dot\lambda\dot\chi}=v_R^{\dot\alpha}(p)\epsilon_{\dot\alpha\dot\beta}u_R^{\dot\beta}(p)\ , \tag{B.23}$$

so that

$$\langle\bar{n}|\mathcal{H}_{\rm eff}|n\rangle_4=-\frac{3\lambda\left(g_1'^{11}\right)^2 g_2^{11}}{8M_1^4M_2^2}|\xi(p)|^2v_R^{\dot\alpha}(p)\epsilon_{\dot\alpha\dot\beta}u_R^{\dot\beta}(p)\ . \tag{B.24}$$

Inserting relations (B.12), (B.16), (B.20), and (B.24) into Eq. (B.8) gives

$$|\Delta m|=|\langle\bar{n}|\mathcal{H}_{\rm eff}|n\rangle|=\frac{3\lambda|\left(g_1'^{11}\right)^2 g_2^{11}|}{2M_1^4M_2^2}|\xi(p)|^2=2\lambda\beta^2\frac{|\left(g_1'^{11}\right)^2 g_2^{11}|}{3M_1^4M_2^2}\ , \tag{B.25}$$

which is exactly Eq. (2.14).

Appendix C

Baryon asymmetry

The diagrams responsible for generating baryon asymmetry in model 1 are shown below.

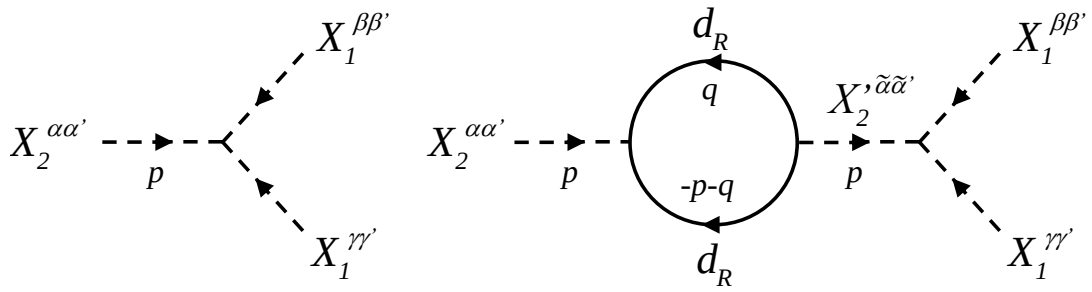

The relevant Feynman rules are listed in Appendix A.

- The tree-level contribution to the amplitude for the process $X_2 \to \bar{X}_1 \bar{X}_1$ is

$$i\mathcal{M}^{\rm tree}_{X_2 \to \bar{X}_1 \bar{X}_1} \;=\; 2i\lambda\, \epsilon_{\alpha\beta\gamma}\, \epsilon_{\alpha'\beta'\gamma'}\;. \tag{C.1}$$

- The one-loop contribution is given by

$$i\mathcal{M}^{1-\rm loop}_{X_2 \to \bar{X}_1 \bar{X}_1} \;=\; \frac{2\,\tilde{\lambda}\,{\rm Tr}(g_2\,\tilde{g}_2^\dagger)}{M_2^2 - \tilde{M}_2^2}\,\epsilon_{\alpha\beta\gamma}\,\epsilon_{\alpha'\beta'\gamma'} \int \frac{d^4q}{(2\pi)^4}\;{\rm Tr}\left(\frac{\not{q}}{q^2+i\epsilon}\,\frac{\not{p}+\not{q}}{(p+q)^2+i\epsilon}\right). \tag{C.2}$$

The loop integral is equal to

$$I = \int \frac{d^4q}{(2\pi)^4}\,\mathrm{Tr}\left(\frac{\not{q}}{q^2+i\epsilon}\,\frac{\not{p}+\not{q}}{(p+q)^2+i\epsilon}\right) = 4\int \frac{d^4q}{(2\pi)^4}\frac{p\cdot q+q^2}{(q^2+i\epsilon)[(p+q)^2+i\epsilon]}\ . \quad \text{(C.3)}$$

We are interested only in the absorptive part,

$$\begin{aligned} I_{\rm abs} &= 4\int \frac{d^4q}{(2\pi)^4}\left[i\pi\delta(q^2)\right]\left[i\pi\delta\left((p+q)^2\right)\right](p\cdot q+q^2) \\ &= \frac{p^2}{16\pi^2}\int d^4q\,\delta(q^2)\,\delta\!\left(\frac{p^2}{2}+p\cdot q\right). \end{aligned} \quad \text{(C.4)}$$

Choosing center of mass coordinates, $p=(M_2,\vec{0})$, the integral takes the form

$$I_{\rm abs} = \frac{M_2}{4\pi}\int d|\vec{q}|\,|\vec{q}|^2\,\delta\!\left(|\vec{q}|^2-\frac{M_2^2}{4}\right) = \frac{M_2^2}{16\pi}\ , \quad \text{(C.5)}$$

therefore

$$i\mathcal{M}^{1-\rm loop}_{X_2\to\bar{X}_1\bar{X}_1} \;=\; \frac{\tilde{\lambda}\,M_2^2\,\mathrm{Tr}(g_2\,\tilde{g}_2^\dagger)}{8\pi(M_2^2-\tilde{M}_2^2)}\,\epsilon_{\alpha\beta\gamma}\,\epsilon_{\alpha'\beta'\gamma'}\ . \quad \text{(C.6)}$$

The sum of the tree-level and one-loop contribution to the amplitude is

$$i\mathcal{M}_{X_2\to\bar{X}_1\bar{X}_1} \;=\; 2i\left[\lambda - i\tilde{\lambda}\frac{M_2^2\,\mathrm{Tr}(g_2\,\tilde{g}_2^\dagger)}{16\pi(M_2^2-\tilde{M}_2^2)}\right]\epsilon_{\alpha\beta\gamma}\,\epsilon_{\alpha'\beta'\gamma'}\ . \quad \text{(C.7)}$$

In order to calculate the decay rate, we compute the squared matrix element summed over the final states,

$$\begin{aligned} \sum_{\text{final colors}} |\mathcal{M}|^2_{\alpha\alpha',\mu\mu'} &= 4\left|\lambda - i\tilde{\lambda}\frac{M_2^2\,\mathrm{Tr}(g_2\,\tilde{g}_2^\dagger)}{16\pi(M_2^2-\tilde{M}_2^2)}\right|^2 \frac{1}{2}\left(\delta_{\beta\nu}\delta_{\beta'\nu'}+\delta_{\beta\nu'}\delta_{\beta'\nu}\right) \\ &\quad\times\frac{1}{2}\left(\delta_{\gamma\lambda}\delta_{\gamma'\lambda'}+\delta_{\gamma\lambda'}\delta_{\lambda\gamma'}\right)\epsilon_{\alpha\beta\gamma}\,\epsilon_{\alpha'\beta'\gamma'}\,\epsilon_{\mu\nu\lambda}\,\epsilon_{\mu'\nu'\lambda'} \\ &\simeq\; 24\left[|\lambda|^2+\frac{M_2^2\,\mathrm{Re}\left(i\lambda\tilde{\lambda}^*\mathrm{Tr}(g_2\,\tilde{g}_2^\dagger)\right)}{8\pi(M_2^2-\tilde{M}_2^2)}\right]\left(\delta_{\alpha\mu}\delta_{\alpha'\mu'}+\delta_{\alpha\mu'}\delta_{\mu\alpha'}\right)\ . \end{aligned} \quad \text{(C.8)}$$

The decay rate is given by

$$\begin{aligned}
\Gamma\left(X_2 \to \bar{X}_1 \bar{X}_1\right) &= \frac{1}{16\pi M_2} \langle |\mathcal{M}_{X_2 \to \bar{X}_1 \bar{X}_1}|^2 \rangle \\
&= \frac{1}{8\pi M_2} \left[|\lambda|^2 + \frac{M_2^2 \,\mathrm{Re}\left(i\lambda \tilde{\lambda}^* \mathrm{Tr}(g_2\, \tilde{g}_2^\dagger) \right)}{8\pi (M_2^2 - \tilde{M}_2^2)} \right] (\delta_{\alpha\mu}\delta_{\alpha'\mu'} + \delta_{\alpha\mu'}\delta_{\mu\alpha'}) \\
&\quad \times \frac{1}{2} (\delta_{\alpha\mu}\delta_{\alpha'\mu'} + \delta_{\alpha\mu'}\delta_{\mu\alpha'}) \\
&\simeq \frac{3\lambda}{8\pi M_2} \left[\lambda - \tilde{\lambda} \frac{M_2^2}{4\pi (M_2^2 - \tilde{M}_2^2)} \mathrm{Im}\left(\mathrm{Tr}(g_2\, \tilde{g}_2^\dagger) \right) \right], \qquad \text{(C.9)}
\end{aligned}$$

where we rotated the X fields in such a way that λ and $\tilde{\lambda}$ are real.

Analogously, one obtains

$$\Gamma\left(\bar{X}_2 \to X_1 X_1\right) \simeq \frac{3\lambda}{8\pi M_2} \left[\lambda + \tilde{\lambda} \frac{M_2^2}{4\pi (M_2^2 - \tilde{M}_2^2)} \mathrm{Im}\left(\mathrm{Tr}(g_2\, \tilde{g}_2^\dagger) \right) \right] . \qquad \text{(C.10)}$$

Appendix D

$\mu \to e\,\gamma$ decay rate

The relevant Feynman rules derived from the Lagrangian (3.3) are the following:

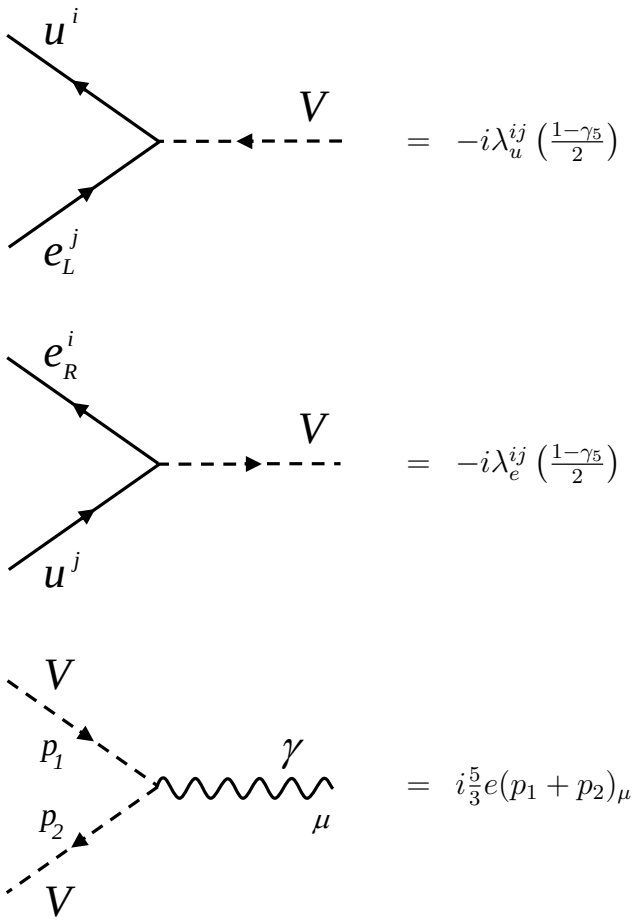

Here we calculate all three contributions to the amplitude for the process $\mu \to e\,\gamma$. For now, let us neglect the Hermitian conjugate part. We will take it into account at the end.

(1) Feynman diagram for the first contribution:

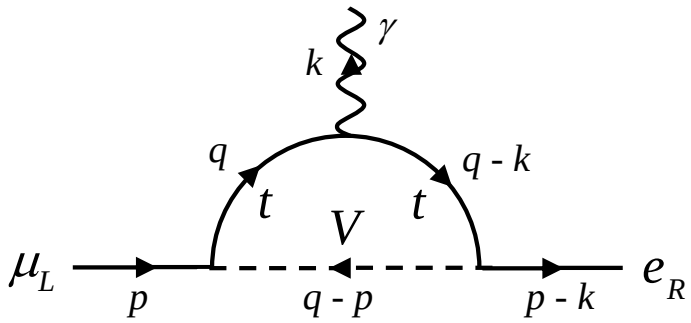

The amplitude is given by

$$\begin{aligned} i\mathcal{M}_1 &= -\frac{2}{3}e\lambda_u^{32}\lambda_e^{13}\,\bar{e}_R(p-k)\int\frac{d^4q}{(2\pi)^4}\left[\frac{\not{q}-\not{k}+m_t}{q^2-m_t^2}\right]\gamma_\mu\left[\frac{\not{q}+m_t}{(q-k)^2-m_t^2}\right] \\ &\quad\times\left[\frac{1}{(q-p)^2-m_V^2}\right]\mu_L(p) \\ &= -\frac{2}{3}e\lambda_u^{32}\lambda_e^{13}m_t\,\bar{e}_R(p-k) \\ &\quad\times\int\frac{d^4q}{(2\pi)^4}\frac{2q_\mu-k_\mu-\frac{1}{2}\,[\not{k},\gamma_\mu]}{(q^2-m_t^2)[(q-k)^2-m_t^2][(q-p)^2-m_V^2]}\,\mu_L(p)\,. \end{aligned} \tag{D.1}$$

Working to linear order in the external momenta, we obtain

$$\begin{aligned} i\mathcal{M}_1 &\simeq -\frac{2}{3}e\lambda_u^{32}\lambda_e^{13}m_t\,\bar{e}_R(p-k)\int\frac{d^4q}{(2\pi)^4}\left[\frac{4\,q\cdot k\;q_\mu}{(q^2-m_t^2)^3(q^2-m_V^2)}\right. \\ &\quad\left.+\frac{4\,q\cdot p\;q_\mu}{(q^2-m_t^2)^2(q^2-m_V^2)^2}+\frac{-k_\mu-\frac{1}{2}[\not{k},\gamma_\mu]}{(q^2-m_t^2)^2(q^2-m_V^2)}\right]\mu_L(p) \\ &= -\frac{2}{3}e\lambda_u^{32}\lambda_e^{13}m_t\,\bar{e}_R(p-k)\left(\frac{-i}{16\pi^2m_V^2}\right)\left[k_\mu\int_0^\infty\frac{y^2\,dy}{\left(y+\frac{m_t^2}{m_V^2}\right)^3(y+1)}\right. \\ &\quad\left.+\,p_\mu\int_0^\infty\frac{y^2\,dy}{\left(y+\frac{m_t^2}{m_V^2}\right)^2(y+1)^2}+(-k_\mu-\tfrac{1}{2}[\not{k},\gamma_\mu])\int_0^\infty\frac{y\,dy}{\left(y+\frac{m_t^2}{m_V^2}\right)^2(y+1)}\right]\mu_L(p) \\ &= -\frac{2}{3}e\lambda_u^{32}\lambda_e^{13}m_t\,\bar{e}_R(p-k)\left(\frac{-i}{16\pi^2m_V^2}\right)\left[\left(\frac{-3+4x-x^2-2\log(x)}{2(1-x)^3}\right)k_\mu\right. \\ &\quad\left.+\left(\frac{1-x^2+2x\log(x)}{(1-x)^3}\right)p_\mu+\left(\frac{1-x+\log(x)}{(1-x)^2}\right)(k_\mu+\tfrac{1}{2}[\not{k},\gamma_\mu])\right]\mu_L(p), \end{aligned} \tag{D.2}$$

where $x=m_t^2/m_V^2$.

(2) Feynman diagram for the second contribution:

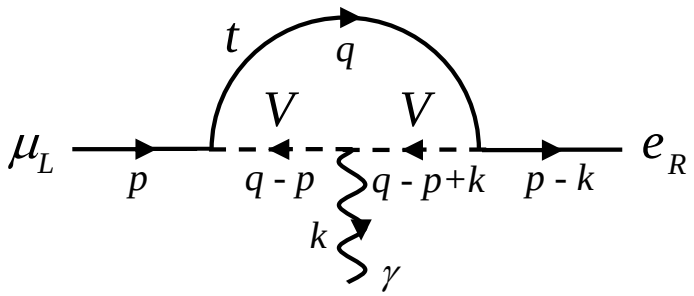

The amplitude is

$$\begin{aligned} i\mathcal{M}_2 &= -\frac{5}{3}e\lambda_u^{32}\lambda_e^{13}\,\bar{e}_R(p-k)\int\frac{d^4q}{(2\pi)^4}(2q_\mu-2p_\mu+k_\mu) \\ &\quad\times\left[\frac{1}{(q-p+k)^2-m_V^2}\right]\left[\frac{1}{(q-p)^2-m_V^2}\right]\left[\frac{\not{q}+m_t}{q^2-m_t^2}\right]\mu_L(p) \\ &= -\frac{5}{3}e\lambda_u^{32}\lambda_e^{13}m_t\,\bar{e}_R(p-k)\,\mu_L(p) \\ &\quad\times\int\frac{d^4q}{(2\pi)^4}\frac{(2q-2p+k)_\mu}{[(q-p+k)^2-m_V^2][(q-p)^2-m_V^2](q^2-m_t^2)}\,. \end{aligned} \tag{D.3}$$

In the low energy regime (where p and k are small) we can expand

$$\begin{aligned} &\frac{1}{[(q-p+k)^2-m_V^2][(q-p)^2-m_V^2](q^2-m_t^2)} \\ &\qquad\simeq\frac{1}{(q^2-m_V^2)^2(q^2-m_t^2)}+\frac{2q\cdot(2p-k)}{(q^2-m_V^2)^3(q^2-m_t^2)}\,, \end{aligned} \tag{D.4}$$

which yields

$$\begin{aligned} i\mathcal{M}_2 &= -\frac{5}{3}e\lambda_u^{32}\lambda_e^{13}m_t\,\bar{e}_R(p-k)\,\mu_L(p) \\ &\quad\times\int\frac{d^4q}{(2\pi)^4}\left[\frac{(2p-k)_\mu}{(q^2-m_V^2)^2(q^2-m_t^2)}+\frac{q^2(2p-k)_\mu}{(q^2-m_V^2)^3(q^2-m_t^2)}\right] \\ &= -\frac{5}{3}e\lambda_u^{32}\lambda_e^{13}m_t\,\bar{e}_R(p-k)\,\mu_L(p)\left(\frac{-i}{16\pi^2m_V^2}\right)(2p-k)_\mu \\ &\quad\times\left[\int_0^\infty\frac{y\,dy}{\left(y+\frac{m_t^2}{m_V^2}\right)(y+1)^2}+\int_0^\infty\frac{y^2\,dy}{\left(y+\frac{m_t^2}{m_V^2}\right)(y+1)^3}\right] \\ &= -\frac{5}{3}e\lambda_u^{32}\lambda_e^{13}m_t\,\bar{e}_R(p-k)\,\mu_L(p)\left(\frac{-i}{16\pi^2m_V^2}\right)(2p-k)_\mu \\ &\quad\times\left[\frac{1-x+x\log(x)}{(1-x)^2}+\frac{1-(4-3x)x-2x^2\log(x)}{2(1-x)^3}\right]. \end{aligned} \tag{D.5}$$

(3) Feynman diagrams for the third contribution:

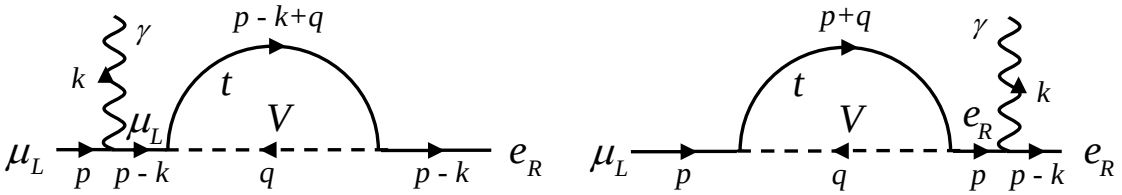

The amplitude,

$$
\begin{aligned}
i\mathcal{M}_3 &= -e\lambda_u^{32}\lambda_e^{13}\,\bar{e}_R(p-k)\,\gamma_\mu\left[\frac{\not{p}+m_e}{p^2-m_e^2}\right]\int\frac{d^4q}{(2\pi)^4}\left(\frac{1+\gamma_5}{2}\right)\left[\frac{\not{p}+\not{q}+m_t}{(p+q)^2-m_t^2}\right] \\
&\quad\times\left[\frac{1}{q^2-m_V^2}\right]\left(\frac{1+\gamma_5}{2}\right)\mu_R(p) \\
&\quad -e\lambda_u^{32}\lambda_e^{13}\,\bar{e}_R(p-k)\left[\frac{\not{p}-\not{k}+m_\mu}{(p-k)^2-m_\mu^2}\right]\int\frac{d^4q}{(2\pi)^4}\left(\frac{1+\gamma_5}{2}\right)\left[\frac{\not{p}+\not{q}+m_t}{(p+q)^2-m_t^2}\right] \\
&\quad\times\left[\frac{1}{q^2-m_V^2}\right]\left(\frac{1+\gamma_5}{2}\right)\gamma_\mu\,\mu_R(p) \\
&= -e\lambda_u^{32}\lambda_e^{13}m_t\,\bar{e}_R(p-k)\,\gamma_\mu\left[\frac{\not{p}+m_e}{p^2-m_e^2}\right]\left(\frac{1+\gamma_5}{2}\right)\mu_R(p) \\
&\quad\times\int_0^1 dx\int\frac{d^4q}{(2\pi)^4}\frac{1}{[(q+px)^2+p^2x(1-x)-m_t^2x-m_V^2(1-x)]^2} \\
&\quad -e\lambda_u^{32}\lambda_e^{13}m_t\,\bar{e}_R(p-k)\left[\frac{\not{p}-\not{k}+m_\mu}{(p-k)^2-m_\mu^2}\right]\left(\frac{1+\gamma_5}{2}\right)\gamma_\mu\,\mu_R(p) \\
&\quad\times\int_0^1 dx\int\frac{d^4q}{(2\pi)^4}\frac{1}{[[q+(p-k)x]^2+(p-k)^2x(1-x)-m_t^2x-m_V^2(1-x)]^2}.
\end{aligned}
\tag{D.6}
$$

Expanding the integral in small momenta yields

$$
\begin{aligned}
&\int_0^1 dx\int\frac{d^4q}{(2\pi)^4}\frac{1}{[(q+lx)^2+l^2x(1-x)-m_t^2x-m_V^2(1-x)]^2} \\
&=\int_0^1 dx\int\frac{d^4q}{(2\pi)^4}\left[\frac{1}{[q^2-m_t^2x-m_V^2(1-x)]^2}+2l^2\frac{x(1-x)}{[q^2-m_t^2x-m_V^2(1-x)]^3}\right] \\
&=F(m_t,m_V)+l^2\left(\frac{-i}{16\pi^2m_V^2}\right)\int_0^1 dx\,\frac{x(1-x)}{\left[x\left(\frac{m_t^2}{m_V^2}-1\right)+1\right]}\,.
\end{aligned}
\tag{D.7}
$$

Neglecting the electron mass and using the relations:

$$\not{p}\mu(p) = m_\mu \mu(p) \ , \quad \bar{e}_R(p-k)(\not{p}-\not{k}) = 0 \ , \tag{D.8}$$

it is easy to see that the contribution of the zeroth order term in the expansion (D.7) cancels out in Eq. (D.6), since $F(m_t, m_V)$ does not depend on the momentum:

$$\begin{aligned} &\bar{e}_R(p-k)\,\gamma_\mu \left[\frac{\not{p}+m_e}{p^2-m_e^2}\right]\mu_R(p) + \bar{e}_R(p-k)\left[\frac{\not{p}-\not{k}+m_\mu}{(p-k)^2-m_\mu^2}\right]\gamma_\mu\,\mu_R(p) \\ &\simeq \bar{e}_R(p-k)\gamma_\mu \frac{m_\mu}{m_\mu^2}\mu_R(p) + \bar{e}_R(p-k)\frac{m_\mu}{-m_\mu^2}\gamma_\mu\mu_R(p) = 0 \ . \end{aligned} \tag{D.9}$$

We are left with

$$\begin{aligned} i\mathcal{M}_3 &= -e\lambda_u^{32}\lambda_e^{13}\left(\frac{-i}{16\pi^2 m_V^2}\right)\int_0^1 dx \frac{x(1-x)}{\left[x\left(\frac{m_t^2}{m_V^2}-1\right)+1\right]}\bar{e}_R(p-k) \\ &\quad \times\left[p^2\,\gamma_\mu\left[\frac{\not{p}+m_e}{p^2-m_e^2}\right] + (p-k)^2\left[\frac{\not{p}-\not{k}+m_e}{(p-k)^2-m_e^2}\right]\gamma_\mu\right]\mu_R(p) \\ &\simeq -e\lambda_u^{32}\lambda_e^{13}\left(\frac{-i}{16\pi^2 m_V^2}\right) m_\mu \bar{e}_R(p-k)\gamma_\mu\mu_R(p)\left[\frac{1-x^2+2x\log(x)}{2(1-x)^3}\right] \\ &= -e\lambda_u^{32}\lambda_e^{13}\left(\frac{-i}{16\pi^2 m_V^2}\right)\bar{e}_R(p-k)(2p_\mu - k_\mu - i\sigma_{\mu\nu}k^\nu)\mu_R(p) \\ &\quad \times\left[\frac{1-x^2+2x\log(x)}{2(1-x)^3}\right], \end{aligned} \tag{D.10}$$

where in the last step we used the Gordon identity.

Putting together formulas (D.2), (D.5), (D.10) and including the Hermitian conjugate gives

$$\begin{aligned} i\mathcal{M} &= -\frac{3\,e\,m_t}{16\,\pi^2 m_V^2}\left[\frac{1-x^2+2x\log x}{2(1-x)^3} + \frac{2}{3}\left(\frac{1-x+\log x}{(1-x)^2}\right)\right]k_\nu\,\epsilon_\mu(k) \\ &\quad \times\Big[\lambda_e^{13}\lambda_u^{32}\,\bar{e}_R(p-k)\,\sigma^{\mu\nu}\mu_L(p) + (\lambda_u^{31})^*(\lambda_e^{23})^*\,\bar{e}_L(p-k)\,\sigma^{\mu\nu}\mu_R(p)\Big]. \end{aligned} \tag{D.11}$$

This leads to Eq. (3.10) upon rotating the couplings as in Eq. (3.12).

Note that the electric dipole moment of the down quark can be computed along similar lines. The only difference is the overall factor coming from the difference in charges between the electron and the down quark.

The spin averaged squared matrix element is:

$$\begin{aligned}\langle|\mathcal{M}|^2\rangle \;=\; & \frac{9\,e^2\,m_t^2}{512\,\pi^4 m_V^4} f\left(\frac{m_t^2}{m_V^2}\right)^2 k_\nu k_{\nu'} \\ & \times\Bigg\{\left|\tilde{\lambda}_e^{13}\tilde{\lambda}_u^{32}\right|^2 \mathrm{Tr}\left[(\not{p}-\not{k}+m_e)\left(\frac{1-\gamma_5}{2}\right)\sigma^{\mu\nu}(\not{p}+m_\mu)\left(\frac{1+\gamma_5}{2}\right)\sigma^{\nu'}{}_{\mu}\right] \\ & +\left|\tilde{\lambda}_u^{31}\tilde{\lambda}_e^{23}\right|^2 \mathrm{Tr}\left[(\not{p}-\not{k}+m_e)\left(\frac{1+\gamma_5}{2}\right)\sigma^{\mu\nu}(\not{p}+m_\mu)\left(\frac{1-\gamma_5}{2}\right)\sigma^{\nu'}{}_{\mu}\right]\Bigg\}.\end{aligned} \tag{D.12}$$

Neglecting the electron mass, both traces can be calculated using the following formula,

$$\mathrm{Tr}\left[\gamma^\alpha\sigma^{\mu\nu}\gamma^\beta\sigma^{\nu'}{}_{\mu}\left(\frac{1\pm\gamma_5}{2}\right)\right] = 4g^{\alpha\nu'}g^{\beta\nu} - 2g^{\alpha\beta}g^{\nu\nu'} + 4g^{\alpha\nu}g^{\beta\nu'}\;. \tag{D.13}$$

Choosing the muon center of mass coordinates, the momenta become: $p = (m_\mu, \vec{0})$ and $k = (m_\mu/2, \vec{p}_e)$, where $|\vec{p}_e| = m_\mu/2$, and the expression for the decay rate becomes

$$\Gamma(\mu\to e\,\gamma) = \frac{1}{16\pi m_\mu}\langle|\mathcal{M}|^2\rangle = \frac{9\,e^2\lambda^2 m_t^2 m_\mu^3}{2048\,\pi^5 m_V^4}\,f\left(\frac{m_t^2}{m_V^2}\right)^2, \tag{D.14}$$

where

$$\lambda \equiv \sqrt{\frac{1}{2}\left|\tilde{\lambda}_e^{13}\tilde{\lambda}_u^{32}\right|^2 + \frac{1}{2}\left|\tilde{\lambda}_u^{31}\tilde{\lambda}_e^{23}\right|^2}\;. \tag{D.15}$$

Appendix E

Fierz identities

(a) We start by proving the first relation in Eq. (3.17). Let us choose the same masses, momenta and spins (m, p, s) for particles 1 and 2, and assume (m', p', s') for particles 3 and 4. The only Lorentz invariant expression which can be written down is

$$\begin{aligned}&[\bar{u}_{1L}(p,s)\, u_{2R}(p,s)]\,[\bar{u}_{3R}(p',s')\, u_{4L}(p',s')] \\ &\qquad = A\,[\bar{u}_{1L}(p,s)\gamma^{\mu} u_{4L}(p',s')]\,[\bar{u}_{3R}(p',s')\gamma_{\mu} u_{2R}(p,s)]\ . \end{aligned} \tag{E.1}$$

Performing a sum over spins on both sides of Eq. (E.1) gives

$$\begin{aligned}&\mathrm{Tr}\left[(\not{p}+m)\left(\frac{1+\gamma_5}{2}\right)\right]\mathrm{Tr}\left[(\not{p}'+m')\left(\frac{1-\gamma_5}{2}\right)\right] \\ &\qquad = A\ \mathrm{Tr}\left[(\not{p}+m)\gamma^{\mu}\left(\frac{1-\gamma_5}{2}\right)(\not{p}'+m')\gamma_{\mu}\left(\frac{1+\gamma_5}{2}\right)\right]. \end{aligned} \tag{E.2}$$

Taking the traces yields

$$4\,m\,m' = A\,m\,m'\ \mathrm{Tr}\left[\gamma^{\mu}\gamma_{\mu}\left(\frac{1+\gamma_5}{2}\right)\right], \tag{E.3}$$

which results in $A = 1/2$ and agrees with the first relation in Eq. (3.17).

(b) In order to prove the second relation in Eq. (3.17), we first choose the same masses, momenta and spins as in the previous case. There are now only two terms which we

can write down on the right-hand side:

$$[\bar{u}_{1L}(p,s)u_{2R}(p,s)][\bar{u}_{3L}(p',s')u_{4R}(p',s')] = B\,[\bar{u}_{1L}(p,s)u_{4R}(p',s')][\bar{u}_{3L}(p',s')u_{2R}(p,s)] + C\,[\bar{u}_{1L}(p,s)\sigma^{\mu\nu}u_{4R}(p',s')][\bar{u}_{3L}(p',s')\sigma_{\mu\nu}u_{2R}(p,s)]\,. \quad \text{(E.4)}$$

Summing over spins gives

$$\begin{aligned}&\mathrm{Tr}\left[(\not{p}+m)\left(\frac{1+\gamma_5}{2}\right)\right]\mathrm{Tr}\left[(\not{p}'+m')\left(\frac{1+\gamma_5}{2}\right)\right]\\ &\quad = B\;\mathrm{Tr}\left[(\not{p}+m)\left(\frac{1+\gamma_5}{2}\right)(\not{p}'+m')\left(\frac{1+\gamma_5}{2}\right)\right]\\ &\quad\quad + C\;\mathrm{Tr}\left[(\not{p}+m)\sigma^{\mu\nu}\left(\frac{1+\gamma_5}{2}\right)(\not{p}'+m')\sigma_{\mu\nu}\left(\frac{1+\gamma_5}{2}\right)\right]. \quad \text{(E.5)}\end{aligned}$$

Taking the trace of both sides yields

$$4\,m\,m' = 2\,B\,m\,m' + \frac{1}{2}\,C\,m\,m'\;\mathrm{Tr}\left[\sigma^{\mu\nu}\sigma_{\mu\nu}\right]\;, \quad \text{(E.6)}$$

which, using the fact that $\sigma^{\mu\nu} = i[\gamma^\mu,\gamma^\nu]/2$, gives $B + 12\,C = 2$.

Next, if we choose the same masses, momenta and spins (m,p,s) for particles 1 and 4, and assign (m',p',s') to particles 2 and 3, we get

$$[\bar{u}_{1L}(p,s)u_{2R}(p',s')][\bar{u}_{3L}(p',s')u_{4R}(p,s)] = B\,[\bar{u}_{1L}(p,s)u_{4R}(p,s)][\bar{u}_{3L}(p',s')u_{2R}(p',s')] + C\,[\bar{u}_{1L}(p,s)\sigma^{\mu\nu}u_{4R}(p,s)][\bar{u}_{3L}(p',s')\sigma_{\mu\nu}u_{2R}(p',s')]\,. \quad \text{(E.7)}$$

Taking the trace yields

$$\begin{aligned}&\mathrm{Tr}\left[(\not{p}+m)\left(\frac{1+\gamma_5}{2}\right)(\not{p}'+m')\left(\frac{1+\gamma_5}{2}\right)\right]\\ &\quad = B\;\mathrm{Tr}\left[(\not{p}+m)\left(\frac{1+\gamma_5}{2}\right)\right]\mathrm{Tr}\left[(\not{p}'+m')\left(\frac{1+\gamma_5}{2}\right)\right]. \quad \text{(E.8)}\end{aligned}$$

This, along with the previous result, gives $B = 1/2$ and $C = 1/8$, which agrees with the second equation in (3.17).

Appendix F

Cancellation of anomalies

The gauge symmetry $SU(3)_c \times SU(2)_L \times U(1)_Y \times U(1)_B \times U(1)_L$ is anomalous in the minimal supersymmetric standard model. We will show here that all the anomalies are cancelled by adding the set of fields introduced in Section 4.2. The subscripts next to each quantum number denote the chiral superfield whose fermionic component enters the calculation. The nontrivial anomaly cancellation conditions are the following:

- $SU(3)^2 \times U(1)_Y$, $SU(3)^2 \times U(1)_B$ and $SU(3)^2 \times U(1)_L$ vanish since the new particles are singlets under the color group.

- $SU(2)^2 \times U(1)_Y$:

$$\begin{aligned} & 3 \times \mathrm{Tr}\,(t_\alpha t_\beta) \times \Big\{ 3 \times \Big[2 \times \left(\tfrac{1}{6}\right)_Q + \left(-\tfrac{2}{3}\right)_{u^c} + \left(\tfrac{1}{3}\right)_{d^c} \Big] \\ & \qquad\qquad + 2 \times \left(-\tfrac{1}{2}\right)_l + (1)_{e^c} + \left(\tfrac{1}{2}\right)_{H_u} + \left(-\tfrac{1}{2}\right)_{H_d} \Big\} \\ & + \mathrm{Tr}\,(t_\alpha t_\beta) \Big\{ 2 \times \left[\left(-\tfrac{1}{2}\right)_\Psi + \left(\tfrac{1}{2}\right)_{\Psi^c} \right] + (1)_{\eta^c} + (-1)_\eta \Big\} = 0 \,. \end{aligned} \tag{F.1}$$

- $SU(2)^2 \times U(1)_B$:

$$3 \times 3 \times \mathrm{Tr}\,(t_\alpha t_\beta) \times 2 \times \left(\tfrac{1}{3}\right)_Q + 2 \times \mathrm{Tr}\,(t_\alpha t_\beta)\,[(B_1)_\Psi + (B_2)_{\Psi^c}] = 0 \,, \tag{F.2}$$

  which requires $B_1 + B_2 = -3$.

- $SU(2)^2 \times U(1)_L$: analogously gives $L_1 + L_2 = -3$.

- $U(1)_Y^3$:

$$3\times\Big\{3\times\Big[2\times\big(\tfrac{1}{6}\big)^3_Q+\big(-\tfrac{2}{3}\big)^3_{u^c}+\big(\tfrac{1}{3}\big)^3_{d^c}\Big]+\;2\times\big(-\tfrac{1}{2}\big)^3_l+(1)^3_{e^c}+\big(\tfrac{1}{2}\big)^3_{H_u}+\big(-\tfrac{1}{2}\big)^3_{H_d}\Big\}$$
$$+\Big\{2\times\Big[\big(-\tfrac{1}{2}\big)^3_\Psi+\big(\tfrac{1}{2}\big)^3_{\Psi^c}\Big]+\big[(1)^3_{\eta^c}+(-1)^3_\eta\big]\Big\}=0\,. \qquad \text{(F.3)}$$

- $U(1)_Y^2\times U(1)_B$:

$$3\times3\times\Big[2\times\big(\tfrac{1}{6}\big)^2\big(\tfrac{1}{3}\big)_Q+\big(-\tfrac{2}{3}\big)^2\big(-\tfrac{1}{3}\big)_{u^c}+\big(\tfrac{1}{3}\big)^2\big(-\tfrac{1}{3}\big)_{d^c}\Big]$$
$$+2\times\Big[\big(-\tfrac{1}{2}\big)^2(B_1)_\Psi+\big(\tfrac{1}{2}\big)^2(B_2)_{\Psi^c}\Big]+\big[(1)^2(-B_1)_{\eta^c}+(-1)^2(-B_2)_\eta\big]=0\,, \qquad \text{(F.4)}$$

which gives $B_1+B_2=-3$.

- $U(1)_Y^2\times U(1)_L$: analogously gives $L_1+L_2=-3$.

- $U(1)_Y\times U(1)_B^2$:

$$3\times3\times\Big[2\times\big(\tfrac{1}{6}\big)\big(\tfrac{1}{3}\big)^2_Q+\big(-\tfrac{2}{3}\big)\big(-\tfrac{1}{3}\big)^2_{u^c}+\big(\tfrac{1}{3}\big)\big(-\tfrac{1}{3}\big)^2_{d^c}\Big]$$
$$+2\times\Big[\big(-\tfrac{1}{2}\big)(B_1)^2_\Psi+\big(\tfrac{1}{2}\big)(B_2)^2_{\Psi^c}\Big]+\big[(1)(-B_1)^2_{\eta^c}+(-1)(-B_2)^2_\eta\big]=0\,. \qquad \text{(F.5)}$$

- $U(1)_Y\times U(1)_L^2$: analogously vanishes.

- $U(1)_Y\times U(1)_B\times U(1)_L$:

$$2\times\Big[\big(-\tfrac{1}{2}\big)(B_1)(L_1)_\Psi+\big(\tfrac{1}{2}\big)(B_2)(L_2)_{\Psi^c}\Big]$$
$$+\;\big[(1)(-B_1)(-L_1)_{\eta^c}+(-1)(-B_2)(-L_2)_\eta\big]=0\,. \qquad \text{(F.6)}$$

- $U(1)_B^2\times U(1)_L$:

$$2\times\big[(B_1)^2(L_1)_\Psi+(B_2)^2(L_2)_{\Psi^c}\big]+\big[(-B_1)^2(-L_1)_{\eta^c}+(-B_2)^2(-L_2)_\eta\big]$$
$$+\;\big[(-B_1)^2(-L_1)_{X^c}+(-B_2)^2(-L_2)_X\big]=0\,. \qquad \text{(F.7)}$$

- $U(1)_B\times U(1)_L^2$: analogously vanishes.

- $U(1)_B^3$:

$$3 \times 3 \times \left[2 \times \left(\tfrac{1}{3}\right)_Q^3 + \left(-\tfrac{1}{3}\right)_{u^c}^3 + \left(-\tfrac{1}{3}\right)_{d^c}^3\right]$$
$$+ 2 \times \left[(B_1)_\Psi^3 + (B_2)_{\Psi^c}^3\right] + \left[(-B_1)_{\eta^c}^3 + (-B_2)_\eta^3\right] + \left[(-B_1)_{X^c}^3 + (-B_2)_X^3\right] = 0\ . \quad \text{(F.8)}$$

- $U(1)_L^3$: analogously vanishes.

- $\text{gravity}^2 \times U(1)_B$:

$$3 \times 3 \times \left[2 \times \left(\tfrac{1}{3}\right)_Q + \left(-\tfrac{1}{3}\right)_{u^c} + \left(-\tfrac{1}{3}\right)_{d^c}\right]$$
$$+ 2 \times \left[(B_1)_\Psi + (B_2)_{\Psi^c}\right] + \left[(-B_1)_{\eta^c} + (-B_2)_\eta\right] + \left[(-B_1)_{X^c} + (-B_2)_X\right] = 0\ . \quad \text{(F.9)}$$

- $\text{gravity}^2 \times U(1)_L$: analogously vanishes.

Appendix G

Annihilation and direct detection cross section

The relevant Feynman rules derived from the Lagrangian (4.31) are:

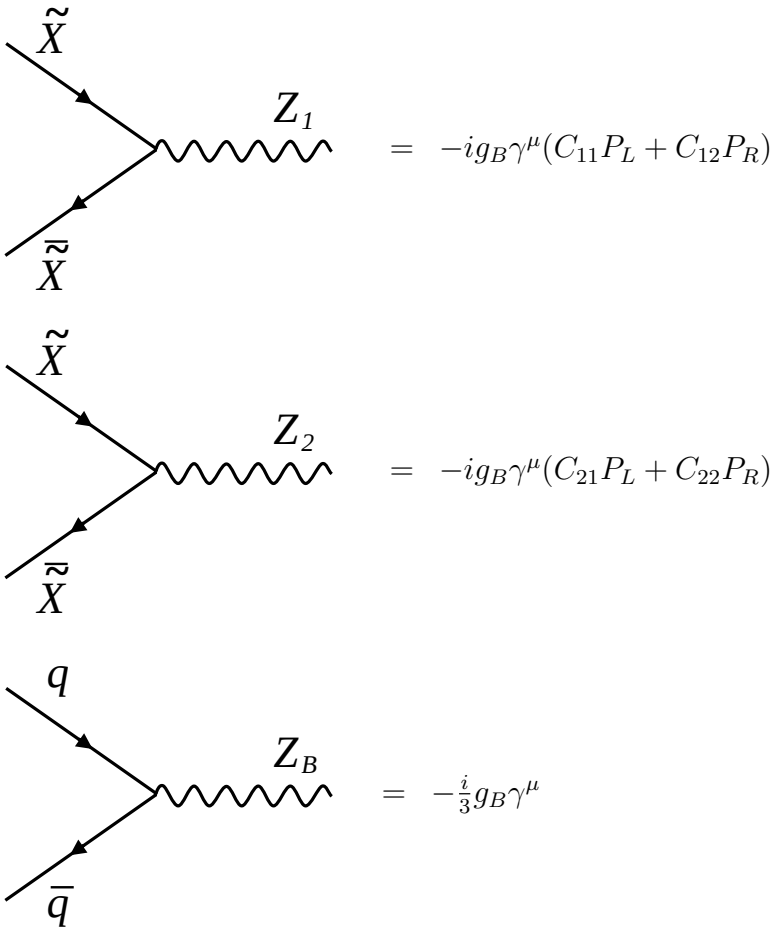

The Feynman diagram for the process $\bar{\tilde{X}}\,\tilde{X} \to Z_1 \to \bar{q}\,q$ is the following:

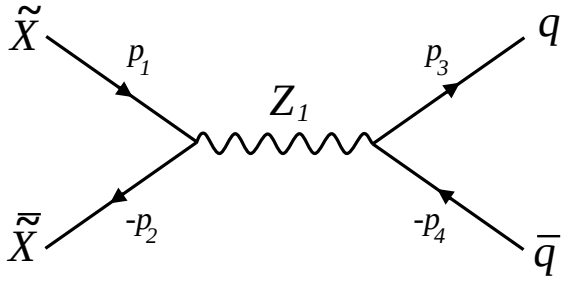

The matrix element is given by

$$\begin{aligned} i\mathcal{M} &= \frac{g_B^2}{3}\cos\theta_{\rm BL}\,\bar{q}(p_4)\gamma^\mu q(p_3)\left[\frac{1}{(p_1+p_2)^2 - M_{Z_1}^2 + iM_{Z_1}\Gamma_{Z_1}}\right] \\ &\quad\times\left[g_{\mu\nu} - \frac{(p_1+p_2)_\mu(p_1+p_2)_\nu}{M_{Z_1}^2}\right]\bar{\tilde{X}}(p_2)\gamma^\nu(C_{11}P_L + C_{12}P_R)\tilde{X}(p_1)\,. \end{aligned} \tag{G.1}$$

After squaring, summing over final states, and averaging over initial ones, it takes the form:

$$\begin{aligned} \langle|\mathcal{M}|^2\rangle &= \frac{g_B^4}{12}\cos^2\theta_{\rm BL}\,{\rm Tr}\left[(\not{p}_4 - m_q)\gamma^\mu(\not{p}_3 + m_q)\gamma^{\mu'}\right]\frac{1}{\left[(p_1+p_2)^2 - M_{Z_1}^2\right]^2 + M_{Z_1}^2\Gamma_{Z_1}^2} \\ &\quad\times\left[g_{\mu\nu} - \frac{(p_1+p_2)_\mu(p_1+p_2)_\nu}{M_{Z_1}^2}\right]\left[g_{\mu'\nu'} - \frac{(p_1+p_2)_{\mu'}(p_1+p_2)_{\nu'}}{M_{Z_1}^2}\right] \\ &\quad\times{\rm Tr}\left[(\not{p}_2 - M_{\tilde{X}})\gamma^\nu(C_{11}P_L + C_{12}P_R)(\not{p}_1 + M_{\tilde{X}})\gamma^{\nu'}(C_{11}P_L + C_{12}P_R)\right]. \end{aligned} \tag{G.2}$$

Using standard formulas for traces and simplifying the resulting expression gives

$$\begin{aligned} \langle|\mathcal{M}|^2\rangle &= \frac{g_B^4}{12}\cos^2\theta_{\rm BL}\left[\frac{1}{[(p_1+p_2)^2 - M_{Z_1}^2]^2 + M_{Z_1}^2\Gamma_{Z_1}^2}\right] \\ &\quad\times\Big\{(C_{11}^2 + C_{12}^2)\Big[(p_1\cdot p_2)\,m_q^2 + (p_1\cdot p_3)(p_2\cdot p_4) + (p_1\cdot p_4)(p_2\cdot p_3)\Big] \\ &\quad + 2\,C_{11}C_{12}\,M_{\tilde{X}}^2\left(p_3\cdot p_4 + 2m_q^2\right)\Big\}\,. \end{aligned} \tag{G.3}$$

Working in the center of mass frame,

$$p_1 = (E, \vec{p}) \,, \quad p_2 = (E, -\vec{p}) \,, \quad p_3 = (E, \vec{k}) \,, \quad p_4 = (E, -\vec{k}) \,,$$
$$\vec{p} \cdot \vec{k} = |\vec{p}||\vec{k}| \cos\theta \,, \quad s = (p_1 + p_2)^2 = 4E^2 \,, \tag{G.4}$$

formula (G.3) can be rewritten as

$$\begin{aligned} \langle |\mathcal{M}|^2 \rangle \;=\; & \frac{g_B^4}{12} \cos^2\theta_{\rm BL} \left[\frac{1}{(s - M_{Z_1}^2)^2 + M_{Z_1}^2 \Gamma_{Z_1}^2} \right] \\ & \times \Big\{ (C_{11}^2 + C_{12}^2) \left[(s - 4m_q^2)(s - 4M_{\tilde{X}}^2) \cos(2\theta) + s(3s + 4m_q^2 - 4M_{\tilde{X}}^2) \right] \\ & + 16\, C_{11} C_{12} M_{\tilde{X}}^2 (s + 2m_q^2) \Big\} \,. \end{aligned} \tag{G.5}$$

The differential cross section is given by

$$\frac{d\sigma}{d\Omega} v = \frac{|p_3|}{16\pi^2 s \sqrt{s}} \langle |\mathcal{M}|^2 \rangle \,, \tag{G.6}$$

and integration over the angles yields

$$\begin{aligned} \sigma v \;=\; & \frac{g_B^4}{36\pi s} \cos^2\theta_{\rm BL} \left[\frac{\sqrt{1 - \frac{4m_q^2}{s}}}{(s - M_{Z_1}^2)^2 + M_{Z_1}^2 \Gamma_{Z_1}^2} \right] \\ & \times \left[(C_{11}^2 + C_{12}^2)(s + 2m_q^2)(s - M_{\tilde{X}}^2) + 6\, C_{11} C_{12} M_{\tilde{X}}^2 (s + 2m_q^2) \right] , \end{aligned} \tag{G.7}$$

which is equivalent to Eq. (4.36), with the definition (4.37), upon summing over the quarks.

The Feynman diagram corresponding to the direct detection is shown below.

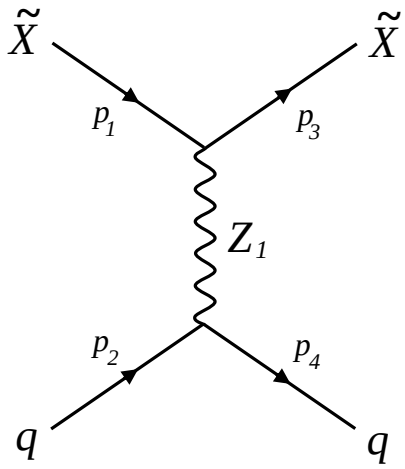

The formula for the direct detection cross section can be obtained from the annihilation cross section result (G.3) by substituting:

$$p_2 \to -p_3 \ , \quad p_3 \to -p_2 \ , \quad m_q \to M_N \ . \tag{G.8}$$

In the nonrelativistic limit

$$p_1 = p_3 = (M_X, 0) \ , \quad p_2 = p_4 = (M_N, 0) \ , \tag{G.9}$$

and the expression for the cross section reduces to

$$\sigma_{\rm SI} = \frac{1}{4\pi} \frac{M_{\tilde{X}}^2 M_N^2}{(M_{\tilde{X}} + M_N)^2} \frac{g_B^4}{M_{Z_1}^4} (C_{11} + C_{12})^2 \cos^2 \theta_{BL} \ , \tag{G.10}$$

which is exactly Eq. (4.43).

Bibliography

[1] J. M. Arnold, B. Fornal and M. B. Wise, *Simplified models with baryon number violation but no proton decay*, Phys. Rev. D **87**, 075004 (2013) [arXiv:1212.4556 [hep-ph]].

[2] J. M. Arnold, B. Fornal and M. B. Wise, *Phenomenology of scalar leptoquarks*, Phys. Rev. D **88**, 035009 (2013) [arXiv:1304.6119 [hep-ph]].

[3] J. M. Arnold, P. Fileviez Perez, B. Fornal and S. Spinner, *B and L at the supersymmetry scale, dark matter and R-parity violation*, Phys. Rev. D **88**, 115009 (2013) [arXiv:1310.7052 [hep-ph]].

[4] S. L. Glashow, *Partial symmetries of weak interactions*, Nucl. Phys. **22**, 579 (1961).

[5] S. Weinberg, *A model of leptons*, Phys. Rev. Lett. **19**, 1264 (1967).

[6] A. Salam, *Weak and electromagnetic interactions*, Conf. Proc. C **680519**, 367 (1968).

[7] H. Fritzsch and M. Gell-Mann, *Current algebra: Quarks and what else?*, in J. D. Jackson and A. Roberts, International Union of Pure and Applied Physics. Proceedings of the XVI International Conference on High Energy Physics 2. National Accelerator Laboratory, Chicago, pp. 135165 (1972).

[8] H. Fritzsch, M. Gell-Mann and H. Leutwyler, *Advantages of the color octet gluon picture*, Phys. Lett. B **47**, 365 (1973).

[9] H. D. Politzer, *Reliable perturbative results for strong interactions?*, Phys. Rev. Lett. **30**, 1346 (1973).

[10] P. W. Anderson, *Plasmons, gauge invariance, and mass*, Phys. Rev. **130**, 439 (1963).

[11] F. Englert and R. Brout, *Broken symmetry and the mass of gauge vector mesons*, Phys. Rev. Lett. **13**, 321 (1964).

[12] P. W. Higgs, *Broken symmetries and the masses of gauge bosons*, Phys. Rev. Lett. **13**, 508 (1964).

[13] A. Manohar and M. B. Wise, *Heavy Quark Physics*, Cambridge Monographs on Particle Physics, Nuclear Physics and Cosmology (2000).

[14] S. L. Adler, *Axial vector vertex in spinor electrodynamics*, Phys. Rev. **177**, 2426 (1969).

[15] J. S. Bell and R. Jackiw, *A PCAC puzzle:* $\pi^0 \to \gamma\gamma$ *in the sigma model*, Nuovo Cim. A **60**, 47 (1969).

[16] N. S. Manton, *Topology in the Weinberg-Salam theory*, Phys. Rev. D **28**, 2019 (1983).

[17] F. R. Klinkhamer and N. S. Manton, *A saddle point solution in the Weinberg-Salam theory*, Phys. Rev. D **30**, 2212 (1984).

[18] G. 't Hooft, *Symmetry breaking through Bell-Jackiw anomalies*, Phys. Rev. Lett. **37**, 8 (1976).

[19] V. A. Kuzmin, V. A. Rubakov and M. E. Shaposhnikov, *On the anomalous electroweak baryon number nonconservation in the early Universe*, Phys. Lett. B **155**, 36 (1985).

[20] A. D. Sakharov, *Violation of* CP *invariance,* C *asymmetry, and baryon asymmetry of the universe*, Pisma Zh. Eksp. Teor. Fiz. **5**, 32 (1967) [JETP Lett. **5**, 24 (1967)] [Sov. Phys. Usp. **34**, 392 (1991)] [Usp. Fiz. Nauk **161**, 61 (1991)].

[21] N. Cabibbo, *Unitary symmetry and leptonic decays*, Phys. Rev. Lett. **10**, 531 (1963).

[22] M. Kobayashi and T. Maskawa, CP *violation in the renormalizable theory of weak interaction*, Prog. Theor. Phys. **49**, 652 (1973).

[23] P. Huet and E. Sather, *Electroweak baryogenesis and standard model CP violation*, Phys. Rev. D **51**, 379 (1995) [hep-ph/9404302].

[24] M. B. Gavela, P. Hernandez, J. Orloff, O. Pene and C. Quimbay, *Standard model CP violation and baryon asymmetry. Part 2: Finite temperature*, Nucl. Phys. B **430**, 382 (1994) [hep-ph/9406289].

[25] H. Nishino *et al.* [Super-Kamiokande Collaboration], *Search for proton decay via* $p \to e^+\pi^0$ *and* $p \to \mu^+\pi^0$ *in a Large Water Cherenkov Detector*, Phys. Rev. Lett. **102**, 141801 (2009) [arXiv:0903.0676 [hep-ex]].

[26] H. Georgi and S. L. Glashow, *Unity of all elementary particle forces*, Phys. Rev. Lett. **32**, 438 (1974).

[27] H. Fritzsch and P. Minkowski, *Unified interactions of leptons and hadrons*, Annals Phys. **93**, 193 (1975).

[28] P. Nath and P. Fileviez Perez, *Proton stability in grand unified theories, in strings and in branes*, Phys. Rept. **441**, 191 (2007) [hep-ph/0601023].

[29] R. N. Mohapatra, *Neutron-antineutron oscillation: Theory and phenomenology*, J. Phys. G **36**, 104006 (2009) [arXiv:0902.0834 [hep-ph]].

[30] K. Abe *et al.* [Super-Kamiokande Collaboration], *The search for* $n - \bar{n}$ *oscillation in Super-Kamiokande I*, arXiv:1109.4227 [hep-ex].

[31] J. Chung, W. W. M. Allison, G. J. Alner, D. S. Ayres, W. L. Barrett, P. M. Border, J. H. Cobb and H. Courant *et al.*, *Search for neutron anti-neutron oscillations using multiprong events in Soudan 2*, Phys. Rev. D **66**, 032004 (2002) [hep-ex/0205093].

[32] M. Baldo-Ceolin, P. Benetti, T. Bitter, F. Bobisut, E. Calligarich, R. Dolfini, D. Dubbers and P. El-Muzeini *et al.*, *A new experimental limit on neutron – anti-neutron oscillations*, Z. Phys. C **63**, 409 (1994).

[33] Y. Kamyshkov, *Search for matter-antimatter transformation with cold neutrons*, Spontaneous Workshop VI, Cargèse, May 11, 2012.

[34] W. J. Marciano and A. I. Sanda, *Exotic decays of the muon and heavy leptons in gauge theories*, Phys. Lett. B **67**, 303 (1977).

[35] B. Pontecorvo, *Mesonium and anti-mesonium*, Sov. Phys. JETP **6**, 429 (1957) [Zh. Eksp. Teor. Fiz. **33**, 549 (1957)].

[36] Z. Maki, M. Nakagawa and S. Sakata, *Remarks on the unified model of elementary particles*, Prog. Theor. Phys. **28**, 870 (1962).

[37] B. Pontecorvo, *Neutrino experiments and the problem of conservation of leptonic charge*, Sov. Phys. JETP **26**, 984 (1968) [Zh. Eksp. Teor. Fiz. **53**, 1717 (1967)].

[38] J. Adam *et al.* [MEG Collaboration], *New constraint on the existence of the* $\mu^+ \to e^+\gamma$ *decay*, Phys. Rev. Lett. **110**, 201801 (2013) [arXiv:1303.0754 [hep-ex]].

[39] W. H. Bertl *et al.* [SINDRUM II Collaboration], *A search for muon to electron conversion in muonic gold*, Eur. Phys. J. C **47**, 337 (2006).

[40] U. Bellgardt *et al.* [SINDRUM Collaboration], *Search for the decay* $\mu^+ \to e^+e^+e^-$, Nucl. Phys. B **299**, 1 (1988).

[41] Y. Kuno *et al.* [COMET Collaboration], *A search for muon-to-electron conversion at J-PARC: the COMET experiment*, Prog. Theor. Exp. Phys. **2013**, 022C01.

[42] R. J. Abrams *et al.* [Mu2e Collaboration], *Mu2e conceptual design report*, arXiv:1211.7019 [physics.ins-det].

[43] S. Dimopoulos and H. Georgi, *Softly broken supersymmetry and* $SU(5)$, Nucl. Phys. B **193**, 150 (1981).

[44] S. P. Martin, *A supersymmetry primer*, In *Kane, G.L. (ed.): Perspectives on supersymmetry II* 1-153 [hep-ph/9709356].

[45] S. M. Barr and X. Calmet, *Observable proton decay from Planck scale physics*, arXiv:1203.5694 [hep-ph].

[46] J. P. Bowes, R. Foot and R. R. Volkas, *Electric charge quantization from gauge invariance of a Lagrangian: A catalog of baryon number violating scalar interactions*, Phys. Rev. D **54**, 6936 (1996) [hep-ph/9609290].

[47] I. Baldes, N. F. Bell and R. R. Volkas, *Baryon number violating scalar diquarks at the LHC*, Phys. Rev. D **84**, 115019 (2011) [arXiv:1110.4450 [hep-ph]].

[48] I. Dorsner, S. Fajfer and N. Kosnik, *Heavy and light scalar leptoquarks in proton decay*, Phys. Rev. D **86**, 015013 (2012) [arXiv:1204.0674 [hep-ph]].

[49] M. D. Litos, *A search for dinucleon decay into kaons using the SK water cherenkov detector*, Ph. D. Thesis, Boston University, 2012.

[50] R. N. Mohapatra and R. E. Marshak, *Local B-L symmetry of electroweak interactions, Majorana neutrinos and neutron oscillations*, Phys. Rev. Lett. **44**, 1316 (1980) [Erratum-ibid. **44**, 1643 (1980)].

[51] T. -K. Kuo and S. T. Love, *Neutron oscillations and the existence of massive neutral leptons*," Phys. Rev. Lett. **45**, 93 (1980).

[52] J. F. Nieves, *Baryon and lepton number nonconserving processes and intermediate mass scales*, Nucl. Phys. B **189**, 182 (1981).

[53] M. Ozer, *Neutron anti-neutron oscillations and renormalization effects for* $\Delta B = 2$ *six quark operators*, Phys. Rev. D **26**, 3159 (1982).

[54] M. I. Buchoff, C. Schroeder and J. Wasem, *Neutron-antineutron oscillations on the lattice*, arXiv:1207.3832 [hep-lat].

[55] Z. Berezhiani and F. Nesti, *Magnetic anomaly in UCN trapping: signal for neutron oscillations to parallel world?*, Eur. Phys. J. C **72**, 1974 (2012) [arXiv:1203.1035 [hep-ph]].

[56] K. S. Babu and R. N. Mohapatra, *Coupling unification, GUT-scale baryogenesis and neutron-antineutron oscillation in SO(10)*, Phys. Lett. B **715**, 328 (2012) [arXiv:1206.5701 [hep-ph]].

[57] S. Weinberg, *Varieties of baryon and lepton nonconservation*, Phys. Rev. D **22**, 1694 (1980).

[58] M. K. Gaillard and B. W. Lee, *Rare decay modes of the K-mesons in gauge theories*, Phys. Rev. D **10**, 897 (1974).

[59] N. Tsutsui *et al.* [CP-PACS and JLQCD Collaborations], *Lattice QCD calculation of the proton decay matrix element in the continuum limit*, Phys. Rev. D **70**, 111501 (2004) [hep-lat/0402026].

[60] S. Rao and R. Shrock, *$n \leftrightarrow \bar{n}$ transition operators and their matrix elements in the MIT bag model*, Phys. Lett. B **116**, 238 (1982).

[61] P. Richardson and D. Winn, *Simulation of sextet diquark production*, Eur. Phys. J. C **72**, 1862 (2012) [arXiv:1108.6154 [hep-ph]].

[62] E. L. Berger, Q. -H. Cao, C. -R. Chen, G. Shaughnessy and H. Zhang, *Color sextet scalars in early LHC experiments*, Phys. Rev. Lett. **105**, 181802 (2010) [arXiv:1005.2622 [hep-ph]].

[63] C. -R. Chen, W. Klemm, V. Rentala and K. Wang, *Color sextet scalars at the CERN Large Hadron Collider*, Phys. Rev. D **79**, 054002 (2009) [arXiv:0811.2105 [hep-ph]].

[64] C. A. Baker, D. D. Doyle, P. Geltenbort, K. Green, M. G. D. van der Grinten, P. G. Harris, P. Iaydjiev and S. N. Ivanov *et al.*, *Improved experimental limit on the electric dipole moment of the neutron*, Phys. Rev. Lett. **97**, 131801 (2006) [hep-ex/0602020].

[65] G. Isidori, Y. Nir and G. Perez, *Flavor physics constraints for physics beyond the standard model*, Ann. Rev. Nucl. Part. Sci. **60** (2010) 355 [arXiv:1002.0900 [hep-ph]].

[66] D. V. Nanopoulos and S. Weinberg, *Mechanisms for cosmological baryon production*, Phys. Rev. D **20**, 2484 (1979).

[67] J. A. Harvey and M. S. Turner, *Cosmological baryon and lepton number in the presence of electroweak fermion number violation*, Phys. Rev. D **42**, 3344 (1990).

[68] K. S. Babu and R. N. Mohapatra, $B - L$ *violating nucleon decay and GUT scale baryogenesis in SO(10)*, Phys. Rev. D **86**, 035018 (2012) [arXiv:1203.5544 [hep-ph]].

[69] J. Adam *et al.* [MEG Collaboration], *New limit on the lepton-flavour violating decay* $\mu^+ \to e^+\gamma$, Phys. Rev. Lett. **107**, 171801 (2011) [arXiv:1107.5547 [hep-ex]].

[70] A. D. Smirnov, *Mass limits for scalar and gauge leptoquarks from* $K_L^0 \to e^\mp\mu^\pm, B^0 \to e^\mp\tau^\pm$ *decays*, Mod. Phys. Lett. A **22**, 2353 (2007) [arXiv:0705.0308 [hep-ph]].

[71] W. Buchmuller, R. Ruckl and D. Wyler, *Leptoquarks in lepton – quark collisions*, Phys. Lett. B **191**, 442 (1987) [Erratum-ibid. B **448**, 320 (1999)].

[72] A. J. Davies and X. -G. He, *Tree level scalar fermion interactions consistent with the symmetries of the standard model*, Phys. Rev. D **43**, 225 (1991).

[73] S. Davidson, D. C. Bailey and B. A. Campbell, *Model independent constraints on leptoquarks from rare processes*, Z. Phys. C **61**, 613 (1994) [hep-ph/9309310].

[74] E. Gabrielli, *Model independent constraints on leptoquarks from rare* μ *and* τ *lepton processes*," Phys. Rev. D **62**, 055009 (2000) [hep-ph/9911539].

[75] R. Benbrik and C. -K. Chua, *Lepton flavor violating* $l \to l'\gamma$ *and* $Z \to l\bar{l}'$ *decays induced by scalar leptoquarks*, Phys. Rev. D **78**, 075025 (2008) [arXiv:0807.4240 [hep-ph]].

[76] I. Dorsner, S. Fajfer, J. F. Kamenik and N. Kosnik, *Can scalar leptoquarks explain the* f_{D_s} *puzzle?*, Phys. Lett. B **682**, 67 (2009) [arXiv:0906.5585 [hep-ph]].

[77] R. Benbrik, M. Chabab and G. Faisel, *Lepton flavour violating* τ *and* μ *decays induced by scalar leptoquark*, arXiv:1009.3886 [hep-ph].

[78] M. Gonderinger and M. J. Ramsey-Musolf, *Electron-to-tau lepton flavor violation at the electron-ion collider*, JHEP **1011**, 045 (2010) [Erratum-ibid. **1205**, 047 (2012)] [arXiv:1006.5063 [hep-ph]].

[79] R. Kitano, M. Koike and Y. Okada, *Detailed calculation of lepton flavor violating muon electron conversion rate for various nuclei*, Phys. Rev. D **66**, 096002 (2002) [Erratum-ibid. D **76**, 059902 (2007)] [hep-ph/0203110].

[80] V. Cirigliano, R. Kitano, Y. Okada and P. Tuzon, *On the model discriminating power of $\mu \to e$ conversion in nuclei*, Phys. Rev. D **80**, 013002 (2009) [arXiv:0904.0957 [hep-ph]].

[81] P. Wintz, [for the SINDRUM Collaboration] *Results of the SINDRUM-II experiment*, Conf. Proc. C **980420**, 534 (1998).

[82] T. Suzuki, D. F. Measday and J. P. Roalsvig, *Total nuclear capture rates for negative muons*, Phys. Rev. C **35**, 2212 (1987).

[83] J. J. Hudson, D. M. Kara, I. J. Smallman, B. E. Sauer, M. R. Tarbutt and E. A. Hinds, *Improved measurement of the shape of the electron*, Nature **473**, 493 (2011).

[84] V. Barger, P. Fileviez Perez and S. Spinner, *Minimal gauged $U(1)_{B-L}$ model with spontaneous R-parity violation*, Phys. Rev. Lett. **102** (2009) 181802 [arXiv:0812.3661 [hep-ph]].

[85] C. S. Aulakh, A. Melfo, A. Rasin and G. Senjanovic, *Seesaw and supersymmetry or exact R-parity*, Phys. Lett. B **459**, 557 (1999) [hep-ph/9902409].

[86] C. S. Aulakh, B. Bajc, A. Melfo, A. Rasin and G. Senjanovic, *$SO(10)$ theory of R-parity and neutrino mass*, Nucl. Phys. B **597**, 89 (2001) [hep-ph/0004031].

[87] K. S. Babu and R. N. Mohapatra, *Minimal supersymmetric left-right model*, Phys. Lett. B **668**, 404 (2008) [arXiv:0807.0481 [hep-ph]].

[88] M. Duerr, P. Fileviez Perez and M. B. Wise, *Gauge theory for baryon and lepton numbers with leptoquarks*, Phys. Rev. Lett. **110**, 231801 (2013) [arXiv:1304.0576 [hep-ph]].

[89] P. Fileviez Perez and M. B. Wise, *Baryon and lepton number as local gauge symmetries*, Phys. Rev. D **82**, 011901 (2010) [Erratum-ibid. D **82**, 079901 (2010)] [arXiv:1002.1754 [hep-ph]].

[90] P. Fileviez Perez and M. B. Wise, *Breaking local baryon and lepton number at the TeV scale*, JHEP **1108**, 068 (2011) [arXiv:1106.0343 [hep-ph]].

[91] M. Duerr and P. Fileviez Perez, *Baryonic dark matter*, arXiv:1309.3970 [hep-ph].

[92] H. An, R. Huo and L. -T. Wang, *Searching for low mass dark portal at the LHC*, Phys. Dark Univ. **2**, 50 (2013) [arXiv:1212.2221 [hep-ph]].

[93] B. A. Dobrescu and F. Yu, *Coupling–mass mapping of di-jet peak searches*, Phys. Rev. D **88**, 035021 (2013) [arXiv:1306.2629 [hep-ph]].

[94] M. S. Carena, A. Daleo, B. A. Dobrescu and T. M. P. Tait, *Z' gauge bosons at the Tevatron*, Phys. Rev. D **70**, 093009 (2004) [hep-ph/0408098].

[95] P. Fileviez Perez and S. Spinner, *The minimal theory for R-parity violation at the LHC*, JHEP **1204**, 118 (2012) [arXiv:1201.5923 [hep-ph]].

[96] R. N. Mohapatra, *Mechanism for understanding small neutrino mass in superstring theories*, Phys. Rev. Lett. **56**, 561 (1986).

[97] D. K. Ghosh, G. Senjanovic and Y. Zhang, *Naturally light sterile neutrinos from theory of R-parity*, Phys. Lett. B **698**, 420 (2011) [arXiv:1010.3968 [hep-ph]].

[98] V. Barger, P. Fileviez Perez and S. Spinner, *Three layers of neutrinos*, Phys. Lett. B **696**, 509 (2011) [arXiv:1010.4023 [hep-ph]].

[99] P. A. R. Ade *et al.* [Planck Collaboration], *Planck 2013 results. XVI. Cosmological parameters*, arXiv:1303.5076 [astro-ph.CO].

[100] E. Aprile *et al.* [XENON100 Collaboration], *Dark matter results from 225 live days of XENON100 data*, Phys. Rev. Lett. **109**, 181301 (2012) [arXiv:1207.5988 [astro-ph.CO]].

[101] P. Fileviez Perez and S. Spinner, *Supersymmetry at the LHC and the theory of R-parity*, arXiv:1308.0524 [hep-ph].

[102] P. Fileviez Perez and M. B. Wise, *Low energy supersymmetry with baryon and lepton number gauged*, Phys. Rev. D **84**, 055015 (2011) [arXiv:1105.3190 [hep-ph]].

[103] K. Ishiwata and M. B. Wise, *Higgs properties and fourth generation leptons*, Phys. Rev. D **84**, 055025 (2011) [arXiv:1107.1490 [hep-ph]].

[104] J. M. Arnold, P. Fileviez Perez, B. Fornal and S. Spinner, *Higgs decays, baryon number violation, and supersymmetry at the LHC*, Phys. Rev. D **85**, 115024 (2012) [arXiv:1204.4458 [hep-ph]].

[105] B. Grinstein, M. Redi and G. Villadoro, *Low scale flavor gauge symmetries*, JHEP **1011**, 067 (2010) [arXiv:1009.2049 [hep-ph]].

[106] A. J. Buras, M. V. Carlucci, L. Merlo and E. Stamou, *Phenomenology of a gauged $SU(3)^3$ flavour model*, JHEP **1203**, 088 (2012) [arXiv:1112.4477 [hep-ph]].

[107] C. S. Fong and E. Nardi, *Quark masses, mixings, and CP violation from spontaneous breaking of flavor $SU(3)^3$*, Phys. Rev. D **89**, 036008 (2014) [arXiv:1307.4412 [hep-ph]].

[108] G. Krnjaic and D. Stolarski, *Gauging the way to MFV*, JHEP **1304**, 064 (2013) [arXiv:1212.4860 [hep-ph]].

[109] E. Nardi, *Naturally large Yukawa hierarchies*, Phys. Rev. D **84**, 036008 (2011) [arXiv:1105.1770 [hep-ph]].

[110] J. R. Espinosa, C. S. Fong and E. Nardi, *Yukawa hierarchies from spontaneous breaking of the $SU(3)_L \times SU(3)_R$ flavour symmetry?*, JHEP **1302**, 137 (2013) [arXiv:1211.6428 [hep-ph]].

[111] R. N. Mohapatra, *Gauged flavor, supersymmetry and grand unification*, AIP Conf. Proc. **1467**, 7 (2012) [arXiv:1205.6190 [hep-ph]].

[112] D. S. Akerib *et al.* [LUX Collaboration], *First results from the LUX dark matter experiment at the Sanford Underground Research Facility*, arXiv:1310.8214 [astro-ph.CO].

[113] P. Schwaller, T. M. P. Tait and R. Vega-Morales, *Dark matter and vector-like leptons from gauged lepton number*, Phys. Rev. D **88**, 035001 (2013) [arXiv:1305.1108 [hep-ph]].